Activation and Regulation of the 4-Hydroxyphenylacetate Decarboxylase System from *Clostridium difficile*

Dissertation

zur
Erlangung des Doktorgrades
der Naturwissenschaften
(Dr. rer. nat.)

dem
Fachbereich Biologie
der
Philipps-Universität Marburg

vorgelegt von
Martin Blaser
aus Frankfurt am Main

Marburg/Lahn, Deutschland 2007

Glücklich ist der Verfasser, der bei Beendigung seiner Arbeit gewiss sein kann, gesagt und überprüft zu haben, was er weiß, und der von sich sagen kann, dass er sein Urteil nach den von ihm erarbeiteten Normen abgegeben hat. Wenn er das Manuskript zum Druck gibt, kann er das beruhigende Gefühl haben, dass er ein lebensfähiges Geschöpf geschaffen hat.

- Janusz Korczak

Die Untersuchungen zur vorliegenden Arbeit wurden von November 2003 bis November 2006 im Laboratorium für Mikrobiologie, Fachbereich Biologie, der Philipps-Universität Marburg unter der Leitung von PD. Dr. T. Selmer durchgeführt.

Vom Fachbereich Biologie
Der Philipps-Universität Marburg
als Dissertation am angenommen.
Erstgutachter: PD. Dr. T. Selmer
Zweitgutachter: Prof. Dr. W. Buckel
Tag der mündlichen Prüfung: .

Abbreviations

5’ Ado	5’ deoxyadenosine
AE	Activating Enzyme
AHT	Anhydrotetracycline
BioB	Biotin Synthase
Bss	Benzylsuccinate synthase
Csd	*Clostridium scatologenes* decarboxylase
DTT	Dithiothreitol
EPR	Electron Paramagnetic Resonance
GRE	Glycyl radical enzyme
Gdh	Glycerol Dehydratase
Hem N	Oxygen-independent coproporphyrinogen III oxidase
HPA	4-Hydroxyphenylacetate
Hpd	4-Hydroxyphenylacetate decarboxylase from *C. difficile*
Hpd-AE	Activating Enzyme of Hpd
HPLC	High Performance Liquid Chromatography
LB	Luria-Bertani medium
LipA	Lipoate synthase
Nrd	Anaerobe ribonucleotide reductase
Pfl	Pyruvate Formate-Lyase
Pfl-AE	Activating Enzyme of Pfl
SAM	S-adenosylmethionine
Tfd	*Tannerella forsythensis* decarboxylase

Zusammenfassung

Der Mensch muss sich damit auseinandersetzen, in einer von Bakterien dominierten Welt zu leben. Alleine die Zahl der Mikroorganismen, die den menschlichen Körper besiedeln, übersteigt die Zahl menschlicher Zellen um das Zehnfache. Ebenso ist die genetische Information, die beispielsweise in den Bewohnern des menschlichen Darmes gespeichert ist, um ein Vielfaches größer als das humane Genom. Viele der hier hinterlegten Informationen können einen direkten Einfluss auf das Wohlbefinden des Menschen ausüben. Das Bemühen, einige dieser Reaktionen genauer zu verstehen, wird daher von der Wissenschaft vorangetrieben und war auch Triebfeder der hier vorgelegten Arbeit, die sich ein vertieftes Verständnis der Aktivierung und Regulation des 4-Hydroxyphenylacetat (HPA) Decarboxylase-Systems aus *Clostridium difficile* zum Ziel gesetzt hatte.

Das HPA Decarboxylase System katalysiert den letzten Schritt der Tyrosinfermentation und setzt als zelltoxisches Endprodukt Kresol frei. Der postulierte Mechanismus dieser Reaktion beinhaltet eine Anzahl radikalischer Zwischenprodukte und ist auf Protein-, wie auch auf Zellebene streng reguliert: Neben zwei Protein-Komponenten (Aktivierendes Enzym: HpdA und Decarboxylase: HpdBC) beinhaltet das System fünf redox-aktive Eisen-Schwefel Zentren und ist abhängig von S-Adenosylmethionin (SAM) als Radikalstarter sowie einer externen Elektronenquelle.

Im Verlauf dieser Arbeit konnte gezeigt werden, dass das aktivierende Enzym drei redox-aktive [4Fe-4S] Zentren enthält. Die anderen Vertreter dieser Proteinfamilie (SAM-Radikal Familie) koordinieren oft nur ein einziges, bereits gut untersuchtes Metall-Zentrum. Die Beschreibung der zwei zusätzlichen Zentren durch Mutationen der Bindungsstellen sowie biochemische Analysen bestätigte deren katalytische Notwendigkeit. Das aktivierende Enzym katalysiert unter Zuhilfenahme von SAM und einer externen Elektronenquelle die Bildung eines Glycyl-Radikals in der Decarboxylase. Eine Quantifizierung des hierbei ebenfalls entstehenden 5'Deoxyadenosin erlaubte nicht nur die Beschreibung eines – dem katalytischen Prozess parallel laufenden – Leerlaufzyklus', sondern bestätigte auch die Abhängigkeit des Aktivierungsprozesses von externen Elektronenquellen, da eine Speicherung nicht möglich scheint.

Im Gegensatz dazu konnte gezeigt werden, dass die Decarboxylase, welche ebenfalls zwei [4Fe-4S] Zentren besitzt, Elektronen in gewissem Umfang speichern und zur Unterdrückung des Glycyl-Radikals verwenden kann. Dieser – erstmals als transiente Aktivierung beschriebene – Prozess unterscheidet die HPA Decarboxylasen von den meisten anderen, gut

untersuchten Vertretern, der Glycyl-Radikal Familie, bei denen das erzeugte Radikalsignal über längere Zeit stabil bleibt.

Die in diesem Zusammenhang gelöste Kristallstruktur von CsdBC gab weiteren Aufschluss über die Koordination der [4Fe-4S] Zentren durch die kleine Untereinheit (CsdC) und bestätigte den für die Katalyse zum Kresol notwendigen hetero-oktameren Komplex des nicht aktivierten Vorläufers.

Sowohl bei der schnellen Aktivierung des Systems als auch bei der intrinsischen Inaktivierung durch die kleine Untereinheit, spielen die Redox-Zustände der [4Fe-4S] Zentren eine entscheidende Rolle bei der Regulation des HPA Decarboxylase Systems.

Summary

Humans must adopt to live in a microbial world. The number of microbes associated with the human body alone exceeds the total number of body cells by more than one order of magnitude. Besides, the overall genetic information harboured by the microbial consortium in the human gut exceeds by many times the human genomic information. Some of these informations exhibit detrimental effects on the human well-being. The endeavour to understand these reactions more precisely does not only inspire the scientific community, but was also the driving force for this work concerning the activation and regulation of the 4-hydroxyphenylacetate (HPA) decarboxylase system of *Clostridium difficile*.

The HPA decarboxylase system catalyses the final step in tyrosine-fermentation, liberating the toxic end product *p*-cresol. The postulated mechanism of this reaction includes a number of radical intermediates and is tightly regulated on the protein as well as on the DNA level. Besides the two protein partners (activating enzyme: HpdA, and decarboxylase: HpdBC) the system includes five redox-active iron-sulfur centres, is dependent on S-adenosylmethionine (SAM) as radical generator and requires an external electron-source.

During the time-course of this work it could be established that the activating enzyme contains three catalytically essential [4Fe-4S] clusters. The other members of this protein-family (SAM radical family) coordinate just one, previously already well characterised cluster. The catalytic need for the additional clusters could be evaluated by mutational analysis of the cluster binding sites and biochemical analysis. In the presence of SAM and an electron source the activating enzyme initiates the glycyl-radical formation in the main enzyme. Quantifying the 5' deoxyadenosine liberated by this reaction, allowed the description of a futile cycle, which runs parallel to the catalytic process. It could also be validated that the activation process is dependent on an external electron-source and that storage of an electron is not possible.

In contrary, the decarboxylase, which also contains two [4Fe-4S] centres, is able to hold back electrons and uses them to dissipate the glycyl-radical over time. This process – first described as transient activation – makes the HPA decarboxylases unique among most other well described members of the glycyl-radical family, where the radical is stable over prolonged incubation times.

In this respect the recently solved crystal structure of CsdBC gave further evidence that the coordination of the [4Fe-4S] clusters is mediated by the small subunit (CsdC) and confirmed the hetero-octameric nature of the complex of the inactive precursor, which is essential for catalysis.

Not only for the fast activation of the system but also for the intrinsic inactivation mediated by the small subunit, the redox-properties of the [4Fe-4S] centres are of utmost importance in the regulation of the HPA-decarboxylase systems.

Content

Figures

Tables

1 Introduction

The evolution of microbial species has focused largely on the expansion of metabolic diversity in contrast to the development of complex cell structures pursued by their higher eukaryotic counterparts. As a result, microbes have freely colonized all aspects of the environment, knowing no geographic borders and are limited only by the accessibility of redox couples with sufficiently high changes in free energy to allow them to survive. In evolutionary simple terms there are two major facts about microbes: They live almost everywhere and they can perform almost every metabolic task.

Following this perspective, humans must adopt to live in a microbial world. As adults, the number of microbes associated with our mucosal surface exceeds our total number of somatic and germ cells by more than one order of magnitude (3). The vast majority resides in our colon where - with cell densities of 10^{11}-10^{12} cells/ml - the highest densities recorded for any microbial habitat are reached (4). Thus, it seems appropriate to view ourselves as a composition of many species and our genetic landscape as an amalgam of genes embedded in our *Homo sapiens* genome and in the genomes of our affiliated microbial partners (5). On the other hand the diversity of the adult flora at the division level is among the lowest; containing only seven of the 55 known bacterial divisions. Among them the *Firmicutes* (e.g. the genus *Clostridium*) and the *Bacteroides* dominated, together accounting for >98% of all 16S rRNA sequences (5).

The composition of the microflora varies along the length of the gut and during the life of the host, but is stable over shorter periods of time and resistant to a number of environmental changes (e.g. nutrition) and may even be used as a personal fingerprint. On the other hand the treatment with antibiotics is often accompanied by a dramatic change in the gut microbiota, and this disturbance is known to account for severe health problems and life threatening diseases. One of the microbes associated with this situation is *C. difficile*.

1.1 *C. difficile*

C. difficile is a slender, gram-positive, anaerobe bacillus that produces large, oval, subterminal spores. It is a member of the normal intestinal flora in <3% of adult humans (6, 7). The organism appears unable to compete successfully in the normal intestinal ecosystem, but can outnumber competitors when the normal flora has been altered by antibiotics. *C. difficile* - associated diarrhoea (CDAD) is initiated by the overgrowth of the intestinal gut microbiota by the pathogen, primarily in the colon.

C. difficile is a major nosocomial pathogen that causes a spectrum of intestinal diseases. The organism proliferates in the disturbed gut ecosystem and secretes two toxins, which primarily act as glucosyl-transferases. The glucosylation of *ras* and *rho* proteins causes cytoskeleton disassembly and is responsible for the cytotoxic and tissue damaging effects (8-10). Clinical symptoms vary widely from mild diarrhoea to severe abdominal pain accompanied by fever and general weakness. Pathology involves primarily the colon, where disruption of brush border membranes occurs, followed by extensive damage of the mucosa. The infection may progress to a pseudomembranous colitis, causing toxic megacolon, intestinal perforation and as a consequence sepsis and death.

Though the recently published genome of *C. difficile* shines some light on the highly mobile mosaic genetic features *C. difficile* employs to be multi-drug resistant, little is known about the virulence factors involved in the ongoing suppression of the gut microbiota following an antibiotic treatment (11). The long known and diagnostically used fermentative formation of *p*-Cresol by *C. difficile* may be an important factor involved.

1.1.1 Fermentation processes in *C. difficile*

Although the role of antibiotic exposure as a predisposing factor to *C. difficile* colonisation and infection is well established, the exact mechanisms by which the colonisation of the gut by the pathogen proceeds are still unclear and need further evaluation. Besides the accumulation of knowledge regarding its pathogenesis, little is known about the metabolic power of *C. difficile* linking the clinical symptoms to metabolic properties or growth parameters.

Its versatile ability to ferment a number of substrates has been recognized since a long time (12, 13), but only recently we start to understand the underlying mechanisms on a molecular basis and the chemically beautiful ways of anaerobe fermentation involved therein.

Clostridia employ a mixed fermentation pathway using a number of complex polysaccharides leading to butyrate, acetate and CO_2. Of special interest is their ability to ferment certain amino acids (12). The abilities to ferment single amino acids and to use several amino acids either as oxidants or reductants, sometimes combined in one organism, was first described by Stickland in 1934 (14). Interestingly, the oxidation reactions are usually similar or identical to corresponding reactions catalyzed by aerobic organisms. The reduction reactions on the other hand vary among clostridia species. Electron acceptors include amino acids, α- and β-keto acids, α, β unsaturated acids or their coenzyme A thiolesters, and protons. The ultimate reduction products include a variety of short-chain fatty acids, succinic acid, δ-aminovaleric acid, and molecular hydrogen (13).

Besides these general patterns a number of unique fermentation pathways are known. Of special interest is the anaerobic degradation of aromatic amino acids leading to aromatic phenolic and indolic compounds (12). Skatole (3-methylindole) and *p*-cresol are common bacterial metabolic end products in animal and human intestine (15-21), which are formed by fermentation of the proteinogenic amino acids tyrosine and tryptophan (12). Considering the life-long exposure, the impact of this compounds is rather obvious, and has been suggested to affect the health status of the host in many ways (22). The compounds are putative risk factors for colon cancer (23, 24) and may cause complications in uremic patients, since they are protein-bound dialysis retention solutes, which can reach toxic levels in blood (25-28). The chronic exposure causes muscle weakness, cardiac arrhymthmias, gastrointestinal and neuropsychatric complaints, and liver, kidney and lung damage. The ruminal formation of skatole from tryptophan has been shown to cause pulmonary edema and ephysema in cattle (29-37). The formation of 4-methylphenol (*p*-cresol) from 4-hydroxyphenylacetate is a feature best described for *C. difficile* and *C. scatologenes,* but also known for *Lactobacilli* (38). This decarboxylation was first demonstrated by D'Ari and Barker in 1985 for cell-free extracts of *C. difficile* (39). Only recently the corresponding enzyme system was described as a new member of the glycyl radical enzyme family (40). Therefore a short introduction into radicals in enzyme chemistry should be given, to approach the HPA decarboxylase system and its complex regulation.

1.2 Radicals in proteins

Since the discovery of a stable organic radical essential in ribonucleotide reductase (41) (an one electron oxidized tyrosyl residue), stable and transiently occurring amino acid-based radicals were detected in proteins, which are stabilized by glycyl-, cysteinyl-, tyrosinyl-, and tryptophanyl residues. All amino acid-derived radicals are synthesized by a posttranslational process involving metal-cofactors located either adjacent to the amino acid being converted to a radical or in a second, "activating" enzyme, which is essential for its formation. Recent genomic analyses revealed that in particular the glycyl radical enzymes (GREs) seem to be more prevalent in obligate and facultative anaerobe microbes than previously anticipated (42). GREs are involved in various reactions (Table 1), for example in the anoxic degradation of pyruvate (Pfl), anaerobic ribonucleotide reduction (Nrd), in the activation of toluene (Bss), coenzyme B_{12}-independent glycerol dehydratation (Gdh) and 4-hydroxyphenylacetate decarboxylation (Hpd). Moreover, a number of novel systems has been identified in the genomes of anaerobes, whose functions remain to be established.

1.2.1 Glycyl Radical Enzymes (GREs)

Most GREs are large enzymes composed of about 900 amino acids. The inactive precursor protein needs to undergo post-translational activation by a specific, SAM-dependent activating enzyme (AE) (reviewed in: (43-45)). Upon activation of GREs, the stable protein-bound glycyl-radical is generated. Work of Knappe et al. on Pfl established that the sp^2–hybridized radical is centered at the α-carbon atom of a specific glycyl residue (46, 47). EPR-spectroscopy revealed that the characteristic glycyl radical EPR signal has a remarkably constant appearance (a doublet with hyperfine coupling of 1.4-1.5 mT centered around g_{iso} = 2.0035 at X-band) in Pfl (47), Nrd (48, 49), Hpd (50), Bss (51, 52), and methylpentylsuccinate synthases (53). The radical is stabilized by delocalization of the free electron over the adjacent peptide bonds in the protein backbone and is regarded as a storage form of the radical.

table 1 Reactions catalysed by GREs

Enzyme/ Organism	Ref.	Reaction catalysed
Pfl/ *E. coli*	(46)	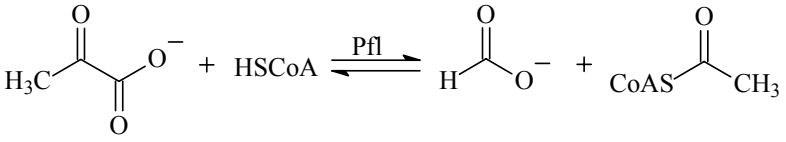 Pyruvate Coenzyme A Formate AcetylCoA
Nrd/ *E. coli*	(54)	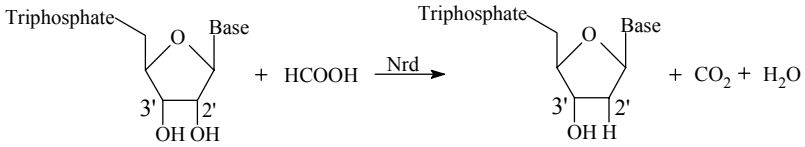 Ribonucleotide triphosphate Formate Deoxyribonucleotide triphosphate
Bss/ *T. aromatica*	(55)	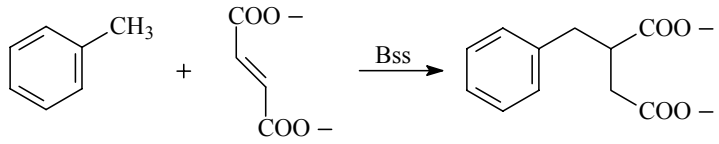 Toluene Fumarate Benzylsuccinate
Hpd/ *C. difficile*	(56)	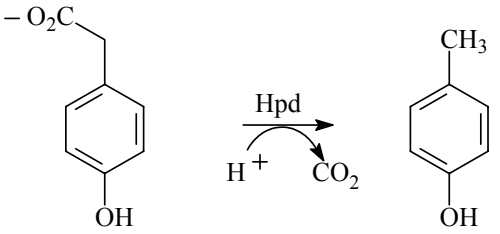 4-Hydroxyphenylacetate 4-Cresol
GD/ *C. butyricum*	(57)	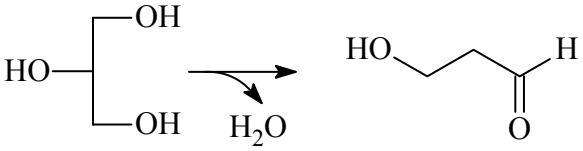 glycerol 3-hydroxy-propionaldehyde

From the crystal structures of Pfl, Nrd and Gdh, it is apparent that these enzymes form homodimers and that these functionally very different polypeptides exhibit a similar three-dimensional fold (58-62). Just recently the crystal structure of Pfl2 from *Archaeoglobus fulgidus* has been solved to a resolution of 2.9 Å (63). In all structures the core is a 10-stranded β-barrel motif assembled by two parallel 5-stranded β-sheets and entirely surrounded by α-helices. All four GRE structures share the presence of two flexible loops protruding into

the central core of β-sheets. While one of these loops carries the glycyl radical site, the second loop carries the active site cysteinyl residue. Unlike the other glycyl radical enzymes described so far, Pfl2 is a homotetramer. *A. fulgidus* is a hyperthermophile and PFL2 appears to be stabilized by several factors including an increased number of ion pairs, differences in buried charges, a truncated N terminus, anchoring of loops and N terminus via salt-bridges, changes in the oligomeric interface and perhaps also the higher oligomerization state of the protein.

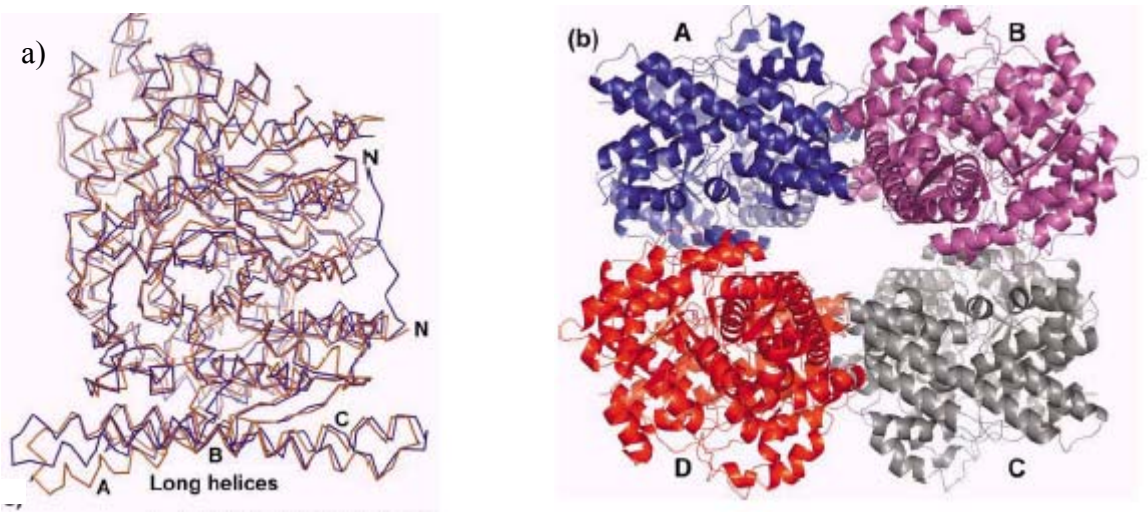

figure 1 Structure of PFL II a) A Cα trace comparing a monomer of PFL2 (brown) with a monomer of Gdh (blue). The N termini have been labelled to show the truncation in PFL2. The long helices that in PFL2 and Gdh are composed of three separate helices are also labelled: A (168–185), B (189–224) and C (226–243 in PFL2 numbering) b) The biologically relevant tetramer of PFL2. The monomers are coloured differently. The view is along one of the 2-fold symmetry axes of the D2-tetramer, which is formed using the crystallographic symmetry operators. Monomers A+B and C+D form the "PFL-like" dimers; the A–D and B–C interfaces are unique to PFL2 (63).

The reaction cycle of all known GREs (figure 2) is thought to be initiated by transferring the radical to the thiol group of the conserved cysteine (1), which is closely neighbored to the glycyl radical site in the tertiary structure. The highly reactive thiyl radical thus generated then abstracts a hydrogen atom from the substrate, yielding an enzyme-bound substrate radical (2-3), which undergoes the reaction to yield an intermediate product radical (3). Finally, the product radical re-abstracts the hydrogen atom from the thiol-group of the enzyme, rendering it back to the active, radical-containing state (4-5). The only deviation from this general scheme is known for Pfl, where the initial radical transfer is relayed on the thiol of a second conserved cysteine and forms a covalent intermediate with the substrate by addition to the β-carbonyl of pyruvate rather than abstracting a hydrogen.

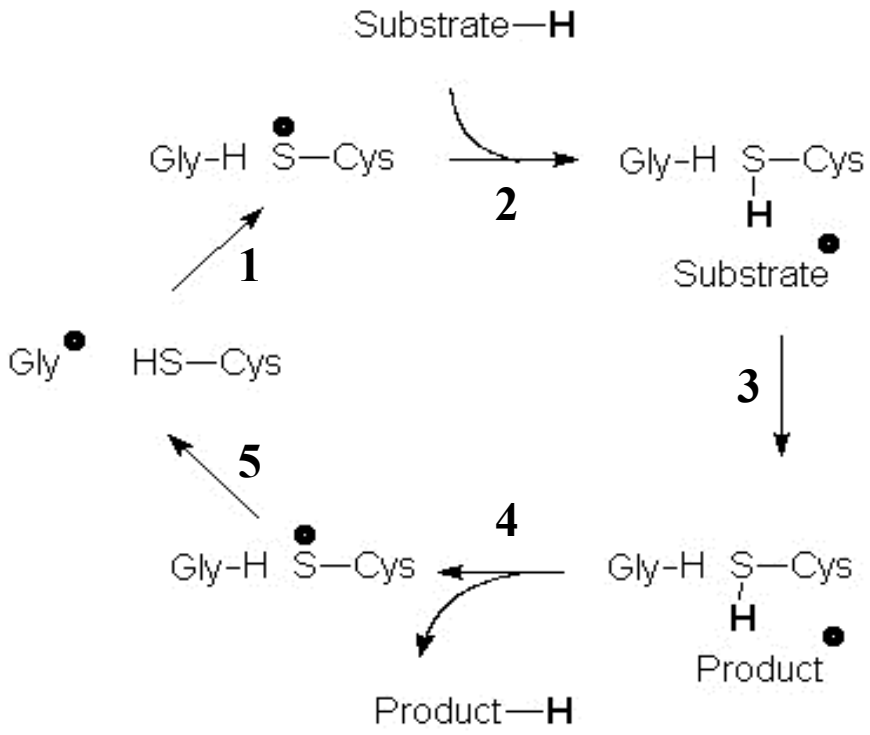

figure 2 General scheme for the mechanism of glycyl-radical enzymes. The glycyl radical abstracts a proton from a conserved cysteine residue in the active site (1). Upon substrate binding (2) and abstraction of a proton to generate a highly active substrate radical, a product-radical is formed (3) (in the case of Hpd by decarboxylation). After re-abstracting the proton from the active site cysteine (4) the product is released and the glycyl radical as stable radical storage form is regenerated (5).

Under *in vitro* conditions the activated glycyl-radical is stable for several hours (1). In the presence of oxygen, however, the glycyl radical becomes highly unstable and the enzyme is irreversibly inactivated by cleavage of the polypeptide chain at the site of the radical (46, 64). Hence, the reversible inactivation aided by unspecific inactivation enzymes (AdhE for Pfl) or as intrinsic property of the GRE itself as postulated for HpdBC (50, 65), might be of physiological relevance. In particular in facultative anaerobes, which occasionally must face sudden exposure toward molecular oxygen, a tight regulation of the system is essential.

1.2.2 A novel subclass of GRE – introducing the HpdBC System

For almost a decade, pyruvate formate-lyase (Pfl, EC 2.3.1.54) and anaerobic ribonucleotide reductase (Nrd, EC 1.17.4.-) have been the only known members of the glycyl radical family (43, 44, 66). During the last decade, a number of novel systems has been functionally characterized. These systems include benzylsuccinate synthase (Bss, EC 4.1.99.11) from *Thauera aromatica* (55, 67, 68), 4-hydroxyphenylacetate decarboxylase

(Hpd, EC 4.11.1.82) from *Clostridium difficile* (56) and a novel type of glycerol dehydratase (Gdh, EC 4.2.1.30) from *Clostridium butyricum* (57).

The decarboxylation of 4-hydroxyphenylacetate (4-HPA) to *p*-cresol is a chemically challenging task, leaving behind a negatively charged methylene group neighbored by an electron dense aromatic π-system. To circumvent this problem, radical chemistry is used for an 'Umpolung' (charge inversion) of the aromatic ring. For this purpose the glycyl-radical is transferred to a cysteine residue in the active site, which than is believed to abstract a hydrogen atom from the substrate (1). The resulting radical anion decarboxylates spontaneously to release CO_2 and forms a product related ketyl-radical intermediate (2). Protonation of this renders the formation of a neutral radical (3), which then re-abstracts a hydrogen atom from the enzyme to yield the product *p*-cresol and regenerating the enzyme bound thiyl-radical (4) (56, 69).

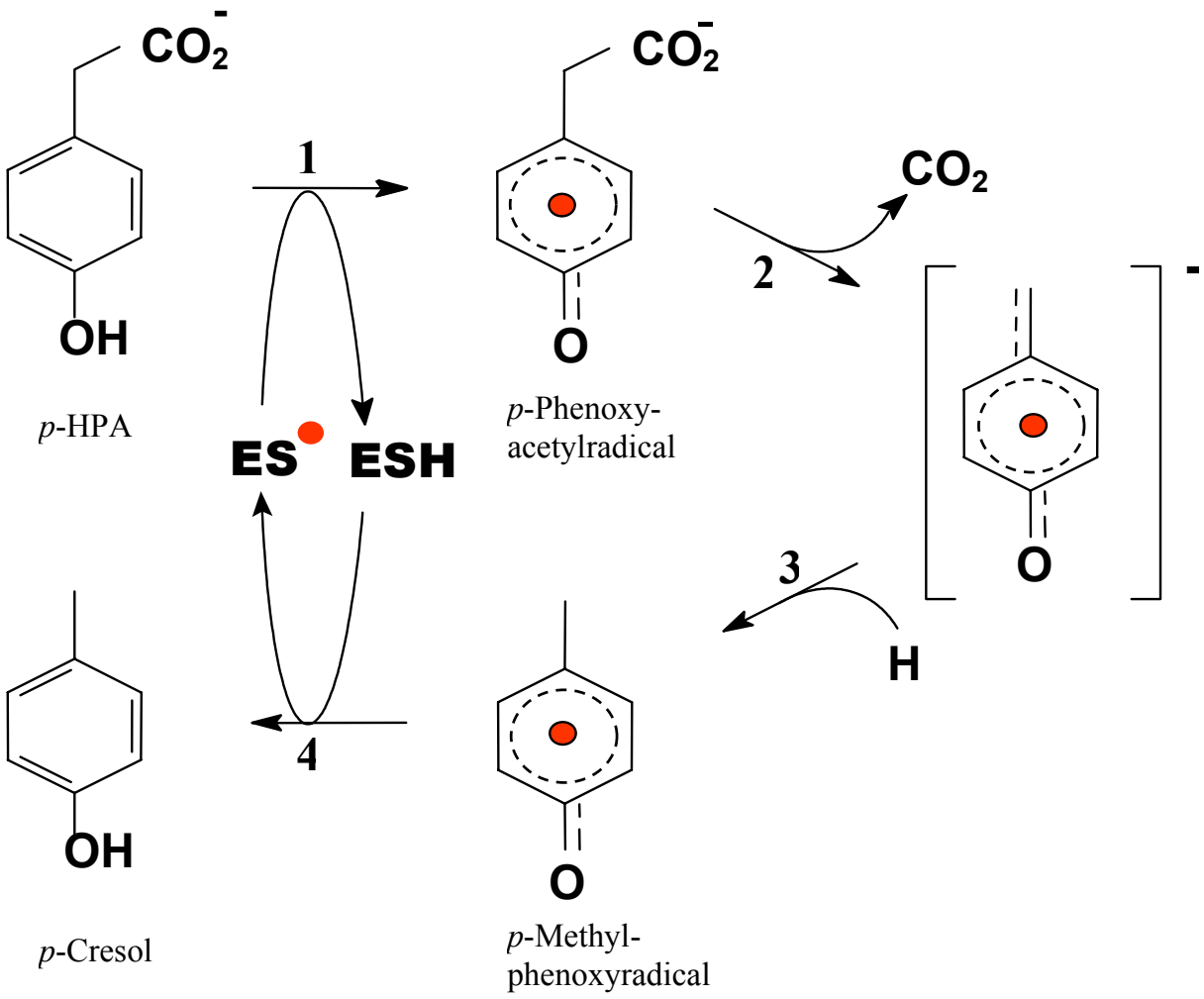

figure 3 Decarboxylation of *p*-Hydroxyphenylacetate to *p*-Cresol by the clostridial HPA-decarboxylase system. Details see text.

So far two systems have been analysed, which are capable of performing this reaction. Both, the 4-HPA decarboxylase systems from *C. difficile* (Hpd) and *C. scatologenes* (Csd), consist of the decarboxylase, which is composed of two subunits, and of its cognate activating enzyme. The large subunit of the decarboxylase (HpdB, 101 kDa, 902 amino acids; CsdB, 101 kDa, 897 amino acids) carries the glycyl radical essential for catalysis, while the functional role of the small subunit (HpdC, 9.5 kDa, 85 amino acids; CsdC, 9.4 kDa, 86 amino acids) seems to be regulatory. The recombinant proteins co-purify in one-step affinity chromatographic purification, which takes advantage of an N-terminally Strep-tag fused to the glycyl radical subunit. They are hetero-octamers ($\beta_4\gamma_4$) and contain sixteen [4Fe-4S] $^{+1/+2}$ clusters per octamer, providing additional enzyme-bound co-factors in addition to the glycyl radical. These clusters were not observed in Pfl, Nrd and Gdh, but are probably also present in Bss. A reversible serine-phosphorylation of HpdB and CsdB was demonstrated, which is believed to regulate complex stability and enzyme activity (50).

The decarboxylase activating enzyme (HpdA, 36 kDa, 316 amino acids, CsdA, 37 kDa, 319 amino acids) is needed for specific activation of the enzymes and may contain up to two [4Fe-4S] clusters in addition to the characteristic SAM-cubane, which is found in all GRE-AEs.

As a third system of unknown function, a glycyl-radical enzyme of *Tannerella forsythensis* has been heterologously expressed. In contrast to the clostridial systems it purifies as a hetero-tetramer ($\beta_2\gamma_2$) with a dramatically reduced iron-sulfur content and is catalytically inactive to all substrates tested so far. The glycyl-radical signal is only 1/10 of the clostridial EPR-signals and by this in the range of the inactivated complexes.

1.2.3 Activation of GREs

When synthesised, GREs are catalytically inactive and must undergo a post-translational activation mediated by hydrogen atom abstraction in order to acquire the catalytically essential glycyl radical. The activation is catalysed by specific activating enzymes (AEs). These AEs are members of the large SAM radical enzyme superfamily and characterised by an unusual C-x_3-C-x_2-C iron-sulfur cluster binding motif and the dependence on SAM as co-substrate (70).

Besides the GRE activating enzymes well-established members of the radical SAM family are the lysine 2,3-aminomutase (LAM), biotin synthase (BioB), Lipoate synthase (LipA) and spore photoproduct-lyase (SPF lyase). More recently characterized members include enzymes like MiaB, a tRNA-methylthiotransferase (71, 72), MoaA/MOCS1A, involved in molyb-

denum cofactor biosynthesis (73), HemN, involved in the oxygen-independent coproporphyrinogen synthesis (74), ThiH, involved in thiamine biosyntesis (75, 76), 7,8-didemethyl-8-hydroxy-5-deazariboflavin synthase (77), AtsB (78), NifB, involved in the synthesis of iron-molybdenum cofactors of nitrogenase (79), HydE and HydG involved in the biosynthesis of the H-cluster of hydrogenases (80) as well as Elp3, which provides one of six subunits in the elongator complex (81).

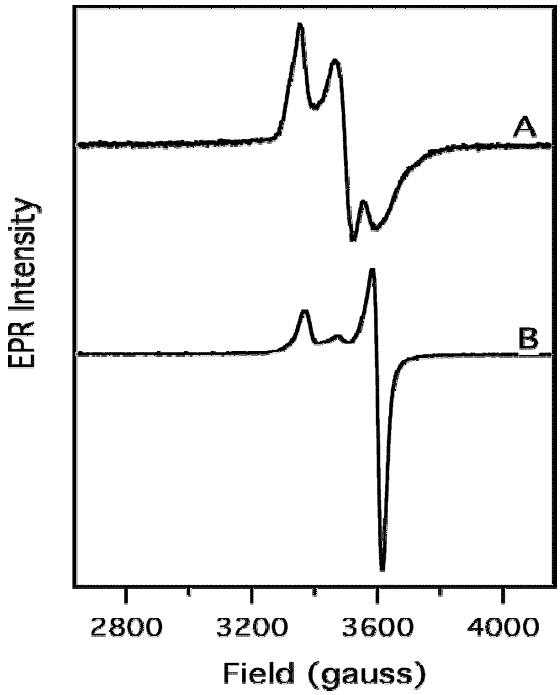

figure 4 EPR signal of Pfl-AE. (A) PFL-AE (0.7 mM); (B) PFL-AE (0.78 mM) photoreduced for 1 h. followed by addition of 2 molar equiv of SAM (1).

In all these SAM radical enzymes a unique [4Fe-4S] $^{+1/+2}$ cluster is directly involved in catalysis, anchoring S-adenosylmethionine (SAM) for cleavage into methionine and a 5'-deoxyadenosyl radical. This transiently formed radical is proposed to abstract the pro-*S*-hydrogen atom from a strictly conserved glycine residue in the GRE, which forms part of a highly conserved finger print motif RVxG[FWY]x_{6-8}[FL]x_4Qx_2[IV]x_2R close to the C-terminus of the polypeptide chain. In the other members the hydrogen is directly abstracted from a non-protein substrate. The unique nature of the SAM cubane can also be seen in EPR, where the signal of the reduced [4Fe-4S] cluster dramatically changes upon SAM binding (figure 4).

A hypothetical mechanism for the Fe-S/SAM-dependent formation of the glycyl radical must consider the notion that the S-C bond dissociation energy in SAM is more than 252kJ/mol and homolytic cleavage would require labilization of that bond by one-electron reduction. This is in agreement with the need for a reducing agent, either an enzymatic system such as NADPH: flavodoxin-reductase: flavodoxin *in vivo* or a chemical agent like dithionite or photoreduced deazaflavin *in vitro* (82-84).

SAM coordinates the unique iron site of the [4Fe-4S] $^{+1/+2}$ cluster in radical SAM enzymes with the amino- and carboxylate groups of its methionine moiety. This

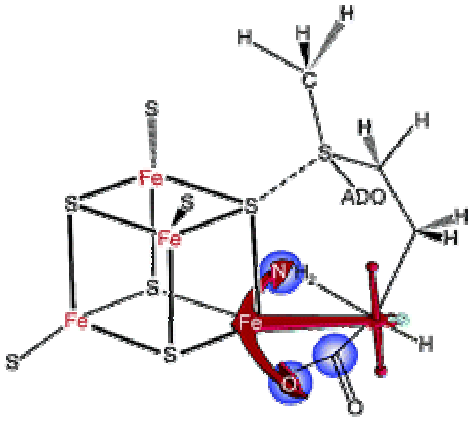

figure 5 SAM bound to the unique [4Fe-4S] cluster (2).

binding mode was first demonstrated by spectroscopic studies of pyruvate formate-lyase activating enzyme and subsequently in crystal structures of four other members of the superfamily (biotin synthase, HemN, MoaA, and lysine 2,3-aminomutase) (1, 2, 73, 85-90). Thus it appears likely that the site-differentiated iron sulfur centre is conserved throughout the radical SAM superfamily due to an essential role of the unique iron, providing a structural element for coordination and anchoring of SAM and for subsequent radical generation.

The SAM cluster anchors the methionine of SAM, whereas the adenosyl-group is bound by a glycine-rich SGG-sequence motif. This motif is located directly adjacent to the cysteines coordinating the SAM cluster in Pfl-AE and Nrd-AE, whereas other GRE-AEs contain a 31 to 64 amino acid insertions between these functional motifs. Within these inserts, 4 to 8 cysteinyl residues are located, which form up to two ferredoxin-like $Cx_{2-4}Cx_2Cx_{7-34}C$ motifs. This might allow the binding of one or two additional [4Fe-4S] clusters as recently found in recombinant Hpd-AE (50).

Interestingly, second clusters have been described for LipA, BioB and MoaA. While recent evidence suggests that this second cluster in LipA and BioB is involved in sulfur insertion (91, 92) other members of the SAM radical family incorporating sulfur during catalysis do not carry a second cluster (MiaB). A recently obtained crystal structure of MoaA containing substrate (5'-GTP) suggests involvement of the second cluster in substrate recognition. Furthermore the second cluster was redox active, allowing a participation in electron transfer during the catalytic cycle (93).

1.3 Aim of this work

Previous studies have shown that the Hpd system from *C. difficile* shows unique properties, which distinguishes this novel GRE system from the well characterized Pfl and Nrd systems. Among these properties are the presence of small subunits and a metal cofactor in the decarboxylase. The decarboxylase activating enzyme also differs in its metal content from the other systems and contains probably up to two iron-sulfur centers in addition to the SAM cubane. Therefore, it was the purpose of this work to contribute to a better understanding of the distinct biochemical properties of these novel systems. The role of the iron-sulfur clusters in the regulation of enzyme activities was of particular interest. The involvement of these additional clusters in the radical formation and dissipation was elucidated biochemically as well as by mutational scanning analysis of the putative cluster binding sites. Additionally, the crystal structure of CsdBC (which is homologue to HpdBC, but originates from *C. scatologenes*) was solved and provided clear evidence for binding of two iron-sulfur-clusters by the small subunits (HpdC and CsdC, respectively) of the decarboxylases.

2 Materials and Methods

2.1 Materials

2.1.1 Chemicals and reagents

All chemicals were purchased from Sigma-Aldrich (Deisenhofen, Germany), Lancaster (Mühlheim, Germany), Fluka (Buchs, Germany) or Merck (Darmstadt, Germany) and were of the highest quality available.

The enzymes used for the molecular biology experiments were from Roche (Mannheim, Germany), MBI Fermentas GmbH (St. Leon-Rot, Germany) or Amersham (Freiburg, Germany).

2.1.2 Instruments, gases and columns

Anoxic experiments were performed in a glovebox (Coy Laboratories, Ann Arbor MI, USA) providing an atmosphere of N_2/H_2 (95%/5%). FPLC system and UV/Vis photometer (Ultrascopec 400) were from Amersham Biosciences (Freiburg, Germany). HPLC was from Sykam (Fürstenfeldbruck). A LiChroCART^{TM} 250 x 4 mm HPLC cartridge (Merck, Darmstadt) filled with LiChrospher^{TM} 100 RP-18 (5 µm) was used for cresol detection. A LC-DABS 150 x 4.6 mm cartridge (Supelco/Sigma, München, Germany) was employed for adenosine derivatives. *Strep*-Tactin MacroPrep column and gravity flow *Strep*-Tactin sepharose columns were from IBA GmbH (Göttingen). N_2 (99.996%), and N_2/H_2 (95:5 v/v) were purchased from Messer-Griesheim (Düsseldorf, Germany).

2.1.3 Bacterial strains and plasmids

table 2 Bacterial strains

Strain	Genotype	Reference/Source
BL21^{TM} (DE3) Codon Plus RIL	*F⁻ ompT hsdS (r_B^- m_B^-) dcm^+ Tet^r gal (DE3) endA Hte [argU ileY leuW Cam^r]*	Fermentas
Rossetta^{TM} (DE3) pLysS	*F⁻ ompT $hsdS_B$ (r_B^- m_B^-) gal dcm (DE3) pLysS/RARE [argU argW ileX glyT leuW [proL] (Cam^r)*	Novagen
DH5α	*F⁻ ϕ80dlacZ ΔM15 Δ(lacZYA-argF) U169 recA1 endA1 hsdR17 (r_k^-, m_k^+) phoA supE44 λ⁻ thi-1 gyrA96 relA1*	Invitrogen

table 3 Plasmids

Plasmid	Characteristic	Reference/Source
pASK-IBA7	Amp^r, cloning and expression vector, providing *tet*A promoter, and N-terminal *Strep*-tag II.	Institut für Bioanalytik, Göttingen

table 4 Molecular biology kits and enzymes

Kit	Company
E.Z.N.A. Cycle pure DNA kit	peqlab (Erlangen)
E.Z.N.A. Plasmid miniprep Kit	peqlab (Erlangen)
T 4 DNA ligase	Fermentas (St. Leon-Rot)
Esp3I	Fermentas (St. Leon-Rot)
BamHI	Fermentas (St. Leon-Rot)
Xba1	Fermentas (St. Leon-Rot)
Taq DNA Polymerase	Fermentas (St. Leon-Rot)
Phusion DNA Polymerase	Finzyme (Espoo, Finland)

2.1.4 Media and plates

All media were autoclaved at 121°C and 1 bar (15psi) for 20 min.

LB medium

Trypton	10.0 g
Yeast extract	5.0 g
NaCl	10.0 g
Distilled water	0.8 L

The medium was adjusted to pH 7.0, filled up to 1 L and autoclaved.

LBG medium

Trypton	10.0 g
Yeast extract	5.0 g
NaCl	10.0 g
Glucose	2.0 g
Distilled water	0.8 L

The medium was adjusted to pH 7.0, filled up to 1 L and autoclaved.

Solid media

Unless otherwise stated, LB (Luria-Bertani Medium) agar plates (1.5%) supplemented with the required antibiotic(s) were used to isolate colonies.

2.1.5 Oligonucleotides

Table 5 Mutagenic primers for the generation of cysteine to serine mutations in the activating enzyme. All the primers used were synthesised by MWG Biotech (Ebersberg).

table 5 Primers used to generate mutants of the cluster binding sites in HpdA

Name	Nucleotide Sequence (5'-3')
HpdC_dsBamHI_as	CGC CAT TTT TCA CTT CAC AGG
SQ_IBA7_s	GAT AGA GTT ATT TTA CCA CTC CC
HpdA_SAMC-S_as	TAA TTT CGT CTC CCA TTT AGA ACT CAG TGG AGA TCC ATT TAA AAA TAC AGT TGT TC
HpdA_SAMC-S_s	ATT AAA CGT CTC AAA TGG TCT GCA AAT CCA GAA AGT TGG ACT G
HpdA_Ib-S_as	TAA TTT CGT CTC CAA AAC TTT CAG AGT CCT TAG AGA TGT TCC AAT CTA TAA CTG GC
HpdA_Ib-S_s	ATT AAA CGT CTC GTT TTG AAA GCG TCA ACT CAT CTT ATT ATA ATG CGT TTA AAT TAT GTG C
HpdA_Ia-S_as	TAA TTT CGT CTC TAG ATC CAT TTT CAT ATT GAG AAG ATA ATT CAC TAA ACA TCA TAT G
HpdA_Ia-S_s	ATT AAA CGT CTC GAT CTA CTG TAT CTC ATG GTA AGT CTA AAA ATG GTG CAT TGA GCT TTA ATC
HpdA(C66S)_as	TCG TCT CTT GAT CCA TTT TCA TAT TGA CAA GAT AAT TCA
HpdA(C66S)_s	TCG TCT CGA GAT ACA GTA CAT CCA TTT TCA TAT TGA CAA G
HpdA(C69S)_as	TCG TCT CGA GAT ACA GTA CAT CCA TTT TCA TAT TGA CAA G
HpdA(C69S)_s	TCG TCT CGA TCT CAT GGT AAG TGT AAA AAT GGT GC
HpdA(C73S)_as	TCG TCT CGA GAC TTA CCA TGA CAT ACA GTA CAT C
HpdA(C73S)_s	TCG TCT CGG TCT AAA AAT GGT GCA TTG AGC TTT AAT CTT G
HpdA(C93S)_as	TCG TCT CGA GAG ATG TTC CAA TCT ATA ACT GGC TTA TTA TC
HpdA(C93S)_s	TCG TCT CGC TCT AAG GAC TGT GAA AGT TTT GAA TGC G
HpdA(C96S)_as	TCG TCT CGA GAG TCC TTA CAG ATC TTC CAA TCT ATA AC
HpdA(C96S)_s	TCG TCT CGC TCT GAA AGT TTT GAA TGC GTC AAC TC
HpdA(C101S)_as	TCG TCT CGG CTT TCA AAA CTT TCA CAG TCC TTA CAG ATG
HpdA(C101S)_s	TCG TCT CGA AGC GTC AAC TCA TGT TAT TAT AAT GCG
HpdA(C105S)_as	TCG TCT CGA GAT GAG TTG ACG CAT TCA AAA CTT TC
HpdA(C105S)_s	TCG TCT CGA TCT TAT TAT AAT GCG TTT AAA TTA TGT GCA AAA CC

2.2 Molecular biology

2.2.1 PCR

PCR strategy to generate mutants

Starting from the sequence of the wild type HpdA, mutational primers were deduced (2.1.5), which generated the desired cysteine to serine exchange and introduced an *Esp3I* cleavage site. For the PCR a plasmid derived primer (SQ_IBA7_s) was incubated with an antisense mutational primer. Likewise a plasmid derived antisense primer (HpdC_dsBamHI_as) was incubated with the sense mutational primer. The two fragments obtained carried the coding sequence of HpdA up to the mutation and ended in an Esp3I site; the second fragment starts with an Esp3I site followed by the mutation and the C-terminal part of the HpdA sequence. The fragments were purified with the Peqlab cycle pure kit, analysed on an agarose gel and triple digested with *Esp3I, Xba1* and *BamH1* (See 2.2.4 and 2.2.5). Since *Esp3I* is an external cutter, this digest removed the *Esp3I* sites from the PCR fragements, leaving sticky overhangs carrying the mutation. Xba1 and BamH1 were used as entry sites into the vector. The digestion was carried out at 37 °C for 1h and repurified with the Peqlab cycle pure kit before ligating the fragments with T4 ligase for 1h at 22 °C. The resulting plasmids were transformed into competent DH5α cells and plated on LB plates containing Carbenicillin (2.2.6). The next day colony PCR was performed using SQ_IBA7_s and HpdC_dsBamHI_as to validate the correct size of the insert. Positive colonies were grown over night in liquid culture. Plasmids were extracted the next day and sequenced to confirm the mutation.

The plasmids thus obtained were further used for heterologe expression of *hpdA* in Rosetta cells. The mutated proteins were purified according to the wild type protocol and analyse for their biochemical behaviour.

Mutational PCR reaction

In this work, the Fusion proofreading DNA polymerase was used for the amplification of target DNA. The composition of individual PCR reactions and the temperature profiles for DNA amplification were as indicated below:

Mutational PCR

Composition of a standard mixture of 100 µl final volume

5x HF buffer	20 µl
10 mM dNTPs solution	2 µl
Primermix 10pmol/µl each (s and as)	5 µl
Template (5ng/µl)	10µl
Polymerase	1 µl
Sterile water	fill to 100 µl

PCR programs used for Fusion polymerase

Initial denaturation:	98 °C	5 min	
Denaturation:	98 °C	10 s	} 29 cycles
Annealing:	58 °C	20 s	
Extension:	72 °C	1 min	
Final extension:	72 °C	5 min	

Colony PCR

Positive colonies were identified by colony PCR. Therefore, individual colonies were picked from the agar and suspended in 10µl sterile water. To this, 15µl of a Colony-PCR premix was added to obtain the following conditions:

Colony PCR (25 µl final volume)

10µl	re-suspended colony
2.5 µl	10x PCR reaction buffer
1µl	Primermix (mixture of HpdC_dsBamHI_as/ SQ_IBA7_s; 10pmol/µl each)
2.5 µl	25 mM $MgCl_2$
0.5 µl	5 mM dNTPs solution
0.1 µl	Taq DNA polymerase (Amersham Pharmacia Biotech)
8.4 µl	sterile H_2O to 25 µl final volume

PCR program used

Initial denaturation:	95 °C	5 min	
Denaturation:	95 °C	45 s	} 35 cycles
Annealing:	58 °C	30 s	
Extension:	72 °C	1 min	
Final extension:	72 °C	10 min	

2.2.2 Plasmid DNA isolation

Plasmid DNA was isolated by using Peqlab Spin Miniprep column according to the supplier's instructions.

5 ml of LB or standard I medium with the required antibiotic(s) was inoculated with bacterial colonies and incubated at 37 °C overnight while shaking. The overnight culture was then harvested by centrifugation. The pellet was re-suspended in 250 µl Buffer I containing RNAse, then lysed by 250 µl Buffer II, and neutralized with 350 µl Buffer III. Precipitates were removed by centrifugation and plasmid DNA was loaded on 2ml high binding columns. The binding was enhanced by washing with 500µl HB buffer; columns were then washed two times with buffer W. The DNA was eluted in 50-100 µl elution buffer or sterile water.

2.2.3 Determination of DNA concentration and purity

DNA concentrations were calculated from the absorption at 260 nm using an absorbance of 1.0 for 50 µg/ml of double-stranded DNA.

$$\text{DNA concentration } (\mu g/ml) = \Delta E_{260} \times 50 \times \text{dilution}$$

2.2.4 DNA gel eletrophoresis

The required amount of agarose was suspended in 1x TAE buffer, boiled in a microwave and cooled to about 55 °C prior pouring onto an object slide or into a mould. After 15-30 min at room temperature, the slot-forming template (comb) was removed gently and the gel was placed in the electrophoresis device and run at 80-100 Volt for 10 - 15 min. The location of DNA was visualised with UV light after staining with ethidiumbromide solution.

2.2.5 DNA restriction and ligation

Unless otherwise stated, restriction digests were performed at 5- to 20- fold over-digestion (e.g. 1 µg of DNA was digested with 10 U endonucleases for 1 h at 37 °C to achieve 10-fold over-digestion). The digested fragments were analysed on agarose gels.
For the HpdA mutants a digest contained the ingredients listed below.
For digesting the PCR product and further ligate it, the following conditions were applied:

Control digest Plasmids

Buffer BamHI	2µl
Plasmid	4µl
BamHI	1µl
Xba1	2µl
H_2O	11µl

Plasmids were digested for 1h at 37 °C and visualized on an agarose gel as described in 2.2.4.

Triple digest of PCR products

Buffer BamHI	5µl
10mM DTT	5 µl
IBA 7 (ca. 100ng/ml)	2 µl
PCR product 1	17.8 µl
PCR product 2	17.8 µl
BamH1	0.5 µl
Xba 1	1 µl
Esp3 1	1µl

PCR fragments were digested for 1h at 37 °C and visualized on an agarose gel and purified with the cycle pure Kit. DNA fragments (16µl) were than re-ligated by incubating 16µl of the aforementioned digest with T4 ligase. 2µl ligase and 2µl buffer for 1h at 22 °C.

2.2.6 Construction of the plasmids for sequencing and protein expression

Construction of expression plasmids

Genes inserted *in frame* with the N-terminal Strep-tag II in the pASK-IBA7 vector are expressed under control of the tetracycline promotor/operator. The strength of the tetA promoter is comparable to that of the lac-UV5 promoter, and it is fully induced by the addition of anhydrotetracycline at a concentration that is not yet antibiotically effective (94). The genes were ligated into the *XbaI*/*BamHI* sites of an empty IBA 7 expression vector. The expression plasmids were named according to table 6.

table 6 List of HpdA mutants

Name	Description
C60->S	Point mutation changing cysteine 60 to serine
C66->S	Point mutation changing cysteine 66 to serine
C69->S	Point mutation changing cysteine 69 to serine
C73->S	Point mutation changing cysteine 73 to serine
C93->S	Point mutation changing cysteine 93 to serine
C96->S	Point mutation changing cysteine 96 to serine
C101->S	Point mutation changing cysteine 101 to serine
C105->S	Point mutation changing cysteine 105 to serine
SAM	Point mutations changing all three cysteines of the SAM cluster (34,38,41) to serines
Ia	Point mutations changing all four cysteines of the Ia cluster (60,66,69,73) to serines
Ib	Point mutations changing all four cysteines of the Ib cluster (93,96,101,105) to serines
SAM only	Point mutations changing all cysteines of the Ia and 1b cluster (60,66,69,73,93,96,101,105) to serines
Ia only	Point mutations changing all cysteines of the SAM and 1b cluster (34,38,41,93,96,101,105) to serines
Ib only	Point mutations changing all cysteines of the Ia and SAM cluster (34,38,41,60,66,69,73) to serines

2.2.7 Transformation of chemically competent cells

Chemically competent cells were used for the generation of expression strains for production of recombinant proteins and for the amplification of plasmid DNA. The transformation of Rosetta (DE3) single™ chemical competent cell and the subcloning efficiency DH5α™ chemically competent *E. coli* cells was performed according to the manufacturers instructions.

2.2.8 DNA sequencing

Custom sequencing of DNA molecules (PCR products and vectors) were performed by MWG-Biotech, Ebersberg. Standard vector-derived primers and internal primers were used for the complete sequencing of DNA templates using dye-terminator chemistry. In order to exclude DNA polymerase-derived mutations, three different clones from three different PCRs were double-stranded sequenced.

2.3 Biochemical Methods

2.3.1 Gene expression and protein purification

Recombinant proteins were produced in *E. coli* BL21 (DE3) Codon Plus-RIL™ or Rosetta (DE3) pLysS™ cells, which were transformed with the individual expression plasmids and kept under selection with 50 µg/ml carbenicillin and 34 µg/ml chloramphenicol during growth. Unless otherwise stated, all cultures were grown aerobically and aerated by constant shaking.

Initially, 250 ml of LBG medium was inoculated with freshly isolated colonies from LB agar plates and grown over night at 37 °C. This pre-culture was used to inoculate 1.5 – 2.0 L of medium (HpdA 22 °C; HpdBC 28 °C). The cells were grown to OD_{578nm} of 0.8-1.0, then 30 – 40 ml ethanol was added (2% final) and the culture was allowed to grow another 30 min prior to induction by anhydrotetracycline (AHT) (50ng/ml HpdA, 100ng/ml HpdBC), and typically harvested 3 h post-induction, washed with TBS and frozen at –80 °C.

2.3.2 Solutions for Protein purification

Basic buffer Decarboxylase

100mM	TRIS-HCl, pH 7.5
150mM	NaCl
5mM	$(NH_4)_2SO_4$
5mM	$Mg\,Cl_2$
5mM	Dithiothreitol (freshly added before use)
	Water up to final volume

Basic buffer Activator

100mM	TRIS-HCl, pH 8.5
150mM	NaCl
5mM	$(NH_4)_2SO_4$
5mM	Mg Cl_2
50mM	Arginine
50mM	Glutamine
5mM	Dithiothreitol (freshly added before use)
	Water up to final volume

Opening Buffer

100ml appropriate Basic buffer (DTT added)

500µM	ATP
5mM	Cysteine
250µM	Iron (NH4)Fe (II)SO4
100µl	DNAse/RNAse (50mg/ml)
15µl/g cells	Avidin (5mg/ml stock)

Elutionbuffer

Basic buffer containing 2 mM Desthiobiotin.

Regeneration Buffer

100mM	TRIS-HCl, pH 7,5
150mM	NaCl
1mM	HABA

2x Activation-/Assay-buffer

200mM	TRIS-HCl, pH 7.5
300mM	NaCl
10mM	$(NH_4)_2SO_4$
10mM	Mg Cl_2

Titanium (III) Citrate

100µl of a 1 M Na_3-Citrate solution were mixed with 50µl of $Ti(III)Cl_3$ in 850µl water and neutralized by the addition of solid Na_2CO_3. This stock solution was freshly prepared every week.

F420

F420 was a generous gift of Rainer Hedderich. The lyophilised powder was resuspended in anaerobe water to give 50mM final concentration. Aliquots were frozen at -20 °C in air tight HPLC vials wrapped with aluminium foil to prevent light damage.

SAM

SAM was anaerobically dissolved in basic buffer decarboxylase to give a 10 mM stock solution and stored at -20 °C in 100µl aliquots. Each aliquot was thawed only once.

All buffers were filtered, boiled in rubber-stoppered flasks and stirred over night in an anoxic chamber.

2.3.3 Protein purification

Unless otherwise stated, all protein purification steps were performed in an anoxic chamber (Coy Laboratoroes, Ann Arbor, MI, USA) with a N_2/H_2 (95 %/5 %) atmosphere at 15-20 °C.
The decarboxylases were typically purified from ~5.0-20.0 g of wet packed cells. The cells were initially suspended in 20 to 60 ml anoxic buffer decarboxylase (100 mM Tris/HCl, pH 7.5, 150 mM NaCl, 5 mM $(NH_4)_2SO_4$, 5 mM $MgCl_2$, 5 mM DTT) supplemented with 0.2 mM $Fe(NH_4)_2(SO_4)_2$, 5 mM L-Cysteine-HCl, 5 mM ATP, 50 µg/ml DNase/RNase and Avidin according to cell mass. The cell suspension was sonicated at 50 W, for 10 min with a Branson sonifier (Branson Ultrasonics, Danbury, CT, USA) under cooling with ice-H_2O in Rossetta flasks. Cell debris and membranes were removed by centrifugation for 60 min at 100,000 x *g* at 18 °C. The clear supernatant was then loaded on 5 ml Streptactin macroprep™ columns. The columns were washed with 3-5 column bed volumes buffer decarboxylase and bound target proteins were eluted in buffer BC containing 2-2.5 mM Desthiobiotin.
The activating enzymes (AEs) were purified accordingly in buffer activator (100 mM Tris/HCl, pH 8.0, 150 mM NaCl, 5 mM $(NH_4)_2SO_4$, 5 mM $MgCl_2$, 50 mM arginine, 50 mM glutamate, 100 mM NaOH, 5 mM DTT). However, significant losses of recombinant AEs

during the washing of the columns was observed and the washing volume was therefore reduced to 3 column bed volumes in AE purifications.

The resulting preparations were concentrated in Vivaspin™ concentrators of appropriate cut-offs (100 kDa for decarboxylases, 10 kDa for activating enzymes) to final concentrations > 5 mg/ml and stored in suitable aliquots in gas tight sealed HPLC sample flasks at –20 °C.

2.3.4 Determination of protein concentrations

The absolute concentration of pure enzymes was calculated from the absorbance at 280 nm in 4 M guanidinium hydrochloride in 0.1 % trifluoroacetic acid. Under these conditions, the iron sulfur clusters of the proteins were destroyed and did not interfere with the measurements. The molar absorbance coefficients and the equivalence values for 0.1 % [w/v] solutions are summarized in table 7.

table 7 The molar absorption coefficients and the absorbance values for 0.1% [w/v] solutions of the individual proteins

Enzyme	Extinction coefficient at 280 nm (units of M^{-1} cm^{-1})	Abs 0.1% (=1 g/l):
HpdA	50070	1.306
HpdBC	135410	1.195
CsdA	56470	1.565
CsdBC	150060	1.329

To correct for the background the flow through of the spin concentrator and the concentrated enzyme were kept separately. To 0.5 ml guanidine HCl solution, 10 µl of the flow through were added, mixed and the $E_{280\ (ft)}$ was read. Then, 10µl of the purified protein solution was added and the value $E_{280\ (pr)}$ was measured. The final protein concentration was calculated according to C_{pr}= (($OD_{280\ (pr)}$*520/10)-(2*$OD_{280\ (ft)}$*510/10))/ε. The molar extinction coefficient ε was determined aided by the Biology Workbench (http://workbench.sdsc.edu/). For the mutants the wild type extinction coefficient was used.

2.3.5 Sodium dodecylsulfate-polyacrylamide gel electrophoresis (SDS-PAGE)

The polyacrylamide was cast as a separating gel topped by a stacking gel and secured in a BioRad electrophoresis apparatus, Mini Protein II, (Heidelberg, Germany). The solution for one gel was prepared as in table 8:

table 8 Protocol for SDS-PAGE gel preparation:

	15%	**12,5%**	**8%**	**6%**	
Bidest.H_2O	540	1.040	650	780	in µl
Tris-HCl pH 8,8	2.250	2.250	-	-	in µl
Tris-HCl pH 6,8	-	-	750	750	in µl
30% Acrylamid/Bis-acrylamide	3.000	2.500	530	400	in µl
10% SDS	60	60	20	20	in µl
5% TEMED	60	60	20	20	in µl
10% APS	90	90	30	30	in µl
	6 mL	6 mL	2 mL	2 mL	

Electrophoresis running buffer	0.3 % (w/v)	Tris
	1.44 % (w/v)	Glycine
	0.1 % (w/v)	SDS

Protein loading buffer	125 mM	Tris, pH 6.8
	4 % (v/v)	Glycerol
	0.1 % (w/v)	Bromophenol blue
	10 mM	DTT (added just before use)

The molecular mass marker used in this study was the unstained Precision Plus Protein Standard (Bio-Rad) (the marker size is 250, 150, 100, 75, 50, 37, 25, 20, 15 and 10 kDa). The protein samples were mixed with protein loading buffer (+ 10 mM DTT) and incubated at 95 °C for 5 -10 min prior loading to the gel. The electrophoresis was performed at a constant voltage of 200 V till the tracking dye reached the bottom of the gel (usually 1h). Then the gel was disassembled and the proteins were stained with Coomassie Brilliant Blue.

2.3.6 Iron sulphur determination

The protocol has already been published elsewhere and should just be mentioned here shortly (95). For the Iron determination, the protein solution was acidified with HCl, neutralized with ammonium acetate and the protein solubilized with SDS. Ascorbic acid was used to reduce all iron to the +II state and iron was detected with a fresh solution of Feren. As iron standard freshly prepared solution of 0.2 mM $(NH_4)_2Fe(SO_4)_2$ x $6H_2O$ (Mohr's Salt) was used (0 to 20 µM $[Fe^{2+}]$ final). The E_{593nm} was measured and the iron content was determined from absorbance plots vs. iron concentrations.

Likewise the acid labile sulfide was determined according to (95) with N, N'-dimethyl-p-phenylenediamine (DMPD). Sulfide stock solutions (2 mM) were prepared from dried crystals of Na_2S x 9 H_2O in 10 mM NaOH under a N_2 inert atmosphere. Iodometric determination of the sulfur standard was carried out to verify the standard concentration.

2.3.7 Size exclusion chromatography

The native molecular masses of the individual decarboxylases and of the AEs were determined by size exclusion chromatographies in purification buffer on a Superdex200 (HR 1.0 / 10) column (Pharmacia, Freiburg), which was calibrated with appropriate molecular mass standard proteins.

2.3.8 UV-visible spectra

UV/vis spectroscopy of the recombinant enzymes was carried out in rubber-stoppered quartz cuvettes with a Hewlett-Packard P 8453 diode array photometer. Freshly purified enzymes (2.5 µM Csd and Hpd, 5 µM HpdA, 10 µM CsdA) were measured in the respective anoxic purification buffer. To reduce the samples sodium dithionite (1mM final) was added via a gas tight syringe. Bleaching was allowed to proceed for 1 h.

2.4 Enzyme activity assays

2.4.1 Activation

The activation was performed by mixing the decarboxylase (0.2-4mg/ml) with a four fold molar excess of its appropriate activating enzyme (0.27-5mg/ml) in buffer A (100 mM Tris-HCl pH 7.5, 150 mM NaCl, 5 mM $MgCl_2$, 5 mM $(NH_4)_2SO_4$, 5 mM cysteine, and 5 mM DTT). As reducing power the mixture was supplemented with Titanium-(III)-citrate plus sodium sulfite (each 2.5mM final), sodium dithionite (1mM final) or F420 (50µM final) and glycine (50mM). After pre-reduction of 5-30 min at 30 °C the activation process was started by adding S-adenosylmethionine (SAM) (250µM final). At different time points samples were withdrawn and tested for 1) 5'-deoxyadensoine (HPLC: 2.4.4) 2) glycyl radical signals (EPR: 2.4.6) or 3) cresol formation (2.4.3).

2.4.2 Photoreduction

If F420 was used as reducing power the reduction was initiated by light. The samples were filled in HPLC glass vials (if needed equipped with a 300µl glass inlay) and placed in front of a 25W Slide projector. The distance to the light source was 20cm. If needed the activation

reaction could be paused by wrapping the probe with aluminum foil and restarted by re-illumination. Note, that with this setting it was not possible to guarantee a stable temperature. For short time experiments (up to 30 min activation) the temperature effect on the activation was neglectable. For some long time experiments the illumination was carried out in a water bath, which kept the temperature at 18 °C. Activation under theses conditions was slightly slower than at 30 °C.

2.4.3 Enzyme Activity

The activity of the decarboxylase was measured taking aliquots of the above mentioned activation mixture at different time points and diluting it 20 - 50 fold in buffer A containing 25 mM 4-Hydroxyphenylacetate as substrate and 1mM dithionite or a mixture of glucose (0.3%), glucose-oxidase (20µg/ml) and catalase (2µg/ml) as oxygen protection system. After incubation for 10 min at 30 °C the reaction was stopped by adding half a volume of 10% perchloric acid. Previous to HPLC measurements the samples were neutralized with half a volume 10% $KHCO_3$ (containing 3mM phenol as internal standard) and centrifuged at 13,000 rpm for 15-30 min to remove the denatured protein and potassium perchlorate.

2.4.4 Reverse-phase HPLC separation of the aromatic compounds

The analysis of the formation of *p*-cresol was performed using a LiChroCART^{TM} 250 x 4 mm HPLC cartridge (Merck, Darmstadt) filled with LiChrospher^{TM} 100 RP-18 (5 µm) and operated at a flow rate of 2 ml·min^{-1} at 50 °C. The eluent contained 0.1 % (v/v) trifluoroacetic acid in 30 % acetonitrile/water. Aromatic compounds were monitored at 275nm.

The concentration of cresol was calculated by comparing the peak intensities of phenol and cresol with a standard solution of 4-HPA, phenol and cresol (500µM each) freshly prepared from a 10mM methanol stock. To determine the specific activity the dilution factor (two) the protein concentration in the assay as well as the assay time were included.

2.4.5 5'-deoxyadenosine detection

To quantify the activation process in more detail the turnover of SAM to 5'-deoxyadenosine was monitored by HPLC. The activating enzyme (0.54mg/ml) was incubated in buffer A (100 mM Tris-HCl pH7.5, 150 mM NaCl, 5 mM $MgCl_2$, 5 mM $(NH_4)_2SO_4$, 5 mM cysteine, and 5 mM DTT) either alone or (to mimic the activation and assay conditions) in the presence of decarboxylase (1.6 mg/ml) or decarboxylase and HPA (25mM). Reduction was performed at 30 °C by applying titanium-(III)-citrate plus sodium sulfite (2,5mM final), sodium dithionite

(1mM final) or F420 (50µM final) and glycine (50mM) as reducing power. The reaction was started by adding 250µM SAM. At different time points 50µl were withdrawn and mixed with 50µl 10% TFA containing 30µM adenosine as internal standard. The denatured protein was removed by centrifugation at 13,000 rpm for 30 min.

5'-deoxyadenosine was detected by developing a LC-DABS cartridge with a gradient of 2-20% acetonitrile in 20mM TAE pH 7.5 and monitoring at 259nm. The amount reached was calculated by comparing the peak intensities with a standard solution containing adenosine, S-adenosylmethionine, S-adenosylhomocysteine, 5'-deoxyadenosine and 2'-deoxyadenosine (30µM each).

2.4.6 EPR Spectroscopy

EPR spectra at X-band were obtained with a Bruker ESP-300E EPR spectrometer equipped with an ER-4116 dual mode cavity and an Oxford Instruments ESR-900 helium-flow cryostat with an ITC4 temperature controller.

Sample preparation for EPR Spectroscopy

Various samples were analysed by EPR spectroscopy. Suitable activity tests were performed in order to confirm functionality of enzymes. In an anaerobic glove box (atmosphere of 95 % N_2 and 5 % H_2), 250 - 300 µl of an activation mixture (2.4.1) were transferred to EPR tubes. Anaerobic tubing was placed over the end of each EPR tube and closed. The EPR tubes were removed from the glove box and immediately frozen in liquid nitrogen prior to analysis by EPR spectroscopy.

For the Fe-S cluster detection, the low temperature experiments were carried out in liquid helium. Unless otherwise stated, EPR experiments were carried out in 100 mM Tris/HCl, pH 7.5, 150 mM NaCl, 5 mM $(NH_4)_2SO_4$, 5 mM $MgCl_2$, 5 mM DTT using 25 µM decarboxylases (4mg/ml) and 100 µM activator (5mg/ml). When required, the samples were pre-reduced with 1 mM sodium dithionite for 30 min at 30 °C and subsequently activated with 0.25 mM SAM at 30 °C for 5 min prior to freezing in liquid nitrogen.

Additional X-band EPR spectra for the glycyl radical signal were recorded in liquid nitrogen.

2.4.7 Redox titration

The redox titration was carried out in the group of Rainer Hedderich in the MPI Marburg. All experiments were performed in an anaerobe atmosphere. The decarboxylase (0.6mg/ml) was provided in the normal assay buffer (100 mM Tris/HCl, pH 7.5, 150 mM NaCl, 5 mM

$(NH_4)_2SO_4$, 5 mM $MgCl_2$) containing a mix of 14 redox-dyes (100µM final prepared from 20 mM stocks) in a final volume of 9ml. The redox-dyes are: 1,4- benzoquinone (274mV), 1,2-naphtoquinone-4-sulfonate (215mV), 1,2-naphtoquinone (134mV), duroquinone (86mV), 1,4-naphtoquinone (69mV), methylene blue (11mV), indigo-disulphonate (-125mV), 2-hydroxy-1,4-naphtoquinone (-145mV), anthraquinone-1,5-disulphonate (-170mV), phenosafranin (-252mV), safranin O (-289mV), neutral red (-325mV), benzyl viologen (-350mV) and methylviologen (-453mV).

The experiment is performed by titrating the sample in the reductive direction with a stock solution of 20 mM sodium dithionite (10-20µl shift ca. 50mV). The sample was continuously stirred until equilibrated at the desired potential. 250µl aliquots were withdrawn and placed in an EPR tube and immediately frozen out of the tent. EPR measurements were performed as previously described. Since the experiment was performed using an Ag/AgCl reference electrode the measured values were corrected for a factor of +197mV.

3 Results

The 4-hydroxyphenylacetate decarboxylase (Hpd) catalyses the last step in tyrosine fermentation by *C. difficile,* the decarboxylation of 4-hydroxyphenylacetate to the cytotoxic end product *p*-cresol (4-methylphenol). In previous work by Dr. Paula I. Andrei and Dr. Lihua Yu, a recombinant expression-system for individual constituents of the three known 4-hydroxyphenylacetat decarboxylase systems was established and kindly provided for this work. Altogether the HPA decarboxylases form a new subfamily of the glycyl radical enzyme family.

The HPA decarboxylase subfamily is characterized by a small subunit, which is necessary to form the activation competent and catalytically active hetero-octameric decarboxylase complex ($\beta_4\gamma_4$). The small subunit also provides binding of two iron-sulfur centers by 4-hydroxyphenylacetate decarboxylases. The decarboxylases and benzylsuccinate synthase (Bss) are the only iron-sulfur proteins among GREs. Hpd as well as Csd contain 32 iron and 32 sulfur per hetero-octamer, suggesting binding of two metal centers by each small subunit. EPR- and UV-visible spectroscopy gave evidence that only $[4Fe\text{-}4S]^{+1/+2}$ centers are present. It should be noted that the iron sulfur content of the Tfd system is significantly lower (around 8 iron / sulfur per hetero-tetramer) suggesting the binding of only one cluster per dimer.

Likewise, the monomeric activating enzymes contain on average 8 irons and 8 acid-labile sulfurs per molecule. Thus, the metal contents of the decarboxylase activating enzymes are significantly larger than previously reported for Pfl- or Nrd-AEs, which exclusively contain the SAM cluster close to the N-terminus of the enzymes.

The additional cofactors of HPA decarboxylases have been suggested to be involved in the highly complex regulation of the enzymes. The regulation effects radical formation and dissipation but also the enzyme activity in response to external triggers, which might be necessary to control *p*-cresol formation beyond the catalytic processes involved. Whereas the glycyl radical can persist anaerobically for several hours in Pfl (1), it is comparably unstable in HPA decarboxylases when substrate is missing. After an initial accumulation of the radical, a slow decline in its intensity was observed. The radical dissipation correlates with loss of enzyme activity. In particular two exciting features of GRE decarboxylases were addressed in this work: 1) The radical formation, which is catalyzed by the cognate AEs and involves two iron-sulfur centres, which are not found in Pfl- and Nrd-AEs, but likely shared with many other GRE-AEs (96). 2) The radical dissipation, which is an intrinsic property of the decarboxylases itself and has been suggested to be most likely mediated by the iron-sulfur centers ligated by the small subunits of 4-hydroxyphenylacetate decarboxylases.

For better understanding of these features and in order to elucidate possible function in regulation of glycyl radical enzymes, biochemical, spectroscopic, and structural parameters of the system were collected. In particular, the activation process (generation of the glycyl radical in Hpd by its cognate activating enzyme, SAM and reducing agent) was uncoupled from the activity measurements (cresol formation by activated Hpd). A HPLC-based method for quantification of SAM turnover to 5'deoxyadenosine and methionine was established, which allowed a quantitative measurement of the activation process. Site–directed mutageneses aimed the identification of iron-sulfur cluster ligands in the decarboxylases and the AEs.

Likewise, the previously mentioned dissipation of the glycyl radical was studied in more detail, supporting that this process is mediated by the decarboxylase alone. To further characterize the involvement of the iron-sulfur clusters of the small subunit in this process, mutational studies were carried out. These studies were guided by the newly available crystal structure of CsdBC, which was solved in collaboration with Prof. Dr. Holger Dobbek and Dr. Berta Martins. The details of this structure will also be described in this work.

3.1.1 The metal centers in Hpd

Recombinant GRE decarboxylases and their cognate AEs exhibited a clearly visible brownish color, indicating the presence of iron-sulfur centers in both, decarboxylases and activating enzymes. This notion was further supported by UV/visible spectroscopy, chemical determinations of non-heme iron and acid-labile sulfur, and EPR measurements (50).

table 9 Physical-chemical properties of the recombinant proteins. The iron content of various (n from 5 to 11) individual preparations (minimum-average-maximum) is given per native structure.

Protein	Native molecular mass	Oligomeric state	Irons per native molecule
Csd-AE	37 kDa	α	5-**7.2**-9
Hpd-AE	38 kDa	α	6-**8.5**-11
Csd	440 kDa	$\beta_4\gamma_4$	26-**31**-32
Hpd	445 kDa	$\beta_4\gamma_4$	28-**29**-32

According to size exclusion chromatography, recombinant Hpd and its homologue from *C. scatologenes* were hetero-octameric ($\beta_4\gamma_4$) proteins and contained 30-32 irons and 28-32 acid-labile sulfurs (table 9). The oxygen sensitive recombinant activating enzymes were monomeric proteins with molecular masses of about 37 kDa and contained on average 8 irons and 8 acid-labile sulfurs per molecule. Thus, the metal content of decarboxylase AEs was significantly larger than the metal content of Pfl- or Nrd-AEs, exclusively containing the SAM cluster with 4 irons and 4 sulfurs.

UV-visible spectroscopy revealed broad charge transfer signals between 300-800 nm without fine structure, which partially bleached upon dithionite reduction. This suggests that only $[4Fe\text{-}4S]^{+1/+2}$ centers were contained. The molar extinction coefficients at 400 nm suggested presence of up to 8 clusters per heteo-octamer in Hpd (56 ± 6 $mM^{-1}cm^{-1}$) and Csd (48 ± 5 $mM^{-1}cm^{-1}$), and 2-3 in the cognate monomeric AEs (11± 3 $mM^{-1}cm^{-1}$ for Hpd-AE and 17 ± 5 $mM^{-1}cm^{-1}$ for Csd-AE) (figure 6).

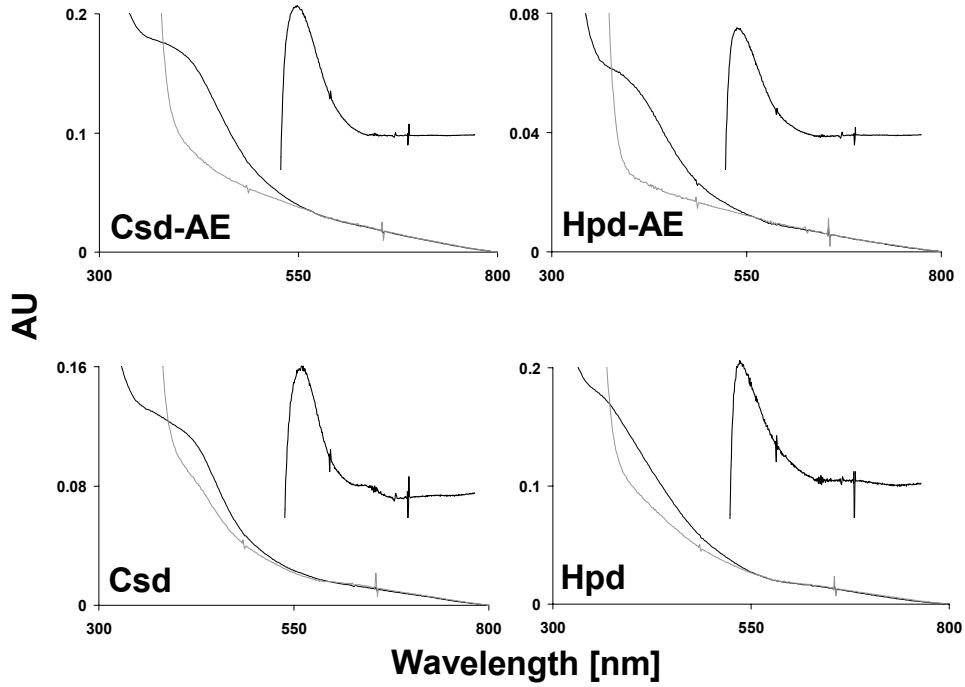

figure 6 UV-visible spectra of the decarboxylases and their cognate AE. Freshly purified enzymes (2.5 µM Csd and Hpd, 5 µM HpdA, 10 µM CsdA) were measured in the respective anoxic purification buffer (black lines). Reduction with sodium dithionite (1mM) for 1 h at room temperature partially bleached the absorbance (grey lines). The insets show the difference spectra between the freshly purified and the dithionite-reduced samples.

3.1.2 EPR spectroscopy of the HPA-decarboxylase systems

The metal centers in the AEs and in the decarboxylase of the Hpd and Csd systems were initially characterized by EPR spectroscopy at low temperature. For these measurements, series of individual samples were prepared and subsequently analyzed by X-band EPR in order to establish properties of the individual constituents of the systems and also to obtain initial indications for interactions between individual paramagnetic centers throughout the activation process.

The purified activating enzymes were entirely silent in EPR (data not shown). Since [3Fe-4S] in the oxidized stated would yield EPR signals, there is no evidence from this

measurements for cluster decay. However, upon reduction with sodium dithionite axial S = ½ EPR signals with g_x = 2.04 and g_y = 1.94 were obtained. These signals are characteristic for spin 1/2 systems, while no additional signals indicating high-spin clusters (spin 3/2) were detectable. The temperature-dependence of the signal clearly showed that these signals arose predominantly from $[4Fe\text{-}4S]^{+1}$ clusters. The detection of very poor signals remaining at higher temperatures suggested that only negligible $[2Fe\text{-}2S]^{+1}$ clusters were present in the samples. Although the overall appearance of the EPR signals and the g-values were similar for HpdA and CsdA, there were also clear differences. The HpdA EPR was significantly broader and less intense than the signal observed for CsdA. Spin integration showed 0.2-0.3 reduced [4Fe-4S] centers, suggesting that only 7-15% of the total 2-3 iron-sulfur centers were reduced.

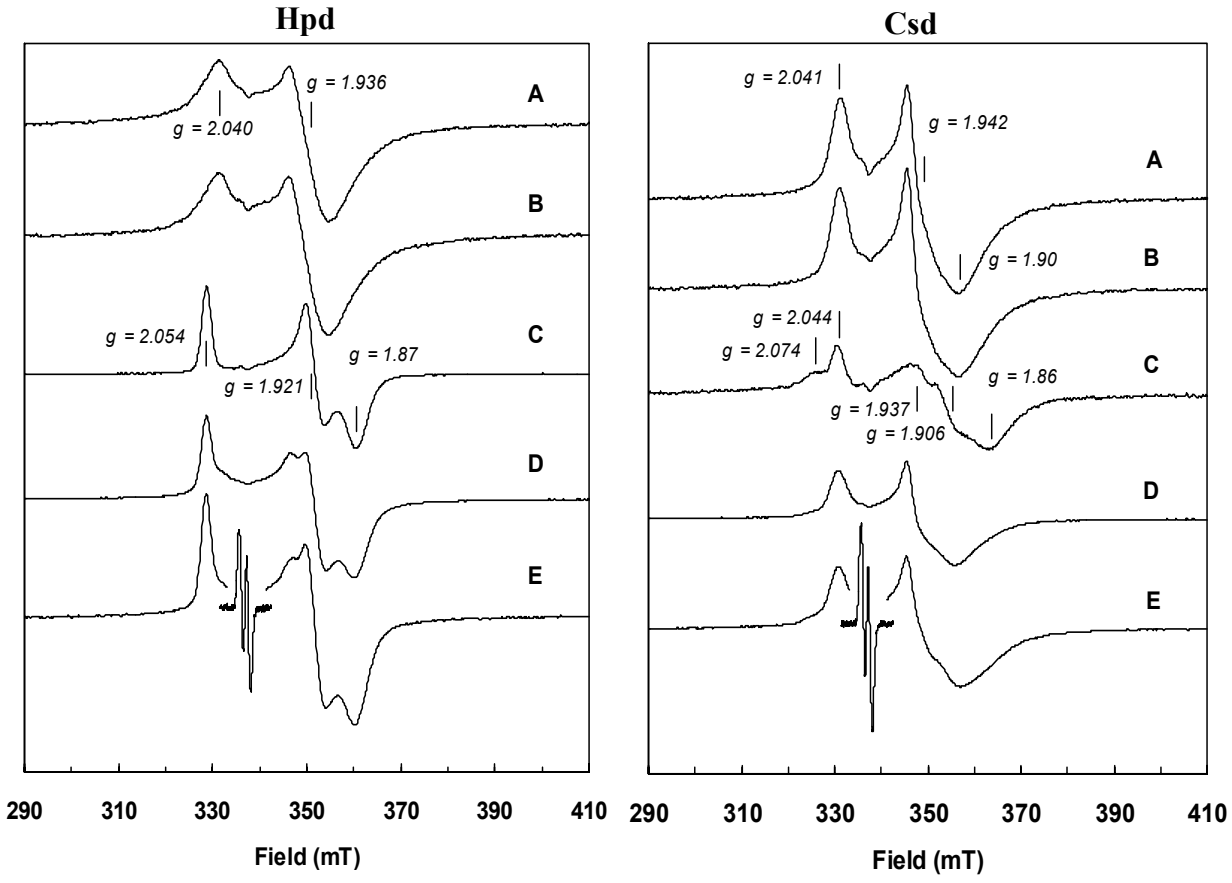

figure 7 EPR spectra of the *p*-hydroxyphenylacetate decarboxylase systems from *C. difficile* (left) and *C. scatologenes* (right). Trace A, HpdA/CsdA (5 mg/ml) in buffer A plus 1 mM dithionite, reduced at 30 °C for 30 min; Trace B, as the samples in trace A plus 0.25 mM SAM for 5 min; trace C, 4 mg/ml HpdBC/CsdBC in buffer A plus 1 mM dithionite (trace C in Csd was enlarged 2-fold), reduced at 30 °C for 30 min; Trace D, 4 mg/ml HpdBC/CsdBC and 5 mg/ml HpdA/CsdA in buffer A plus 1 mM dithionite, reduced at 30 °C for 30 min; trace E, the sample was treated as in trace D, then SAM was added to 0.25 mM. After 5 min incubation, sample was frozen for EPR measurement (the central part with the very intense glycyl radical signal was saturated and therefore the inset has been recorded with different settings). Spectra were recorded at 10 K (60 K for the inset of trace E); microwave power, 0.8 mW (0.13 mW for the inset of trace E); microwave frequency, 9.459-9.460 GHz; modulation frequency, 100 kHz; modulation amplitude, 1.25 mT (0.45 mT for the inset of trace E).

Interestingly, there were virtually no changes in the appearance of the EPR signal of HpdA upon addition of SAM. The CsdA spectrum also showed only minor changes, predominantly a small increase in signal intensity rather than the expected changes in line shape, which have been reported for other GRE-AEs to occur when SAM binds to the SAM-cubane.

The EPR of reduced Hpd showed intense rhombic signals with g-values of 2.054, 1.921, and 1.87, which integrated to 2.9 spins/(β4γ4). In Csd, a mixture of two rhombic species with gx = 2.074/2.044 and gy = 1.937/1.906, and g_z ca. 1.86 were found, which integrated to 1.3 spins/($\beta_4\gamma_4$). These signals broadened out above 30 K, supporting the $[4Fe\text{-}4S]^{+1/+2}$ centers indicated by UV-visible spectroscopy. From these data it can already be anticipated, that only one of the two clusters is redox active.

Since the purified decarboxylases already exhibit a signal for a reduced [4Fe-4S] cluster, it may be suggested, that either the redox potential is quite high and a reduction by DTT might cause partial reduction, or that these clusters are very stable in the reduced state and, therefore, purified from *E. coli* in the reduced form. To further elucidate this, redox-titration experiments were carried out with both decarboxylases using a number of redox dyes as mediator. Since it was known that Csd is only partially reduced (compare figure 7 c), it was applied twice as concentrated (1.2mg/ml) as Hpd (0.6mg/ml); still the signal to noise ratio did not allow to determine the redox potential. For the cubanes in Hpd, however, only a single midpoint potential of around -287 ± 4 mV was determined (figure 8). This is rather surprising since two clusters are predicted for Hpd, which could not be differentiated in this experiment. Either both clusters exhibit a very similar redox-potential, or only one of the clusters can be reduced. A notion that could be further supported by the hybrid-constructs described later on.

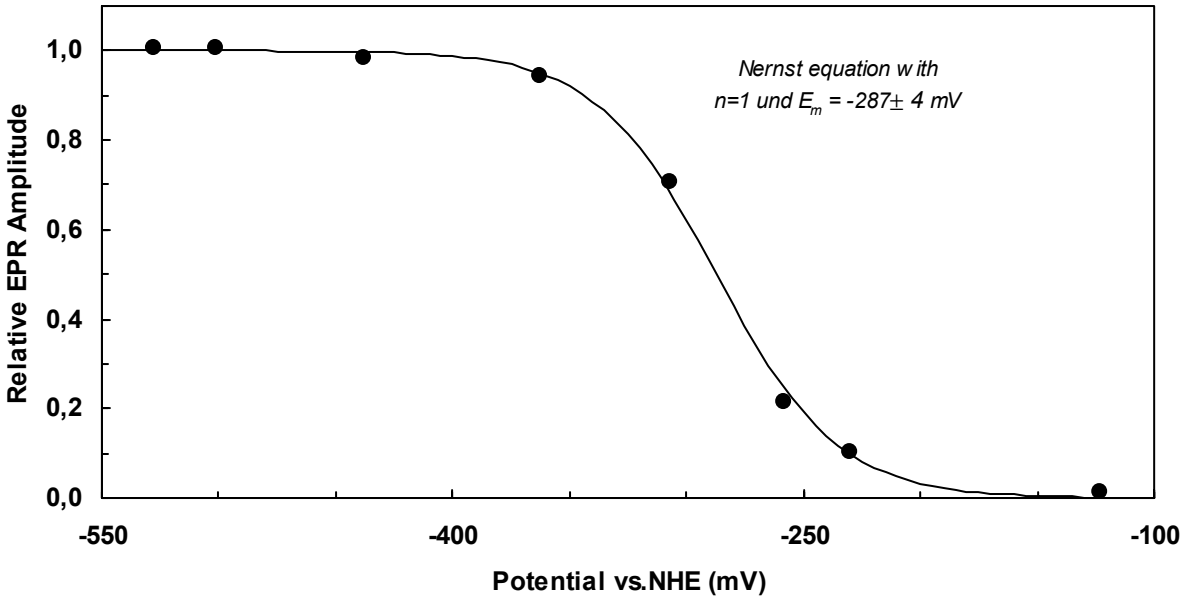

figure 8 Redox titration of Hpd. To determine the mid point potential of the $[4Fe\text{-}4S]^{+2/+1}$ clusters in the decarboxylase, 0.6mg/ml Hpd were mixed in a buffer containing several redox dyes. The sample was completely reduced by addition of Dithionite and re-oxidized by ferrycyanid. Glycylradical signals were collected at the depicted redox states. The values were collected against an Ag/AgCl electrode and corrected to fit N.H.E.

When the decarboxylases were reduced in presence of their cognate activating enzymes, the resulting EPR spectra showed features expected from a summation of those spectra obtained for the individual enzymes. Since there were only minor changes in the overall appearance of the iron-sulfur center spectra, there is no clear indication for magnetic interaction between the individual clusters or any of the clusters with the glycyl radical. A quantitative analysis of minor changes was not possible at present and must await the characterization of the clusters in the individual proteins by Mössbauer-spectroscopy.

3.2 The crystal structure of Csd

A big step in understanding the complex regulation of arylacetate decarboxylases on a molecular level was the elucidation of the CsdBC crystal structure. In co-operation with Prof. Dr. Holger Dobbek and Dr. Berta Martins from the University of Bayreuth, the crystal structure of non-activated Csd was solved at 1.8 Å resolution. Not only did the data confirm the hetero-octameric nature of the catalytically competent complex, but it also exemplified for the first time the three-dimensional structure of the small subunit and confirmed the metal binding properties of this protein. As a third finding a different binding mode of the substrate HPA was deduced from soaking experiments and is currently investigated in our laboratory. Additionally, the structural information was used to generate specific mutants. Besides the constructs with an altered binding mode of the metal centers, which are partially presented in this work, mutants with changed residues in the complex interfaces as well as in the putative electron-channel, connecting the active site glycyl radical with the redox active (radical quenching) cluster of the small subunit, are on the way.

3.2.1 Crystallization

The Csd decarboxylase was crystallized under strictly anoxic conditions (atmosphere of 95% N_2 and 5% H_2, with a palladium catalyst and oxygen sensor) in an anaerobic chamber (Coy Laboratory Products, Ann Arbor, USA). First crystallization conditions were obtained by the sitting drop vapour diffusion method at 16 °C by mixing 2µl of protein solution (~ 40mg/ml in 100mM Tris-HCl pH 7.5, 150mM NaCl, 5mM $(NH_4)_2SO_4$, 5mM $MgCl_2$, 5mM DTT and 2mM Desthiobiotin) plus 2µl of precipitant (Index Screen, Hampton Research, Aliso Viejo, USA).

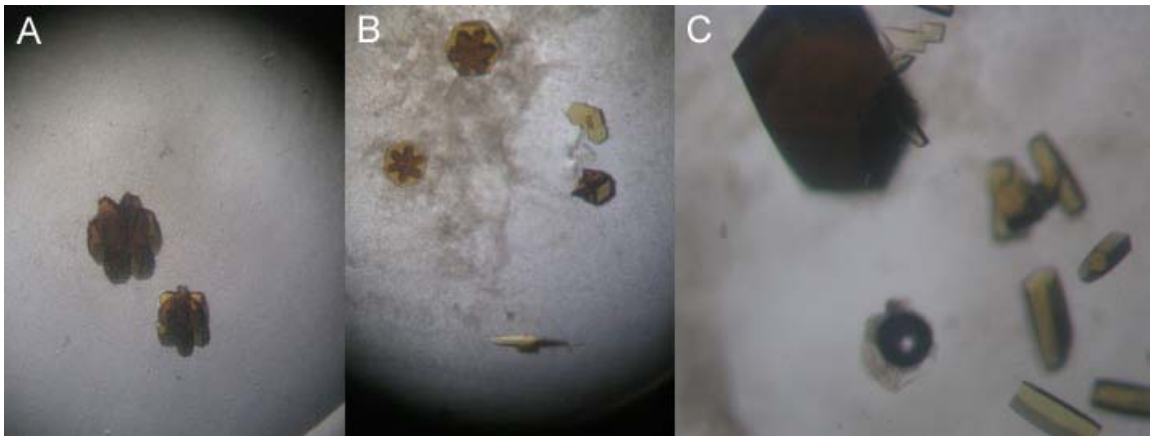

figure 9 Crystals of CsdBC grown in the presence of PEG MME 550, $MgCl_2$, Tris/HCl pH 7.5-8.4. (A): 22% PEG MME 550, 30mM $MgCl_2$, pH 8.0; (B): 22% PEG MME 550, 100mM $MgCl_2$, pH 7.5; (C): 21% PEG MME 550, 20mM $MgCl_2$, pH 8.0.

Optimization grid screens resulted in the growth of elongated plate-shaped crystals in 15-20% PEG 3350 and 100-250mM DL-malic acid pH 7.0 within 2-3 weeks. After optimizing the crystallization conditions flower-like and well-shaped hexagonal crystals grow within 1-2 weeks displaying dark yellow/brown colour (figure 9).

For diffraction quality tests at 100K, the crystals were harvested in a cryo-protectant solution (precipitant supplemented with PEG MME 500) and frozen in a nitrogen stream (Oxford Cryosystems, Oxford, UK). Diffraction tests were performed using an in-house Nonius FR591 X-ray rotating anode generator providing CuKα radiation (λ=1.5418 Å) (Bruker AXS, Karlsruhe, Germany) coupled to a mar345dtb image plate detector system (Marresearch, Norderstedt, Germany). The diffraction pattern displayed a maximum resolution of around 2 Å and a complete dataset was collected. The crystals belong to the orthorhombic crystallographic system $C222_1$ with cell constants of a = 133 Å, b = 227 Å, c = 148 Å and $\alpha = \beta = \gamma = 90°$.

To determine the crystal structure, first Molecular Replacement was performed with the available coordinates of glycerol dehydratase (59). Second, the phases of the replacement solution were used to locate the [4Fe-4S] centres in anomalous difference Fourier maps. In total, 16 individual Fe ions (from 4 [4Fe-4S] centres per asymmetric unit) were used for SAD phasing using in-house dataset to a resolution of 1.8 Å. Phases from the SAD measurement were used for automatic model building with ARP/wARP resulting in a largely complete model without the metal centres. The model was refined and manually adjusted using CNS and Main, respectively, resulting in an R-factor of 20.7 % and free R-factor of 23.0 %.

3.2.2 Overall crystal structure

As depicted in figure 10 the refined model displays a tetramer of heterodimers with each heterodimer being built up by two subunits CsdB (big subunit with the active site) and CsdC (small subunit with two [4Fe-4S] clusters). The contacts between the four Hpd heterodimers were primarily mediated by the big subunits forming a cloverleaf structure with the small subunit capping the outside of the glycyl-radical subunits.

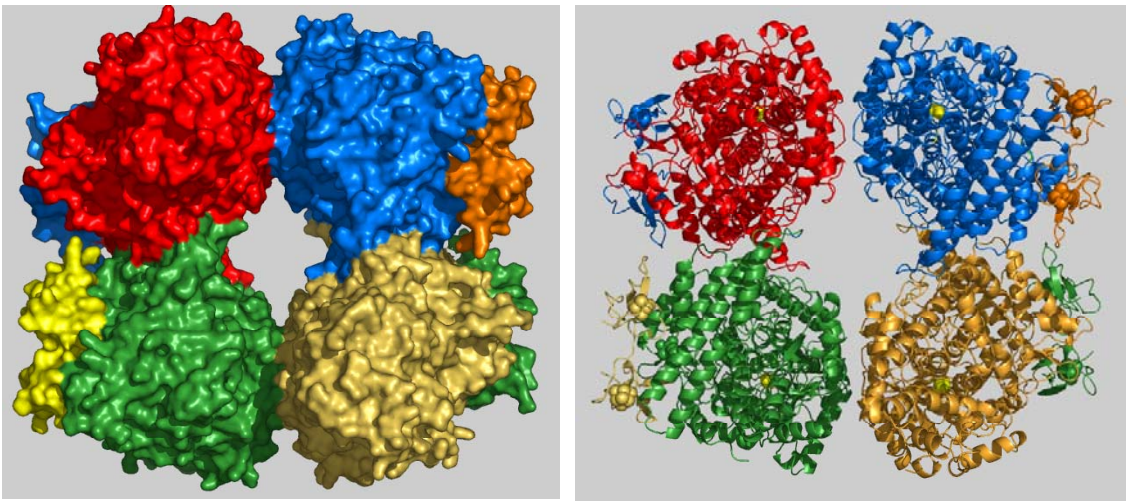

figure 10 Crystal structure of Csd. The left picture shows a surface presentation, and the right is the Ribbon diagram, which shows the binding of the small subunit and the Fe-S clusters in these unique constituents of GRE decarboxylases. Each heterodimer is composed of a big and a small subunit. The 4[Fe-4S] centres are displayed in spheres (2 per small subunit) and the catalytic active residue glycine is displayed as yellow sphere.

It became evident, that the small subunits are predominantly involved in binding two [4Fe-4S] clusters. To interfere with the active site (depicted in yellow) a distance of 40 or 41 Å between the closest iron and the glycyl radical site has to be bridged.

This detachment of the clusters makes a direct interaction with the glycyl-radical site impossible. Nevertheless an interaction can be postulated, since the observed intrinsic inactivation of the glycyl-radical highly favors the participation of a reduced [4Fe-4S] cluster. To bridge this long distance a reorientation of the structure upon activation may be speculated which opens away for inactivation. On the other hand, a long-distance electron transport mediated by aromatic amino acid residues may be postulated. A similar mode of action has been described for the activation of the ribonucleotide reductase (class I), where a distance of 35 Å needs to be bridged during activation. This distance derives from docking models of the individually solved crystal structures of both reaction partners and has been shown to involve a tyrosine residue not seen in the structure (97, 98). Recent EPR distance measurements could confirm this long range electron transfer and make a similar mode of action for the radical quenching in arylacetate decarboxylases possible (98).

Although the refinements of the structure is still on the way, preliminary comparison with other known structures suggests, that the overall structure of the individual glycyl radical subunits is quite similar to the ones already described (43, 59, 60, 63): Two parallel five-stranded β-sheets forms a core 10 -stranded β-barrel motif, that is assembled in an anti-parallel manner. This β-barrel core is completely surrounded by α-helices and has been

termed a β/α -barrel structure. Protruding into this barrel two finger like loops bring together the active site glycine (glycine 873) with the active site cysteine (cysteine 502), which is involved in radical transfer to the substrate (HPA). The close proximity of these catalytically essential residues to the substrate (HPA) is depicted in figure 11.

3.2.3 The active site

Interestingly the methylene-group of the substrate (which has been soaked into the crystal) is orientated to the active site cysteine. This suggests that a hydrogen is abstracted at the C_α position rather than from the aromatic ring itself, which has been previously postulated (56, 69). To validate the orientation of HPA during catalysis, ongoing experiments are carried out in our laboratory with C_α –deuterated substrate.

It also may be speculated that the orientation reflects an inactive state of the protein, since it could be deduced from EPR measurements that only one site per hetero-octamer is catalytically active (50). Therefore the majority of the active sites is not activated and may be inhibited by an ‘incorrectly’ orientated substrate.

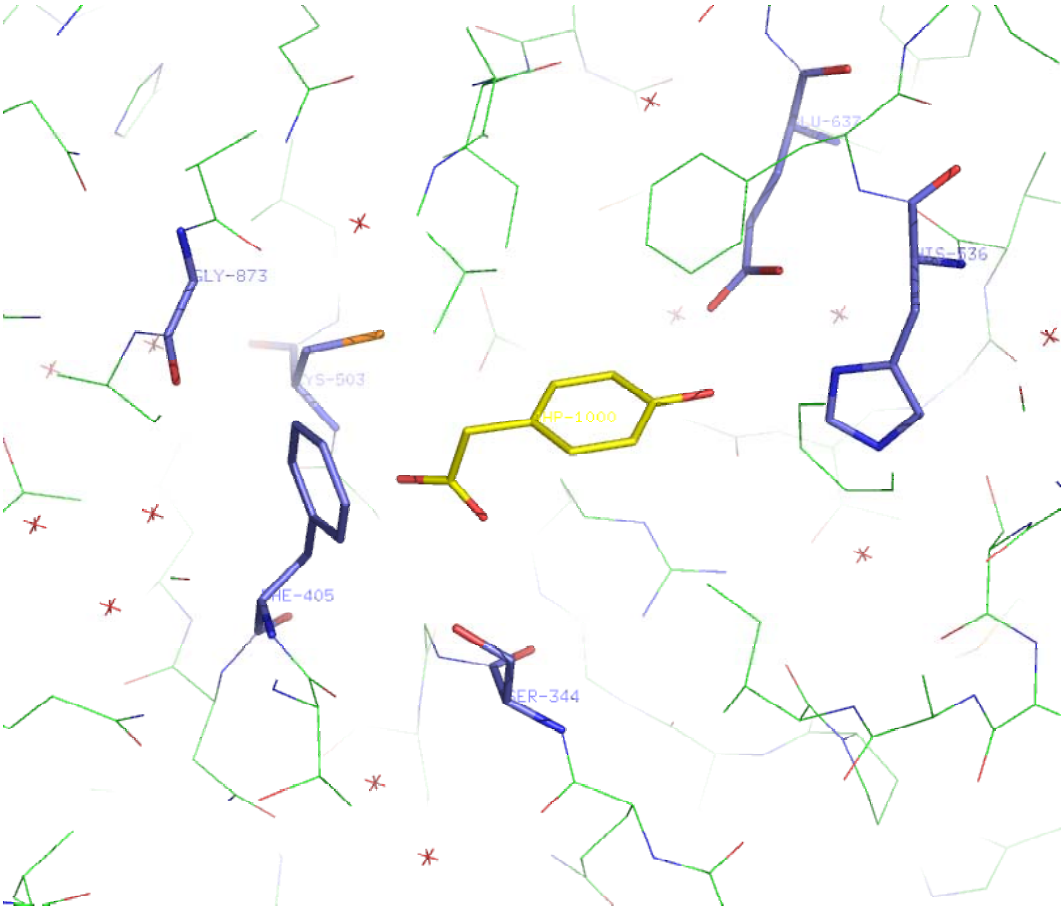

figure 11 Active site of CsdB. The substrate HPA (depicted in yellow) was soaked into the crystal. The catalytically important residues glycine 873 and cysteine 503 are marked, as well as the residues presumably involved in substrate binding.

3.2.4 The small subunit

Concerning the fine structure of the small subunit, the binding mode of the two identified [4Fe-4S] clusters could be studied. The N-terminal cluster is bound by three cysteines (C6, C14, C19) and one histidine (H3); the C-terminal cluster by four cysteine ligands (C45, C48, C62, 80). The edge-to-edge distance between the clusters within a small subunit is 21 Å. While the N-terminal cluster is quite exposed to the environment, the C-terminal one is entirely shielded by β sheets.

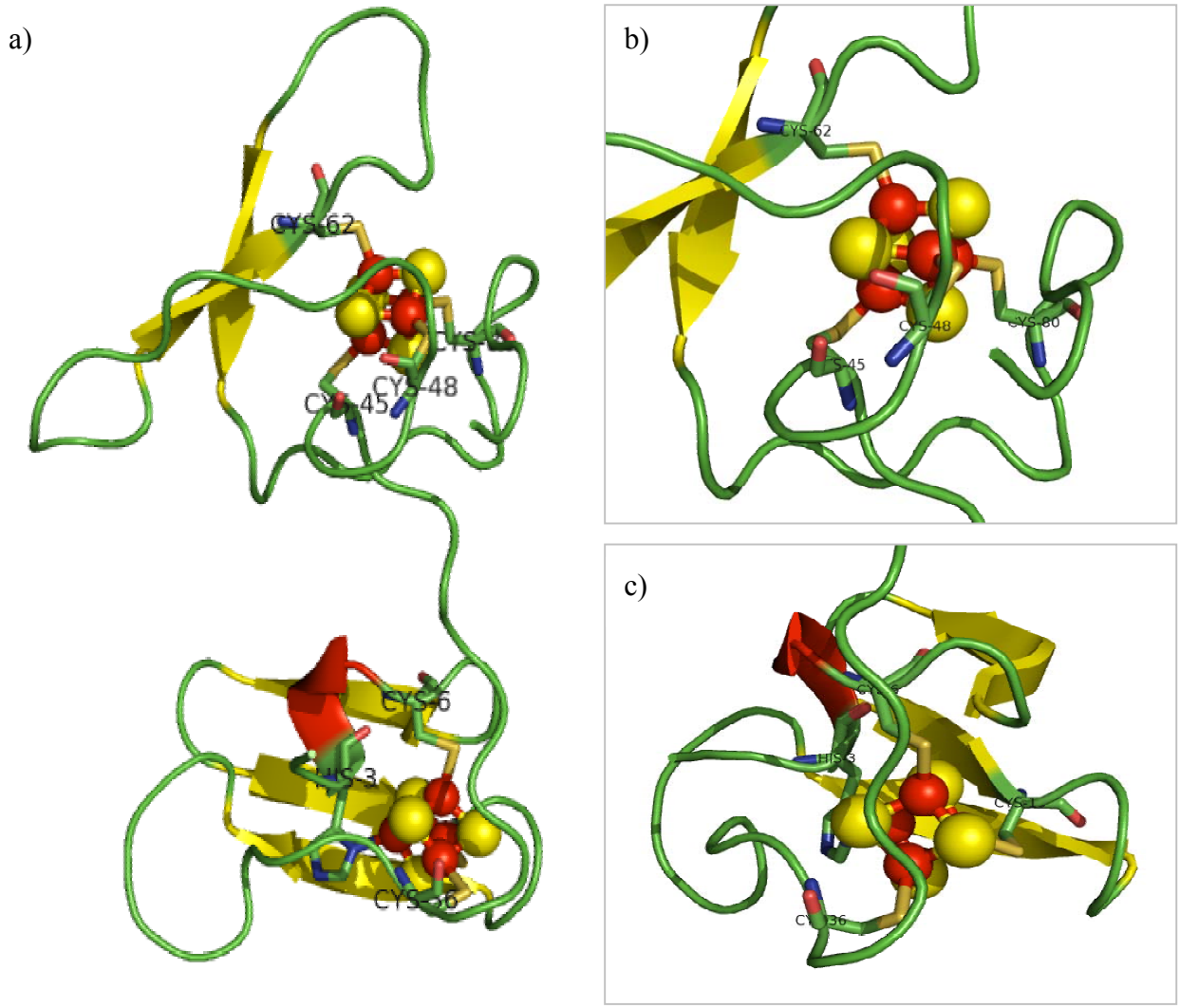

figure 12 Csd small subunit carrying the two iron sulphur clusters. The residues involved in cluster binding are highlighted. a) Overall structure of CsdC; b) the N-terminal cluster of CsdC c) the C-terminal cluster of CsdC.

It has been postulated, that the small subunit is essential to form the catalytically active hetero-octameric complex. While the well characterized Nrd and Pfl are catalytically active dimers, the dimer of HpdB previously reported was almost inactive (56, 99). Nevertheless, only one finger-like loop links two CsdC molecules and may directly contribute to the

complex stability. In the same interface the P-loop structure of the big subunit is located. Together this interface opens a pocket large enough for a big nucleotide-derivative. First experiments indeed suggest NAD as binding partner. It is also worth noticing that according to the amino acid alignments of the small subunits the binding mode of the N-terminal cluster is not conserved and seems to be missing in TfdC (figure 13).

```
CsdC    ---MRHYDCKNYINLDCEKGLCALTKGMVPIDGEGREASPNFKPAEKCGNCKNF-CNPDK
HpdC    --MRKHSDCMNFCAVDATKGICRLSKQMINLDD---AACPEIKVMPKCKNCKNF-VEAND
TfdC    MEERIYKNSLNYIPIDVAKGIDRRTGKRVNADD----VDPNYERMPKCMHCVNFTLNQEK

CsdC    YGLGTCTGLEKENWAYATCGASACPSYKAE--
HpdC    EGIGKCVGLEKEDWVYSTLNAITCEGHVFNE-
TfdC    IGLGICR-MGKEFIAYPDMAAVTCTGYKERGA
```

figure 13 Sequence alignment of the small subunits of the known arylacetate decarboxylases. Highlighted in red are the ligands involved in the binding of the iron sulfur clusters.

The N-terminal phosphorylation site of CsdB, which has been previously shown and was suggested to contribute in the complex stability (50), could not be visualized in the structure. The N-terminal part of the decarboxylase (CsdB), which is phosphorylated (Andrei & Selmer, unpublished) was unordered in the structure, so that the first 35 amino acids could not be annotated. However, this flexible part of the structure may be stabilized in a phosphomimetic mutant (Ser->Glu). It may be envisioned that this N-terminal tail forms a flexible linker, not only responsible for sensing an incoming phosphorylation signal, but also capping the small subunit and contributing further to its binding.

Further investigations concerning the structural architecture of arylacetate decarboxylases will include attempts to solve the structure of HpdBC as well as TfdBC. Likewise co-structures with the activating enzymes would be extremely desirable; as well as soaking experiments with the substrates HPA, DHPA or the postulated effector NAD.

3.3 Activation in the assay

When the recombinant Hpd system was reconstituted *in vitro*, cresol formation was linear over time. In these experiments the activating enzyme was combined with the decarboxylase in a buffer containing a reducing agent and HPA as substrate. The reaction was started by the addition of SAM and cresol formation was monitored by HPLC. Once the full activation was achieved, the cresol concentration in the test increases linear over time, suggesting specific activities of more than 10 U/mg for the decarboxylation of HPA by Hpd. Later on, a decrease in activity – most probably due to substrate limitation was observed (figure 14, dotted line)

On the other hand, when the activation was performed in the absence of substrate, it was of transient nature, with initially high specific activity slowly declining throughout extended periods of incubation. The maximum activity (up to 10 U/mg) was reached after 5-10 min followed by an asymptotic drop thereafter. However, the radical dissipation was not complete, leading to an equilibrium of activation and inactivation. This baseline activity was usually around 10% of the maximum activity and was stable for several hours (figure 14 black line).

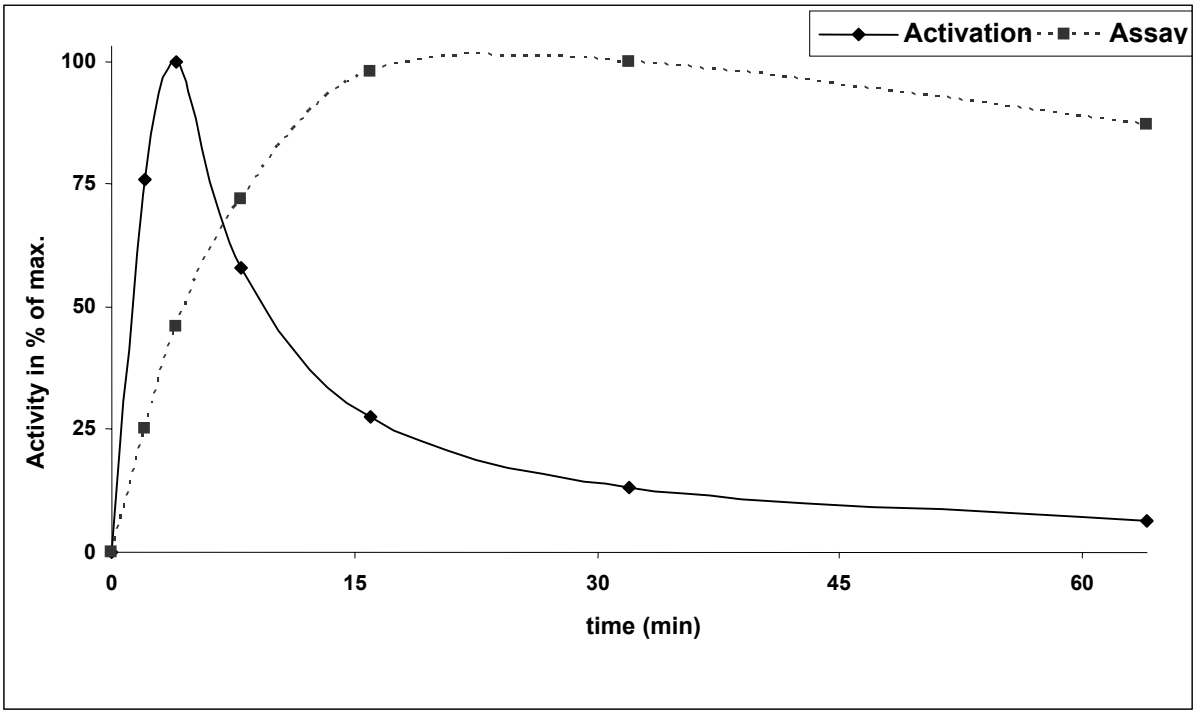

figure 14 Specific activity of Hpd. Comparison specific activity under assay conditions (assay) when 25mM HPA was present and under activation conditions, when the glycyl radical was formed in the absence of HPA (activation). For better comparison the data are given in % of maximum activity (Assay 12U/mg; Activation 17U/mg).

To characterize this unusual radical dissipation, a series of experiments was performed. But neither changing the protein concentration or ratio, nor altering the amount of SAM used or the source of electrons, altered the overall line shape. The activation/inactivation process seemed to be an intrinsic property of the system when substrate is missing.

The transient nature of the activation process was further validated by EPR measurements. As depicted in figure 15 the loss of activity was paralleled by a quenching of the glycyl radical signal of the decarboxylase, revealing that the loss in activity relies indeed on radical dissipation. Further studies carried out in our laboratory by Yan Ling supported the notion that the site of inactivation is the glycyl radical rather than the intermediately formed thiyl radical at the active site. Mutants, carrying a serine instead of the active site cysteine, were

unable to decarboxylate HPA, but showed a transient glycyl radical signal compared to the wild type (100). However, the fate of the glycyl radical during inactivation remains enigmatic.

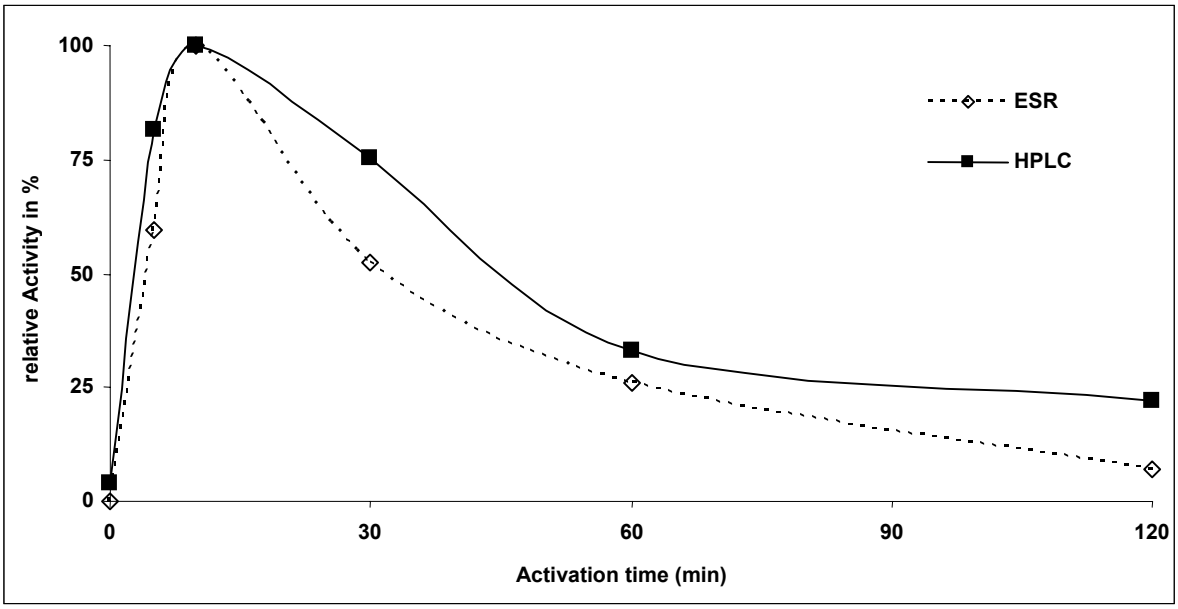

figure 15 Transient activation The activation was carried out by mixing the HpdBC (2mg/ml final) with a four fold molar excess of HpdA (2.7 mg/ml final) in buffer A (100mM TRIS-Cl pH 7.5, 150mM NaCl, 5mM $(NH_4)_2SO_4$, 5mM $MgCl_2$) freshly supplemented with 5mM DTT, 5mM cysteine and 1mM dithionite. The reaction was started by adding SAM to a final concentration of 250µM. At various time points 250µl of the activation mixture were withdrawn into EPR tubes and frozen in liquid nitrogen; in parallel 10µl of this activation mixture were diluted in 1ml assay buffer. The reaction was stopped after 10 min by adding perchloric acid, neutralized and measured by RP-HPLC for cresol formation.

Noteworthy, the analogue Csd-System from *Clostridium scatologenes* behaves almost identically. As already shown elsewhere (50, 101) it exhibits similar activation/inactivation properties. Since the glycyl-radical signal of the other well known systems (Pfl, Nrd) is quite stable over time, having a half life time of several hours (1), the intrinsic inactivation seems to be a characteristic property of clostridial arylacetate decarboxylases. To get a better understanding of this unusual process, both the activation and the inactivation processes, were characterised in more detail.

3.4 Radical dissipation – a regulatory role of the small subunit?

Since the transient nature of the activation and the observed radical dissipation distinguishes the arylacetate decarboxylases from other GREs, further experiments with the recombinant enzymes essentially attempted to dissect activator-dependent radical formation and the radical dissipation. The easiest way to quench the glycyl radical would be the incorporation of a hydrogen atom. This may be provided in form of one electron by a reduced $[4Fe\text{-}4S]^{+1}$ cluster,

followed by protonation of the glycyl-radical anion thus formed by a proton from the environment.

3.4.1 Gelfiltration

Altogether there are up to five individual iron-sulfur clusters present in the HPA-decarboxylase system (two in the decarboxylase and up to three in the activating enzyme); only the SAM-cluster in HpdA has been functionally characterized in orthologue systems (Pfl and Nrd) so far. The initial attempt to characterize the [4Fe-4S] centers more individually was to separate both protein partners (decarboxylase and activating enzyme) after a short initial activation period by gel filtration. The composition of the resulting preparations was verified on SDS-PAGE and showed, that indeed a complete separation of the decarboxylase and the AE occurred. Re-purified Hpd revealed a similar rate of inactivation as the non-separated control, suggesting that the inactivation process is an intrinsic property of the decarboxylase itself and does not rely on the presence of the activating enzyme (figure 16). The half life time is 60-120 min for both processes.

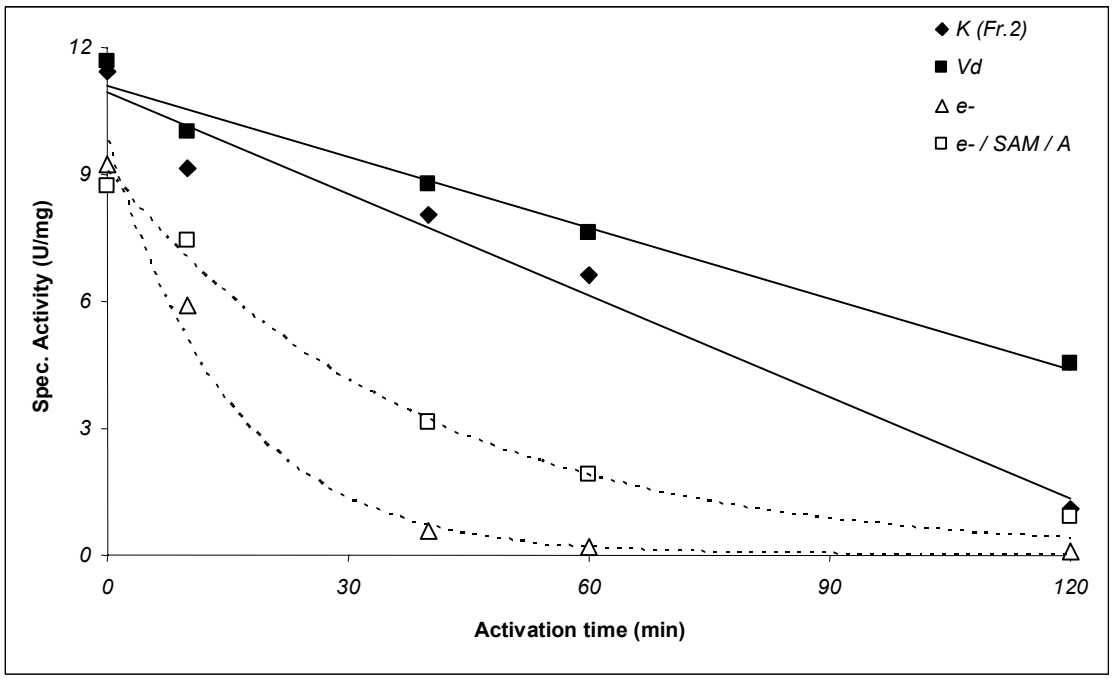

figure 16 Gel filtration. A highly concentrated activation mixture was activated for five minutes in the presence of SAM before loaded onto Superdex 200 (HR 10/30) gelfiltration column. The fractions containing only the decarboxylase (K) were measured for their ability to convert HPA. As a control the initial activation mixture was diluted to give a comparable concentration of HpdBC (Vd). In both cases a similar rate of inactivation was observed. When a reducing agent was added to the gel-filtered HpdBC the inactivation process was faster (e-). Even the re-addition of all components needed for activation could not restore full activity nor prevent the inactivation.

The re-addition of reducing agents after gel filtration accelerated radical decay; the half life time is reduced to approximately 15 min. Even the re-addition of individual components including SAM and activating enzyme to restore activation conditions could not fully restore activity (half life time 30 min); suggesting that the process of inactivation, once on the way could not be reverted.

Due to the low capacity of the gel filtration, EPR measurements for quantification of the glycyl-radical or the reduction state of the [4Fe-4S] cluster of HpdBC during radical dissipation could not be performed. Therefore, photoreducing experiments were performed as an alternative way to dissect the two processes.

3.4.2 Activation under photoreducing conditions

While chemical reduction of the decarboxylase system *in vitro* requires excess of the reductant, which is difficult to remove and causes artificial over-reduction, the photoreduction provides sufficient reducing equivalents to drive the activation process to completeness, but allows also stopping the electron supply to the system at defined time points (figure 17). Since it has been shown that the activating enzyme cannot stabilize the reduced cubanes for longer times (compare: figure 22), one can predict that the termination of illumination provides experimental access to the fate of the glycyl-radical and of the reduced cubane in the decarboxylase.

Noteworthy, under the conditions described above (figure 17) the activation is slowed down by using equal molar ratios of both enzyme components to elucidate that the inactivation process could be started independently of the activation. When the usual four fold molar excess of AE over Hpd was used, the activation proceeded within the first ten minutes and was then stable in time (data not shown). Interestingly the radical dissipation diminished under permanent light, while shading of the samples leads to rapid decline in specific activity. It may be speculated that the observed stability under assay conditions (presence of HPA) or permanent light is due to an equilibrium between the activation and inactivation, while the net inactivation, which was observed with chemical reductants might be caused by damage of the activating enzyme. Taking into account this notion, photoreduction creates an electrochemical environment also found under assay-conditions, were the presence of substrate either stabilizes the activating enzyme or, more likely, slows down the intrinsic radical dissipation of the decarboxylases.

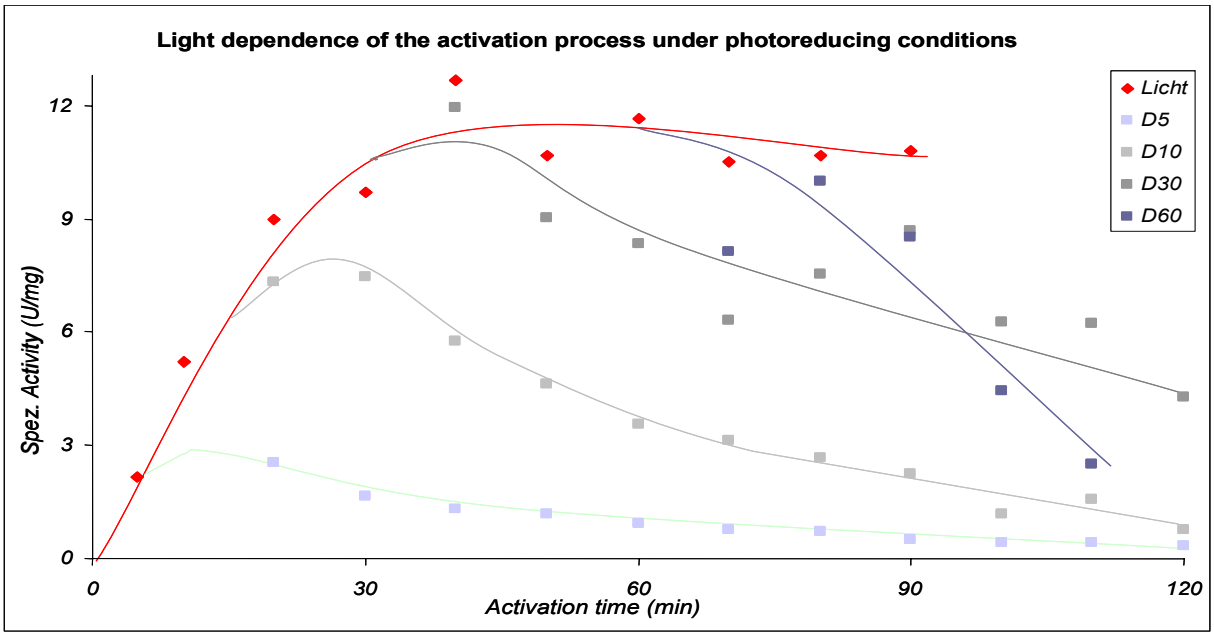

figure 17 Light dependence of activation. An activation mixture containing both enzymes and SAM in a TRIS buffered solution was photoreduced for 90min. Note that the Ratio of HpdA to HpdBC in this experiment was 1:1; resulting in a slower activation process! At the dedicated time points (D5 = 5min, D10 = 10min, D30= 30min, D60 = 60 min) an appropriate aliquot was taken and further incubated at 30 °C in darkness to allow the inactivation process to quench the reaction. At the dedicated time points samples were taken from the activation mixture and diluted into assay buffer. Cresol formation was monitored following standard protocols.

3.4.3 Reduction impact on activation

To determine the processes involved in inactivation, the decarboxylase, activating enzyme and SAM were illuminated in the presence of F420 and the accumulation of the glycyl radical and of activity were monitored. As shown in figure 18, continued illumination caused a rapid and stable formation of glycyl radical signals and decarboxylase activity.

The samples withdrawn for EPR detection of the glycyl radical were also analyzed for the paramagnetic metal centers at low temperature and exhibited almost pure signals characteristic for the decarboxylase cubane(s), without disturbance by the AE signals. Neither specific activity nor the intensities of the glycyl radical or the reduced cubane changed significantly upon prolongated illumination. The continued formation of 5'-deoxyadenosine further supports the conclusion that under these conditions the system is at equilibrium, where radical formation and dissipation occur at more or less constant rates.

However, the picture changed dramatically when previously illuminated samples were transferred to the dark and incubated for defined periods of time prior to activity measurements or EPR sampling. Noteworthy, the liberation of 5'-deoxyadenosine immediately stops after transfer of the samples in the dark, further supporting an almost

immediate re-oxidation of the iron-sulfur centers in the activating enzyme in the absence of continued electron supply. In these samples, a slow decline in specific activity was observed, which was accompanied by significant radical dissipation. Most interestingly, the signal for the reduced decarboxylase iron-sulfur centers also diminished slowly in time. These findings further supported the notion that the radical dissipation relies on a reduction of the glycyl radical on the expense of metal center oxidation. Indeed, both processes occurred parallel in time and quantitative data evaluation suggested that approximately 1.3 electrons from the reduced cubanes are consumed per glycyl-radical quenched.

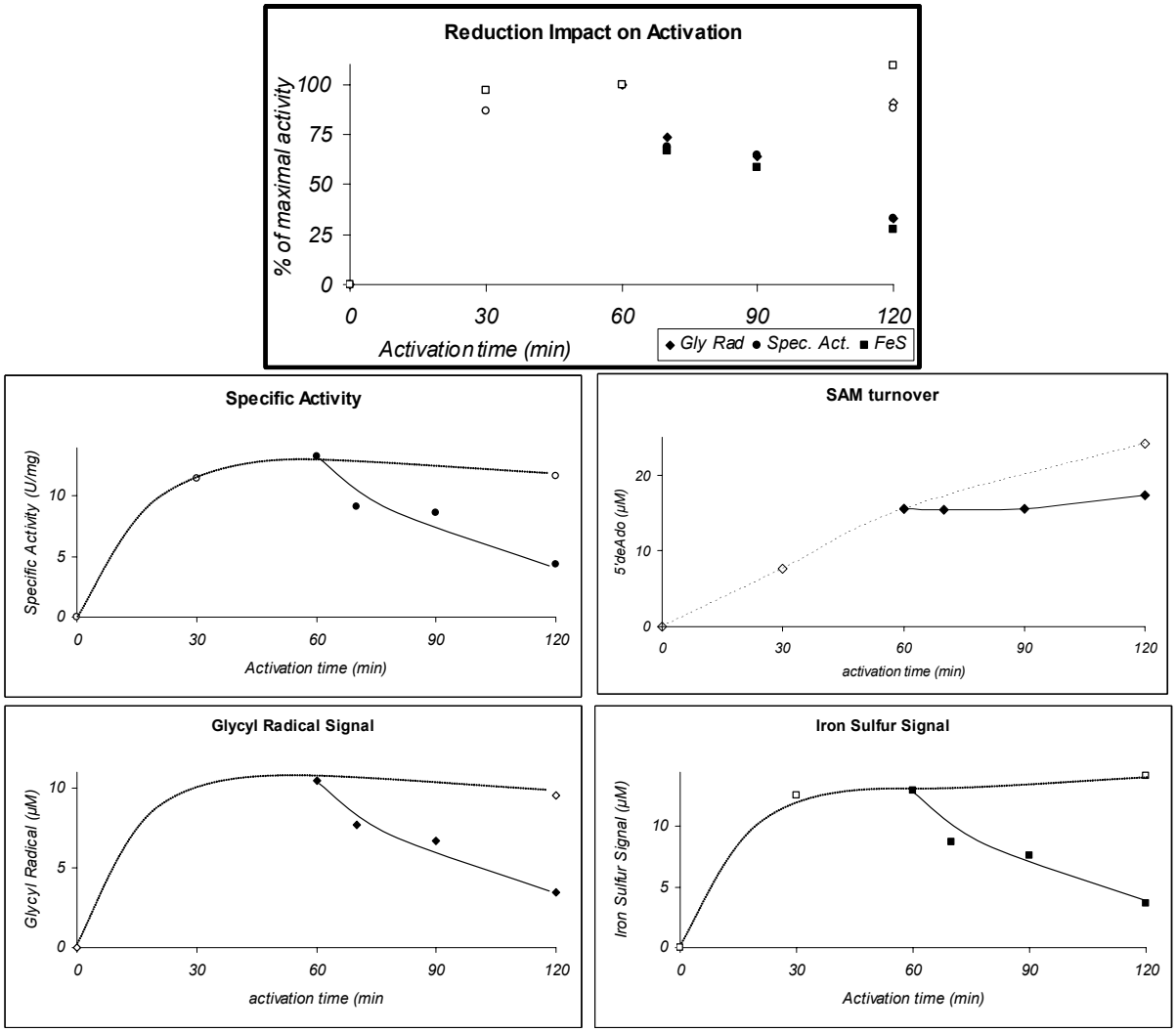

figure 18 Reduction impact on activation. An activation mixture containing 5mg/ml HpdA and 4mg/ml HpdBC was activated under photoreducing conditions. At the timepoints dedicated an aliquot of this mixture was withdrawn and analysed for its ability to form cresol; a second aliquot was frozen in liquid nitrogen and analysed by EPR for glycyl-radical intensity as well as the presence of reduced [4Fe-4S] clusters. This aliquot was later used to quantify the amount of 5' deoxyadenosine liberated during activation (shown as inlay). The dotted line represents the darkened samples, while the solid line depicts the 5' deoxyadenosine production under light.

3.4.4 Reactivation

To check whether an inactivated sample can be reactivated, molar ratios of both enzymes were incubated in photoreduction experiments and illuminated for 30 minutes (until maximum activity was reached). Transfer of the samples in the dark caused the inactivation process to proceed for 90 minutes before a second round of illumination was started. The latter of which was paralleled by an aliquot of the original activation mixture, which was kept in darkness for four hours and served as a control.

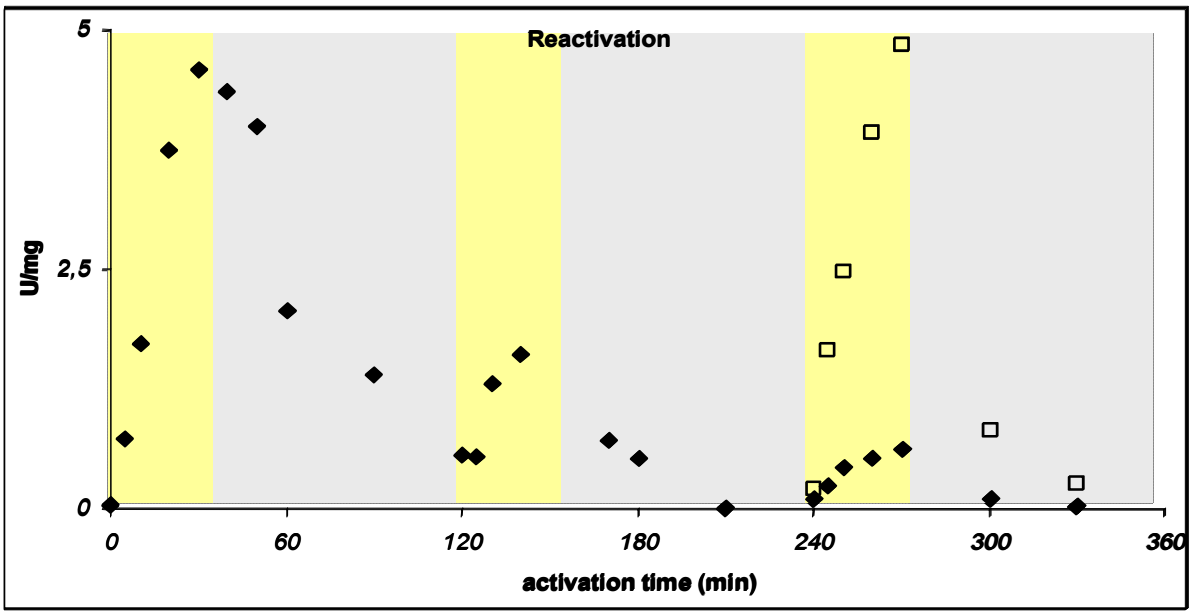

figure 19 Reactivation of Hpd. An activation mixture containing HpdA (0.28 mg/mL) and HpdBC (0.8 mg/ml) was photoreduced in the presence of SAM for 30 min (light yellow) and than kept in dark for 90 min (light grey). Note that the molar ratio of HpdA and HpdBC is 1:1. At the time points indicated, samples were withdrawn and tested for cresol formation following standard protocols. This illumination cycle was carried out three times (black diamonds). To validate the stability of the reaction mixture a control sample was kept in dark for 4h and illuminated parallel to the last cycle (open squares).

Using chemical reductants as electron sources, the poor stability of the activating enzyme has been noted. It could be shown in photoreduction experiments, however, that transiently inactivated samples were re-activated by re-illumination with an efficiency of 43% (16% for the third round). Since the enzymes were applied in equal molar ratios, un-reacted excess of HpdA could not be the driving force of the observed re-activation. Hence it appeared that the AE is catalytically active under photoreduction conditions. The decline of the efficiency in re-activation is most likely due to the instability of one of the reaction partners. Since the control samples are not affected, one of the reaction partners seems to undergo a permanent change during the activation / inactivation process.

3.5 Hybride decarboxylases – defining the role of the small subunit

To fully understand the complex regulatory mechanism found for arylacetate decarboxylases and the intrinsic inactivation in the absence of substrate, it is of utmost importance to elucidate the role of the small subunit (HpdC, CsdC, TfdC) during catalysis. From the crystal structure presented earlier on, it could be deduced that the small subunit harbors two [4Fe-4S] clusters; one of which is redox active and exhibit a mid-point potential of -287mV. From the biochemical studies it became evident that the decarboxylase itself is able to eliminate the glycyl radical; most probably by using a reduced cluster of the small subunit. It is also known from previous work, that the small subunit significantly influences the formation of the catalytically competent hetero-octameric complex, which could not be obtained for the *Tanneralla forsythensis* system. It has also been described, that an inactivated HpdB dimer can be purified from *C. difficile* wild type, while the recombinant system is only soluble in the presence of the small subunit.

From all this data it could be concluded, that the small subunit is a) involved in the formation of the catalytically competent hetero-octameric complex and b) essential for the radical dissipation in the absence of substrate. Therefore, to elucidate the functional role of the small subunit during catalysis, it is not only necessary to further understand the participation of the reduced [4Fe-4S] cluster in radical-quenching, but also to deepen our knowledge concerning the catalytically needed complex formation.

To validate the influence of the small subunit during complex formation, hybrid enzymes composed of the individual small subunits with different glycyl radical subunits were generated by genetic fusion of individual genes. Note that all hybrid-decarboxylases and small subunit mutants presented in this work were created by Dr. Lihua Yu and kindly provided for the biochemical characterization presented here. The biochemical data for the resulting hybrids are summarized in table 10 (see also: (101))

table 10 The hybrid decarboxylases. Wild type is depicted in bold; the oligomerisation state, the phosphorylation as well as the iron-sulfur content are illustrated. The wild type values are marked in bold.

	Csd B			**Hpd B**			**Tfd B**		
	oligomeric state	**phosphor**	**[Fe-S]**	**oligomeric state**	**phosphor**	**[Fe-S]**	**oligomeric state**	**phosphor**	**[Fe-S]**
Csd C	**β4γ4**	**yes**	**32**	β2γ2	**yes**	**16**	**insoluble**		
Hpd C	**insoluble**			**β4γ4**	**yes**	**32**	βγ	**yes**	**8**
Tfd C	**insoluble**			β2γ2	**yes**	**8**	**β2γ2**	**yes**	**8**

Only the wild type decarboxylases could be activated by their cognate AEs to give glycyl-radical signals in EPR. The intensity observed for TfdBC, however, was only about 10% of

the two other wild type decarboxylases. Since the soluble hybrids exhibit a lower oligomeric state when compared to the wild type, it was deduced that the oligomerisation is an important regulator of the enzyme activity and mediated by the small subunit.

To understand the differences in complex formation and activity, the amino acid sequences of the individual small subunits was compared. It became immediately evident that only the C-terminal cluster is conserved throughout all three decarboxylase small subunits and that the N-terminal cluster is missing in *T. forsythensis* (compare: figure 13).

From this data it could be speculated that the C-terminal cluster – at least in *T. forsythensis* – is essential for an initial complex formation, while the N-terminal cluster may be needed to fully assemble the catalytic complex. This hypothesis would structurally differentiate the two observed functions of the small subunit (complex formation and radical dissipation) and assign different functions for the two clusters. Interestingly, first EPR measurements with the purified reduced TfdBC exhibits only a negligible amount of reduced iron-sulfur cluster, supporting a functional differentiation of the two clusters.

To further elucidate this hypothesis mutants of the small subunit were generated. One approach eliminated the individual ligands of the two clusters of CdsC by replacing them with serines (histidine to glutamate in the case of the N-terminal cluster). In another setup the N-terminal cluster of CsdC was fused to the C-terminal cluster of HpdC; likewise the N-terminal cluster of HpdC was fused to the C-terminal cluster of CsdC. These fusions should further elucidate the functional role of the two clusters in complex formation and catalysis. The preliminary results for these mutants are summarized in table 11.

table 11 Initial characterisation of small subunit mutants. The small subunit mutants carrying a single amino acid exchange are depicted for the N-terminal cluster ligands; the C-terminal mutations were insoluble. Likewise some hybrids sharing the two domains of different small subunits are showed Depicted is the oligomeric state, the iron-sulfur content and the specific activity (U/mg) after 10 (t 10) and 40 (t 40) min activation. * Due to the gelfiltration experiment it could be estimated, that these mutants are mixtures of different species, dominated by hetero-octamers. Therefore the measured activities may reflect only a smaller portion of active proteins, than anticipated by protein determination.

	Oligomeric state	**[Fe-S]**		**t 10 [U/mg]**	**t 40 [U/mg]**
CsdBC	β4γ4	**7.0**		**5.0**	**1.0**
CsdBC H3G	β4γ4	**4.2**		**1.3**	**0.3**
CsdBC C6S	(β4γ4)*	**(0.8)***		**(0.2)***	**(0.1)***
CsdBC C14S	β4γ4	**6.6**		**2.2**	**0.3**
CsdBC C19S	(β4γ4)*	**(1.9)***		**(0.2)***	**(0.1)***
CsdB CsdC-NHpdC-C	**aggregate**	**5.5**		**3.6**	**1.0**
CsdB HpdC-NCsdC-C	β4γ4	**3.7**		**0.8**	**0.3**
TfdB CsdC-NHpdC-C	**aggregate**	**1.7**		**0.2**	**0.1**

The ligand exchange of the cluster-coordinating residues revealed, that the mutants lacking the C-terminal cluster were insoluble, while the mutants of the N-terminal cluster could be purified and analyzed. A ligand exchange in the N-terminal cluster does not affect the oligomeric state of the mutants, but reduces their ability to properly coordinate the [4Fe-4S] clusters (table 11). In concordance with this finding is their impaired ability to form the glycyl radical, while their ability to inactivate is not completely abolished. Further studies with a full cluster knock-out are needed to establish the functional role of this cluster. If this cluster indeed is of regulatory importance it would be expected to resemble the wildtype in the EPR. Likewise, the C-terminal cluster is confirmed to be the structurally important, complex forming cluster, since mutations in this region completely abolished the solubility and function of the enzyme.

The small subunit hybrid mutants on the other hand are soluble and of brownish colour. Nevertheless, the fusions containing the N-terminal cluster of CsdC aggregated during gel filtration while the one containing the N-terminal cluster binding motif of HpdC appeared as a hetero-octameric complex. This observation further supported the functional importance of the C-terminal cluster in solubility and complex formation.

The two mixed chimeras of the small subunit, combining the two cluster-binding sites of the clostridial small subunit of Hpd and Csd, were fused to CsdB. While a fusion of wild type HpdC to CsdB was insoluble, these chimeric constructs were soluble and could be activated by CsdA. When the N-terminal cluster was exchanged to the HpdC counterpart, the chimeric construct was almost as active as the wild type; the exchanged C-terminal cluster could only be activated to 23% of the wild type activity. Therefore, an intact C-terminal cluster seems to be essential for proper activation and recognition of the AE.

Interestingly, the TfdB fused with CsdC-NHpdC-C is active (even though below 10% of wild type) and even though aggregating during gel filtration contains some hetero-octamers. This was the first reported active form of the *Tannerella* system on a substrate level. Since the active site of the TfdB (binding HPA) was not altered, it could be deduced, that the Tfd also belongs to the HPA-decarboxylase family.

Further studies should include activation of the constructs described here with Hpd-AE to confirm the importance of the N-terminal cluster during activation. Additionally EPR measurements may be used to confirm the impaired cluster binding of the single amino acid mutants as well as the hybrids of the small subunit. Also of interest would be the functional characterization of a hybrid containing TfdB and HpdC-NCsdC-C.

3.6 The activation process

As already shown, the recombinant Hpd system could be reconstituted in vitro, resulting in specific activities of up to 20 U/mg. In contrast to the well characterized GRE-AEs, where the activation-mixture needs to be pre-reduced for 30 to 60 min, the activation process of the Hpd system proceeds smoothly and within minutes after adding the reducing agent and SAM. Since there are up to two additional clusters in the activating enzymes of the arylacetate decarboxylases, it may be speculated that these unique metal centers are involved in the fast reduction of the SAM cluster. The first indication for unusual redox properties of these clusters was obtained by EPR-spectroscopy.

Though the purified AEs were EPR silent, the reduced clusters gave rise to a clear but SAM-independent spin ½ signal (compare figure 7). It should be noted that the EPR signal of the other studied GRE-AEs exhibit a dramatic change upon SAM binding (1). To further understand the underlying mechanisms of the activation process, the turnover of SAM was measured directly. By this it could be shown, that the activating enzyme itself is able to convert SAM to 5’ deoxyadenosine in the absence of the decarboxylase at very low rates. Mutants of the activating enzymes were generated, which lacked one or more of the putative binding sites of the [4Fe-4S] clusters.

3.7 5' deoxyadenosine detection

In addition to the decarboxylases themselves, three components are needed to generate the glycyl radical: 1) the cognate activating enzyme, which belongs to the SAM radical superfamily and harbors at least one [4Fe-4S] cluster, 2) S-adenosylmethionine (SAM), which is converted to methionine and a highly reactive 5’ deoxyadenosyl-radical, capable to abstract the pro-S hydrogen of a conserved glycyl-residue in the target protein, and 3) a source of electrons, which is provided in vitro by a strong reducing agent (by sulfuranyl or by F420/deazaflavine-semichinol radicals).

To quantify the activation process either the glycyl-radical can be measured by EPR, or the amount of 5’ deoxyadenosine or methionine could be quantified. To gain deeper insight into the activation process a direct HPLC-based method was established to determine the turnover of SAM to 5' deoxyadenosine (5'Ado), since methionine, which is frequently measured to determine this turnover may also arise from hydrolysis of SAM.

Based on a 30 µM standard containing 5' deoxyadenosine, SAM, S-adenosylhomocysteine, adenine (as internal standard) and 2'deoxyadenosine, the formation of 5' deoxyadenosine was measured for the activator alone or under activation conditions (HpdA alone, HpdA with

HpdBC) as well as under assay conditions (HpdA, HpdBC and HPA) and corrected for the internal standard: the appropriate protein(s) were mixed in TRIS buffer (pH 7.5) containing DTT, cysteine, and a reducing agent. The standard protein concentration was 0.54 mg/ml HpdA (15 µM) and either 0.4 mg/ml (4 µM) or 1.6 mg/ml (15 µM) HpdBC. HPA was provided with 25 mM final concentration when assay conditions were applied. The reaction was started by adding SAM to a final concentration of 250 µM and allowed to proceed while incubated at 30 °C in a heating block. The reaction was stopped at various time points by addition of an equal volume 10% TFA (containing 30 µM Ado as internal standard). The column was developed in a linear gradient of 2-20% ACN over 20 min. Detection was at 259nm. Samples containing substrate were additionally tested for cresol formation following the standard procedure. Concentrations as low as 2µM 5'-deoxyadenosine could be reliably detected by this method.

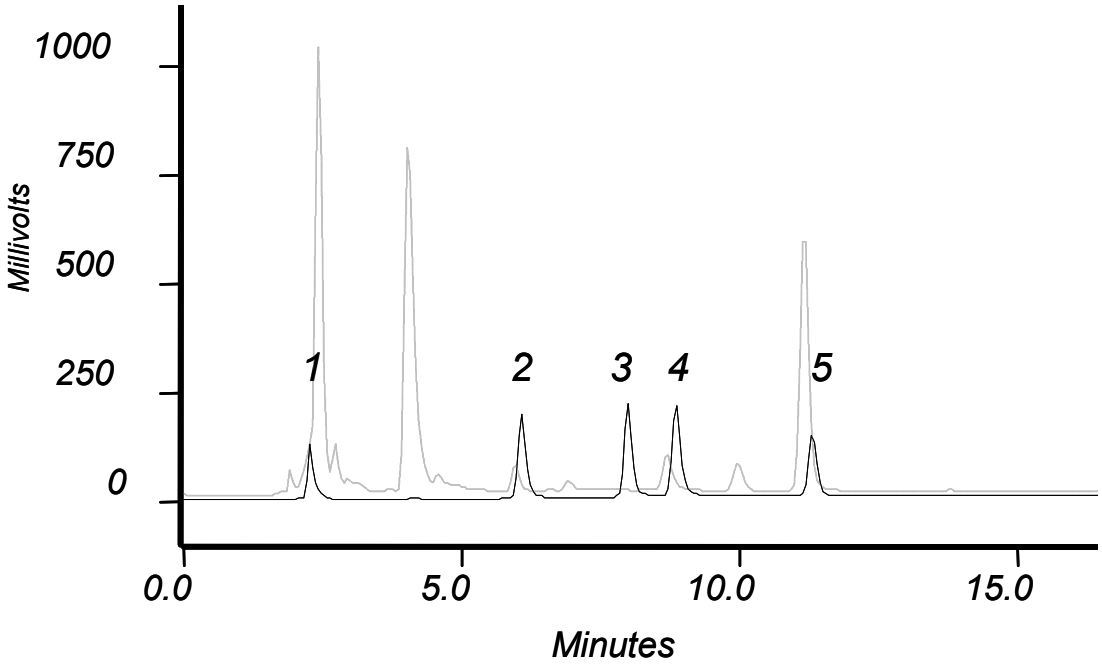

figure 20 HPLC traces of SAM derivatives. The standard depicted in black contained 30µM of each SAM derivative. A clear baseline separation of S-adenosylmethionine (1), adenosyl-homocysteine (2), adenosine (3), 2'deoxyadenosine (4), and 5' deoxyadenosine (5) could be established. The grey line shows an example of an assay containing 4mg/ml Csd-AE and 250µM SAM after 60 min incubation. The sample contained 15µM 2'deoxyadenosine as internal standard. Note that the depicted graph is shortened to about 16 min; further time needed to re-equilibrate the column is omitted.

3.7.1 5' deoxyadenosine under activation and assay conditions

It became evident, that the activating enzyme alone is able to catalyze the cleavage of SAM to liberate 5' deoxyadenosine with an efficiency of 4-5 turnovers per AE per hour. This futile cycle was linear over the time measured.

When the decarboxylase was present, additional turnover was observed – most probably due to the liberation of the 5' deoxyadenosyl-radicals and by this formation of glycyl-radicals in the decarboxylase. It should be noted that the additional turnover observed in the presence of HpdBC mainly happens within the first 10 minutes upon SAM addition – the time normally needed to accomplish full activation of the decarboxylase (6 per hour). Later a return to baseline turnover could be seen.

Under assay conditions however, SAM was exclusively used to generate the glycyl radical, as could be shown by subtracting the two curves where substrate is missing from one another. Under these conditions the turnover in the first ten minutes reaches more than 5 per hour, dropping to 1-2 per hour later on.

This further supported the notion that the futile cycle and the activation are independent, additive processes. And, even though the turnover numbers in the beginning of an assay suggest high rates of catalysis, the final concentration of 5'-deoxyadenosine never exceeded 23-30 µM suggesting that each AE (15µM final) is able to catalyze a maximum of two turnovers under these conditions. This may suggest, that each activating enzyme catalyses only 1.5 - 2 turnovers, when HPA is present.

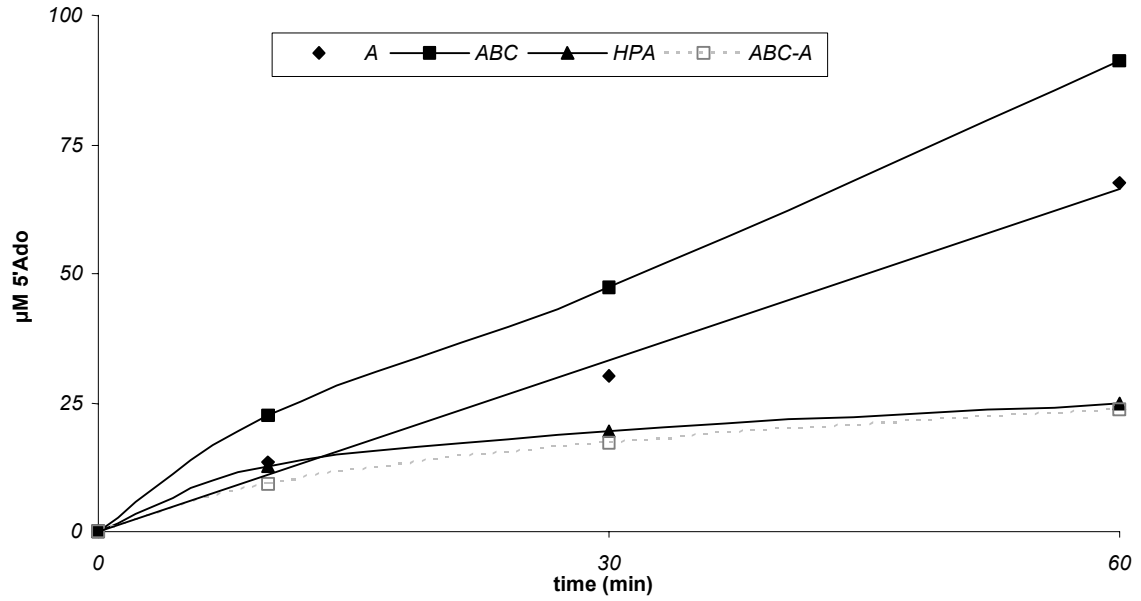

figure 21 5' deoxyadenosine detection. SAM turnover of 15µM HpdA alone (A), mixture of HpdA and HpdBC in a ratio of 4:1 (ABC) and turnover under assay conditions containing both enzymes and 25mM HPA (HPA). When the futile cycle was subtracted from the activation process (ABC-A), the amount of 5' deoxyadenosine was equal to the one detected under assay conditions. Cresol formation for the sample containing HPA was measured separately using standard protocols.

To further investigate this dramatic change in SAM turnover upon addition of HPA, inhibitor studies were performed. It could be shown, that neither methionine nor S-adenosine-homocysteine, 5' deoxyadenosine, or adenosine had any impact on the measured turnovers. Neither HPA (in the absence of HpdBC) nor HPAA (in the presence of HpdBC), a known inhibitor of the decarboxylase, showed any effect on the futile cycle, though HPAA inhibited Hpd-dependent turnover resulting in 5' deoxyadenosine production similar to HpdA alone. On the other hand first measurements with cresol indicate, that this compound completely abolished the futile cycle.

Since a similar but DTT dependent futile cycle has been described for the activating enzyme of Nrd, the impact of DTT was tested. For this purpose a concentrated sample containing the activating enzyme was desalted on NAP columns in TRIS buffer containing neither DTT nor DTB (the absence of DTT was monitored by Ellmann's reagent (Dithiobisnitrobenzoate). The thiol-free activator preparation cleaved SAM at rates accounting for only 26% of the spontaneously occurring cleavage in the presence of DTT. Re-addition of DTT resulted in partial reconstitution of the decarboxylase-independent 5' deoxyadenosine formation at specific activities, which reached 75% of the starting sample. Similar results could be obtained by DTT- free purified activator. This suggests that the activation is only partially dependent on DTT, which may more likely be involved in complex stability than serve as secondary electron source for quenching the SAM radical to 5'-deoxyadenosine.

Photoreduction

In previous work, the reconstituted system was chemically reduced by either dithionite or a mixture of titanium-(III)-citrate and Na_2SO_3 as sources of sulfuranyl radicals to achieve maximal activity (101). It is likely that the redox state of the individual clusters is regulated more precisely under *in vivo* conditions. For a better understanding of the electron flow during activation, light sensitive F420 was employed to substitute these chemical reducing agents by photoreduction.

To show that the reduction achieved via photoreduction was comparable to chemical reduction, the activation was monitored by 5' deoxyadenosine production of the activating enzyme in absence of decarboxylase. The liberation of 5' deoxyadenosine was similar to that observed with chemical reductants, but was completely light dependent; the production of 5' deoxyadenosine paused by switching off the light and could be restarted by re-illumination.

Even overnight, 60-70% of initial activity could be received, suggesting that the AE is very stable under photoreduction conditions.

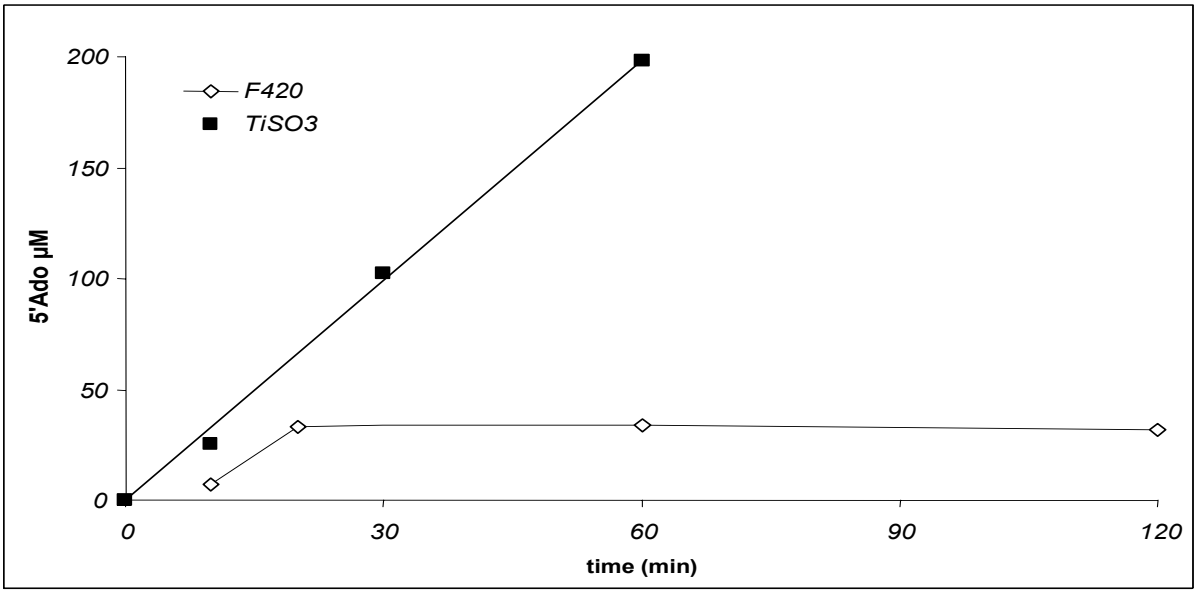

figure 22 Photoreduction compared to chemical reduction. An activation mixture containing 50 µM activating enzyme was reduced in the presence of SAM (250µM final) was reduced either with Ti(III)Citrate, Na_2SO_3 (2.5 mM each) or a mixture of F420 (50 µM final) and glycine (50 mM). Both samples were illuminated for 20 min. with a 25W slide projector. The turnover-number for the chemical reduction is 3.7 h^{-1}.

When the activator was pre-reduced in the absence of Hpd under these conditions, delayed addition after illumination-stop yielded only negligible decarboxylase activity, as indicated by trace amounts of cresol formed. In agreement, there was no detectable cleavage of SAM to 5' desoxyadenosine, which exceeded the spontaneously occurring liberation throughout the light-period of the experiment. Moreover, photoreduced HpdA was EPR silent, suggesting that $[4Fe\text{-}4S]^{+1}$ are very unstable in the absence of continuously ongoing reduction, which is easily provided by an excess of chemical reductant but not by photoreduction in the dark. Together, these observations strongly suggest that the reduced clusters in the activating enzyme are very short-lived.

While it has been previously shown, that the full activation requires the presence of a sulfuranyl radical (101) – provided by dithionite or titanium-(III)-citrate/Na_2SO_3 – titanium-(III)-citrate by its own was able to support the futile SAM cycle. This observation may be a valuable tool to dissect the activation process from the futile SAM-cycle.

3.8 HpdA Mutants

As already mentioned, the iron-sulfur content of the activating enzyme provided evidence for the existence of at least two [4Fe-4S]-clusters. The activation proceeds smoothly without

the need of prolonged pre-reduction times; the EPR signal of the AE is not sensitive to the presence of SAM and SAM is intrinsically cleaved in the absence of substrate or decarboxylase.

To fully understand these unique features of the AE, the participation of additional clusters was focused. Comparing the sequence alignments of the known activating enzymes revealed possible binding sites for up to two clusters in addition to the well known SAM cubane. Interestingly, all conserved cysteines, possibly involved in this cluster binding, are located in a 60 amino acid stretch, which is missing in the activating enzymes of Pfl and Nrd, but found in many GRE-AEs of as yet not functionally characterized systems. Likewise the EPR-signal of the purified arylacetate decarboxylase AEs showed no significant change upon SAM binding. It may be that the insert clusters are predominantly reduced under the conditions applied and significantly contribute to the obtained EPR-signal.

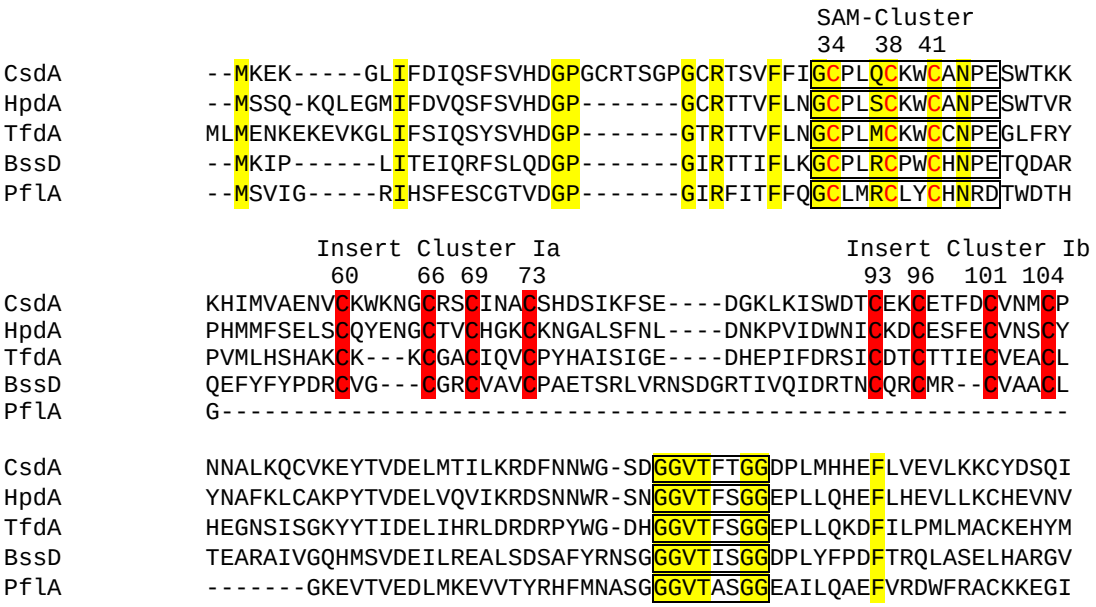

figure 23 Alignment of the N-terminal amino acid sequences of glycyl radical enzyme activating enzymes (GRE-AE). The N-terminal half of the amino acid sequences of HpdA, CsdA and TfdA are compared to the sequences of PflA from *E. coli* and BssD from *Thauera aromatica*. The SAM-binding motif (SAM-cluster and glycine-rich motif) is boxed. The completely conserved amino acid sequences are shadowed in yellow. The cysteines of the SAM-cluster are red lettered. The 8 conserved cysteinyl residues within an approximately 60 amino acids long insert as compared to PflA are shadowed in red. Note that only about 1/3 of the amino acid sequences of the individual AEs is shown.

To elucidate the role of these putative clusters in the regulation of the decarboxylase activity, the possible binding sites of the individual clusters were mutated either separately or in combination, eliminating all binding sites of individual putative clusters (**Fehler! Verweisquelle konnte nicht gefunden werden.**).

All mutated activating enzymes were purified under the conditions described for the wild type. All exhibited brownish color indicating the presence of remaining iron-sulfur clusters. To initially characterize these clusters the amount of iron-sulfur bound to the enzyme was determined and proven to be reduced when compared to wild type. Initial EPR measurements elucidated that all clusters exhibit similar properties as the wild type form. The catalytic performance of all mutants was dramatically reduced when compared to the wild type.

Since most radical SAM enzymes contain only one cluster, it was believed in the beginning of that work, that only one cluster is present in the activating enzyme. Later, the presence of additional clusters was postulated, and confirmed by the unusually high iron-sulfur content of the protein. (The as purified protein contains normally 4-6 iron/sulfur; initially good preparations or reconstituted samples up to 8-11.) For this reason it was believed, that the cluster binding is quite tight and that there is no need to further reconstitute the clusters. Therefore, the reported values of the HpdA mutant have been recorded with purified proteins and may be differ if the clusters are properly reconstituted. Initial experiments with the wild type indeed showed, that the as purified clusters can be reconstituted *in vitro*.

table 12 Iron content of HpdA mutants and EPR spin intensity. The iron content of the individual mutants was calculated separately and the percentage of the particular wild type Hpd-AE was evaluated. The EPR spin was calculated for each sample versus a Cu standard. Protein concentration during EPR measurements was set to 4mg/ml.

	Fe (%)	EPR Spin (µM)
Wild type	**100**	**17.3**
SAM	**60**	**6.3**
Ia	**87**	**10.3**
Ib	**62**	**7.0**
SAM only	**36**	**n.d.**
Ia only	**34**	**n.d.**
Ib only	**43**	**n.d.**

	Fe (%)	EPR Spin (µM)
Reconstituted Wild type	**166**	**n.d.**
C60->S	**66**	**18.8**
C66->S	**55**	**21.2**
C69->S	**89**	**5.8**
C73->S	**n.d.**	**22.3**
C93->S	**55**	**11.5**
C96->S	**n.d.**	**13.3**
C101->S	**40**	**10.0**
C105->S	**45**	**3.2**

Single cluster mutants

In a first round cluster mutants were generated, which lacked the binding sites for whole clusters. All four (three for the SAM cubane) binding sites of one cluster were mutated. The resulting construct was believed to contain two unaffected clusters. Indeed, from the Iron-sulfur content it could be estimated, that the cluster mutants harbor only 2/3 of the wildtype metal centers.

While the ΔSAM mutant still harbored the two insert clusters, the EPR-signal for the reduced [4Fe-4S] clusters was dramatically lowered compared to the wild type Hpd-AE. Likewise the catalytic activity towards SAM as well as towards HpdBC was gone (figure 24).

Interestingly, an elimination of the second insert cluster (ΔIb) – leaving the SAM cubane as well as the Ia cluster unaffected – resulted in a similar EPR-picture. The ΔIa mutant on the other hand harbored more reduced clusters than the other two mutants of this group. It is therefore likely that the contribution of the Ia cluster to the wild type EPR is only marginal. Since the elimination of the SAM cluster as well as Ib dramatically affect the EPR-signal a major contribution of this clusters to the wild type signal may be stated.

The activation capacity of the two insert mutants towards the decarboxylase was around 17 ± 7 % of the wild type (3 vs. of 16 U/mg). They exhibited SAM turnovers of 14 ± 6 % of the wild type when the futile cycle was measured and 8 ± 2 % under assay conditions. These results demonstrate that the insert clusters are kinetically competent for maximum activity of the AE, while the SAM cluster is essentially needed to convert SAM to 5' deoxyadenosine and methionine.

Double cluster knock-outs

Having the single cluster mutants at hand, double cluster knock-outs were generated harboring only one unaffected cluster. Upon purification they exhibit a brownish color and their metal content was estimated to be 1/3 of the wild type; suggesting the presence of one residual [4Fe-4S] cluster. While the double cluster knock-outs carrying only one of the insert clusters (Ia only, Ib only) were completely inactive, the mutant containing only the SAM cluster (SAM only) converted SAM to 5' deoxyadenosine with residual activity accounting for about 5% of the wild type. The EPR signal for these mutants could not be obtained yet.

Single cysteine to serine mutants

Since both insert clusters seems to participate in catalysis, single cysteine to serine exchanges were performed to elucidate the binding of the cluster. From the structurally similar clostridial ferredoxins, it is known that the binding of the clusters is not consecutive with the amino acid sequence but happens in a cross-over fashion. To understand the contribution of the eight cysteines found in the inserted 60 amino acid sequence to the cluster binding, single exchanges of individual cysteines to serines were performed.

The resulting mutants highly differed in their ability to coordinate iron and sulfur, as reflected in their heterogenous metal contents. Like the two insert cluster mutants (ΔIa, ΔIb) their catalytic performance was dramatically reduced. In EPR, three different signals could be differentiated: While the C60S, C66S and C73S mutants showed EPR signals comparable to

the wild type, the C93S, C96S and C101S gave only around half the EPR intensity and C69S as well as C105S harbored only a small fraction of reduced [4Fe-4S] cubanes (figure 24). From these findings it can be deduced that cysteine 69 and cysteine 105 significantly contribute to the cluster binding, while the involvement of Cys60, Cys66 and Cys73 seems to be unlikely. Still it remained unclear if one or two additional clusters are coordinated by the insert motive.

Form all these data's it can be concluded, that indeed three individual clusters may be present in the AE. The SAM cluster could be confirmed as being catalytically essential, while the additional clusters also participate in the electron-flow during catalysis. The exact binding of the two clusters however remains to be unsolved; from the mutants generated so far a cross over binding in a similar fashion but with different spacing compared to the one known for clostridial ferredoxins may be postulated.

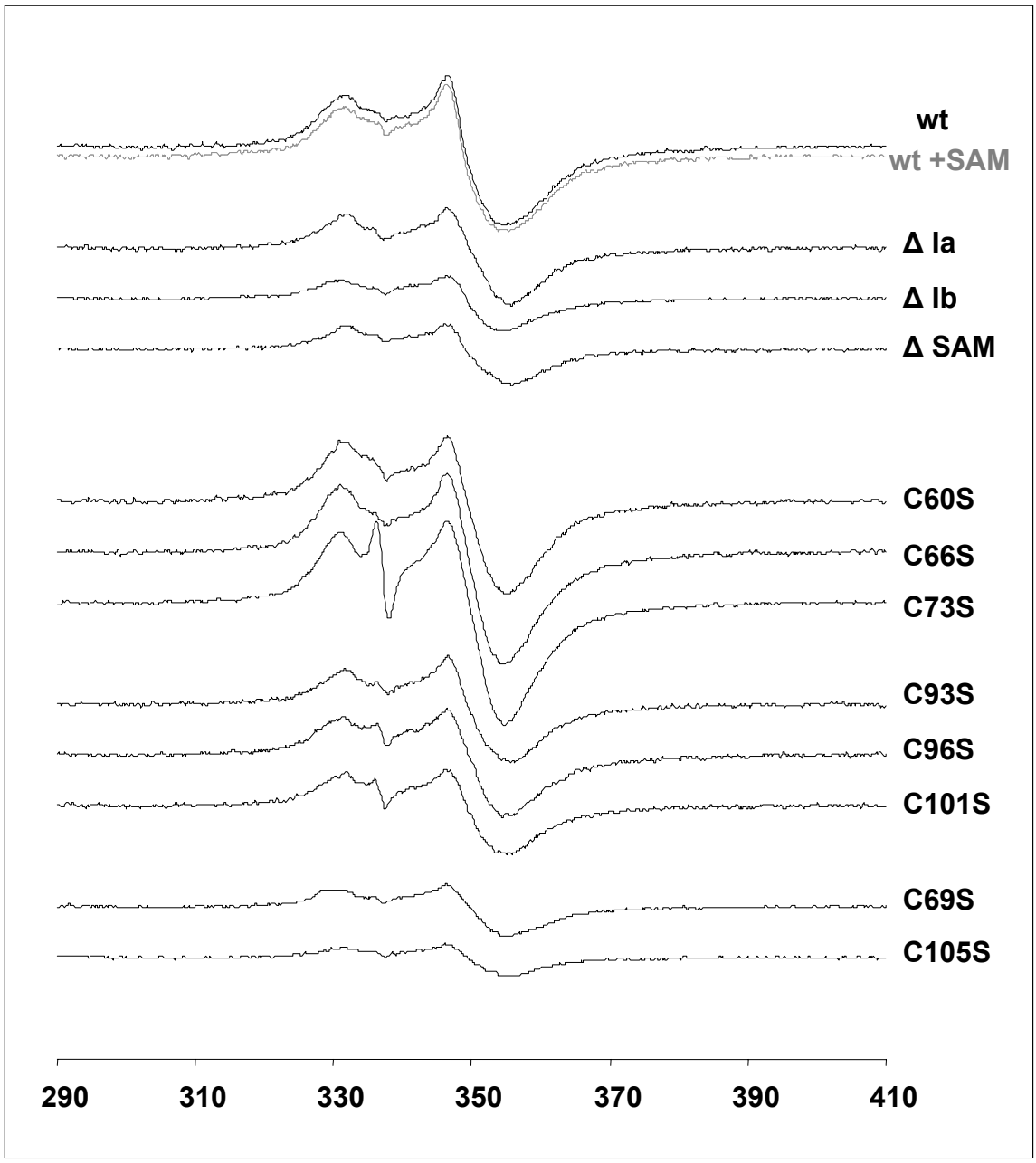

figure 24 EPR spectroscopy of HpdA mutants showing the signal of the reduced [4Fe-4S] cluster. Protein concentration was adjusted to 4mg/ml. The samples were reduced with 1mM dithionite for 5-10 min.

4 Discussion

The aim of this work was to elucidate the regulatory mechanisms involved in the activation and inactivation process of the clostridial arylacetate decarboxylases. Besides the well known system of *C. difficile,* closely related systems from *C. scatologenes* and *T. forsythensis* were also included in some experiments.

When compared to other members of the glycyl radical family, the here described members differ in the presence of additional [4Fe-4S] clusters in both protein partners, the additional presence of a small, regulatory subunit and a phosphorylation of the glycyl radical subunit. Biochemically they seem to be tighter regulated than their previously studied counterparts. Noteworthy, only a limited number of publications concerns the regulation (especially Nrd (102)) or radical dissipation (Pfl (65)) of glycyl-radical proteins. To fully understand the complex regulatory machinery described in this work, a broader view on cresol formation by *C. difficile* may be needed:

4.1 Regulation of cresol formation

- a concerted mechanism involving different cell parameters

The fast production of Cresol by *C. difficile* in its normal habitat – the mammalian gastro-intestinal system - may be of importance for proliferation of this organism after antibiotic treatment. Under physiological conditions HPA but not tyrosine is the inducer of the genes coding for the decarboxylase system and is seemingly fast activated, reaching cresol levels exceeding 10 mM in the medium. In line with this observation is the fast activation of the system on a molecular level, seen in the *in vitro* reconstituted system.

Interestingly, *C. difficile* cannot detoxify cresol, and its formation is suicidal for batch cultures in media, which do not promote sporulation. Therefore cresol formation causes a considerable risk of self-elimination for the pathogen. Hence a tight regulation of cresol formation and the co-ordination with other elemental cellular processes is absolutely necessary in order to avoid detrimental effects on the producer. Therefore the observed inactivation of the *in vitro* system may be of regulatory relevance under natural conditions.

The simplest way to control the decarboxylase activity may be imagined as a feedback inhibition by cresol, while a certain threshold of the process could be established by co-operative substrate binding to the multimeric enzyme. Since the decarboxylase requires a post-translational activation, this process may account for an alternative site of regulation. However, the recombinant decarboxylase is not inhibited by cresol as indicated by a linear

increase of cresol concentrations yielding values above 5 mM in enzymatic tests, and the enzyme exhibits typical Michaelis-Menten kinetics (101). Moreover, the activation of recombinant precursors proceeds smoothly in the presence of cresol (3.2 mM). The slow inactivation by the small subunit described for the reconstituted system may account for an alternative mode of regulation. Nevertheless a more sophisticated regulatory scheme is required for a meaningful regulation of the Hpd system.

The required regulatory mechanism needs to expand the regulatory variables beyond the enzymes' catalytic reactants, which links Hpd activity with elemental cellular processes including energy metabolism and internal redox potential. Such specialized and dedicated regulatory mechanisms are provided by allosterism, covalent modification or redox mediators.

Allosterism and covalent modification

Indeed, it is known from the very first analysis of the amino acid sequence of HpdB that this enzyme contains a P-loop motif (Walker A), which could indicate a nucleotide-dependent allosteric regulation of the enzyme. First experiments – based on the newly available crystal structure of CsdBC – suggest NADH as possible partner.

Additionally, there is clear evidence for a serine-specific phosphorylation of the glycyl radical subunit of all three wild type systems, which can easily link the cresol formation to other cellular processes in a reversible manner, and may allow a tuning of the Hpd activity according to the actual needs of the organism (101).

Likewise from the very beginning it is known, that the *in vivo* clostridial decarboxylase can be purified as an almost inactive dimer of HpdB; while the catalytically competent complex of the *in vitro* system purifies as a hetero-octameric complex of HpdBC. Already this initial observation suggested a regulatory role of the small subunit HpdC during catalysis. Together with previously published data the results presented in this work suggest two regulatory properties for the small subunit: a) complex formation / stability and b) radical dissipation (50, 99, 101).

Both functions are linked to the two residual [4Fe-4S] clusters seen in the crystal structure. It could be established, that only one cluster is redox active (mid point potential: -278 mV), suggesting a more structural function of the second cluster. This notion is supported by the *Tannerella forsythensis* system, which naturally lacks the N-terminal cluster and exhibits a lower oligomeric state than its clostridial counterparts. Likewise, a lower oligomeric state can be found in the soluble hybrid decarboxylases, which were generated by fusing the different small and big subunits, of the three known systems, and in the hybrid decarboxylases, which

carry the different cluster binding sites of the small subunit and an unaltered big subunit. The same holds true for the single cysteine to serine mutants of the *C. scatologenes* small subunit: there exchanged ligants of the N-terminal cluster resulted in a hetero-octameric complex, which can be activated by its cognate AE. The C-terminal cluster in contrary is essentially needed for solubility and complex formation. All mutations in these sites completely abolished the function of the protein, which hinders further studies to differentiate the exact functions of the two clusters. To fully establish their function and the regulatory role of the small subunit further mutational as well as EPR measurements are needed.

Taking the structural information into account the evidence for the structural importance of the C-terminal cluster becomes even more evident, since this region of the small subunit is highly involved in the formation of the active complex. The N-terminal part seems to be more flexible. It may be hypothesized that this region is needed to cooperate with the N-terminal phosphorylation site of the big subunit to establish the catalytically competent hetero-octameric complex. Since the N-terminal 35 amino acids of CsdB are unordered in the crystal, their role as flexible linker, receiving the phosphorylation signal and stabilizing the catalytically essential complex, remains to be established.

The functional small subunit derivatives (hybrid small subunits as well as the mutants of the N-terminal cluster) are catalytically competent hetero-octamers and yield about 10-40% of the wild type maximal activity. They inactivate in a similar to the wild type, which further stresses the function of the altered N-terminal cluster during complex formation as well as activation. Additionally these data may suggest that the redox active cluster needed for radical quenching is the residual C-terminal cluster. In the *T. forsythensis* wild type this cluster may not be fully reduced since the wild type TfdBC complex is almost EPR silent.

Of special interest for the participation of the small subunits in the transient activation, are some observations of the *Tanneralla forsythensis* system: This system has been initially characterized as inactive hetero-tetrameric complex of unknown function and limited ability to be activated by its cognate AE. However a construct, which contained TfdB a chimeric small subunit composed of the N-terminal half of HpdC and the C-terminal half of TfdC, could be activated by CsdA to yield 9% of wild type clostridial decarboxylase activity towards HPA. This was the first reported activity for the *Tannerella* system on a substrate level. Since the active site of TfdB (binding HPA) was not altered, it could be deduced from this experiments, that the Tfd as well as Csd and Hpd may be grouped in the arylacetate decarboxylase family. This unusual gain of function mutant further supports the hypothesized role of the C-terminal cluster as being essential for the solubility of the complex and the N-

terminal cluster as being essentially needed for the formation of the catalytically competent hetero-octameric complex, which can be activated *in vitro*.

In the *in vivo Tannerella forsythensis* system the missing N-terminal cluster may be substituted by a yet unknown constituent, which is lacking in the recombinant protein. Indeed the *tfd* operon contains an open reading frame for an additional – most probably membrane bound – protein (TfdD) similar to the major facilitator protein superfamily. Since these proteins usually act as secondary carriers, which use electrochemical gradients to thrive active transport of small molecules across the cytoplasma membrane, TfdD might act in substrate uptake or be involved in the formation of the catalytically active complex and act as redox mediator for the small subunit (103, 104). It may be hypothesized that TfdD is essentially needed to assemble a membrane bound, catalytically active, hetero-octameric complex.

Conclusively, the two clusters in the small subunit are highly involved in the complex regulation of the system. They not only are essential for the formation of the hetero-octameric complex, which can be activated *in vitro*, but likewise are needed to solublize the complex and quench the glycyl-radical signal. An additional mode of regulation to the previously suggested regulation via phosphorylation and allosterism (complex formation of hetero-octameric HpdBC) was found in the redox state of the [4Fe-4S] clusters, which may allow a regulation mediated by the metabolic/redox state of the clostridial cell.

4.2 A redox driven regulation of enzyme activity – evidence and perspective

From the data presented in this work two redox dependent processes could be differentiated: a) the slower radical dissipation mediated by the cluster(s) of the small subunit and b) the fast activation of the glycyl radical precursor by its AE. (Additionally, as an *in vitro* side reaction a redox dependent futile SAM cycle could be established.)

4.2.1 Trans activation – the role of the small subunit in inactivation

One way of terminating cresol formation would be the dissipation of the glycyl radical. Nevertheless, the fate of the rather stable glycyl radical *in vivo* is still unknown and the means of inactivation far from being understood.

Therefore the observed intrinsic inactivation of the decarboxylase complex is of significant importance, to get hints about the radical dissipation under *in vivo* conditions. Nevertheless, it should be noted that the observed inactivation for the *in vitro* reconstituted system only takes

place in the absence of substrate and, therefore, provide a switch-off mechanism when HPA is depleted.

If the recombinant arylacetate decarboxylase system is reconstituted *in vitro* without the addition of HPA, the glycyl radical formation is of transient nature. After an initial fast activation, the obtained glycyl radical signal measured by EPR as well as the specific activity of the decarboxylase decline over prolonged incubation times.

In analogy to the Pfl and Nrd system, the glycyl radical established upon activation needs to be transferred to a conserved cysteine in the active site, before it can react with HPA. It could be shown, that the radical quenching is independent of the active site cysteine, since an exchange of the active site cysteine to serine – thought it completely abolished the turnover of HPA to cresol – had no detrimental effect on glycyl radical signal formation nor quenching (100). From this finding it can be deduced that the activation as well as the radical dissipation involve directly the storage glycinyl residue rather than involving the active site thiol.

Since the radical dissipation can be envisaged as a one electron reduction followed by an addition of an environmental proton, an involvement of reduced [4Fe-4S] clusters as electron donor seems likely. Altogether there are up to five redox active clusters in the arylacetate decarboxylase system present. Three are bound by the activating enzyme and two are coordinated by the small subunit of the decarboxylase.

To elucidate the role of these clusters, gel filtration experiments were performed, which separated the two protein components of the system. The fraction containing the decarboxylase alone could be inactivated by the addition of chemical reductants; the further addition AE and SAM could not reverse the observed inactivation. These findings suggest that the inactivation of the glycyl radical is not only an intrinsic property of the decarboxylase – most probably mediated by the [4Fe-4S] clusters of the small subunit – but also is irreversible under highly reductive conditions.

A similar result could be obtained by photoreduction of the system. Since all measurable reactions of Hpd AE are highly dependent on an external electron source and immediately stop, when the light is switched off in photoreduction experiments, it may be argued that the inactivation process seen in darkened samples is mediated by the $[4Fe\text{-}4S]^{+1/+2}$ clusters of the small subunit. These clusters – already reduced upon irradiation – seem to be readily re-oxidised and deliver the electrons to the active site glycyl-radical, when substrate is absent. An almost equimolar ratio of cluster re-oxidation and radical-quenching further supports the participation of the reduced cluster in the small subunit during radical dissipation. However, if

the clusters are continuously re-reduced by excess of chemical reductants, an ongoing futile cycle of activation and re-inactivation is generated.

From the presented experiment it can be deduced that the radical dissipation is an intrinsic function of the decarboxylase complex and that the radical quenching is accompanied not only by a loss in specific activity but simultaneously by an equimolar oxidation of the reduced cluster(s) of the small subunit. However, the crystal structure of CsdBC illustrates a distance between the clusters in the small subunit and the active site of 40 to 41 Å. A distance to far for an unattended electron transfer. Nevertheless a similar distance (35 Å) needs to be bridged during the activation of anaerobic ribonucleotide reductase and it has been suggested that specific amino acid residues are involved in this long range electron transfer (98, 105).

Likewise, the crystal structure of CsdBC verifies the presence of two [4Fe-4S] clusters; at least one is redox active (mid point potential of -278 mV in HpdBC). Of special interest in defining a functional role of the two clusters during catalysis is their impact on complex formation as well as radical dissipation, which was addressed in mutational analysis.

Taken together all findings, the mutants suggest, that the C-terminal cluster may be involved in complex formation and primarily have a structural role, while the N-terminal cluster seems to be essential for full activation and may be the redox active cluster needed for radical dissipation. Further studies with this and other mutants (gelfiltration, Fe-S determination, transient activation, EPR, crystallization, etc.) are desirable to fully characterize the function of the two clusters.

Possible candidates for new mutants are found in the metal binding sites of the two clusters (single amino acid exchanges as well as cluster knock-outs or further chimeric recombination) as well as residues in the putative electron-channel connecting the clusters with the active site in the decarboxylase, which may be deduced from the structure.

4.2.2 Activation - does the insert cluster speed up the activation process?

The tight regulation of cresol formation by *C. difficile* can already be monitored on a genetic level where the presence of 4-hydroxyphenylacetate (HPA) in the growth medium readily initiates the transcription and translation of the *hpd* system (100). In line with that is the observation of a fast responding activation process. While recombinant Nrd and Pfl need to be pre-reduced for 30 to 60 min in vitro to gain maximum activation, the Hpd system is readily reduced within 5 to 10 min with chemical reductants. This observation together with the fact that the EPR signal obtained for the reduced [4Fe-4S] clusters did not change upon the addition of SAM, gave first evidence that Hpd-AE indeed harbors additional clusters.

Likewise, the as purified activating enzyme contained enough iron and sulfur to build two to three [4Fe-4S] clusters and was catalytically active without having been reconstituted further. The mutational analysis presented in this work gave further evidence for the presence of three individual clusters coordinated by the AE. However the interpretation of the obtained data is still not fully conclusive:

The SAM cluster and mutations in related SAM-radical enzymes

The structural and functional role of the SAM cluster is well established in literature. (2, 85) and has therefore been individually addressed in this work. The cluster mutants presented verified that the SAM cubane is essential for catalysis. Nevertheless, the tight SAM binding, which causes distinct changes in the EPR spectra of Pfl-AE (106) and Nrd-AE (83) upon addition of SAM, could not be observed. Although a similar binding mode can be predicted for the decarboxylase AEs, no significant SAM-dependent changes of the EPR signals of the reduced [4Fe-4S] centers were found. To understand the very similar EPR signals of the presented mutants, an overview about mutational analysis of SAM enzymes should be given:

Mutational studies in the well studied Nrd-AE and Pfl-AE, which carry only the SAM cubane, revealed the catalytic importance of this cluster. The cysteine to serine mutations of the Pfl-AE as well as a cysteine to alanine exchange abolished the function of the AE (107, 108), which is in line with the results of the SAM cluster mutants presented in this work.

Since Pfl and Nrd carry only the SAM cluster, a comparison with other members of the SAM-radical family is needed to evaluate the insert cluster mutants. So far a second cluster has been described for BioB, LipA and MoaA and is speculated to be present in Gdh-AE and Bss-AE (40, 59, 109). The second cluster in BioB and LipA is believed to be involved in sulfur insertion and able to switch from an [4Fe-4S] to an [2Fe-2S] cluster during catalysis; a role quite different to the one postulated for the additional clusters of Hpd-AE (93, 110).

Similar to the observations for BioB the Hpd-AE mutants presented in this work show only minor changes concerning their iron-sulfur content and EPR-fingerprints. It is likely that the observed EPR signal is a mixture of individual signals, but the contribution of the individual clusters is extremely difficult to address:

Cluster binding and structural considerations – defining an electron wire

Looking at the binding sites of the clusters, decarboxylase AEs evidently contain one or two iron-sulfur center(s), which are coordinated by a 60 amino acid insert between the SAM cluster motif (GCx_3Cx_2CxN) and the SAM-binding motif II (Gx_4GG) (70). The insert

provides eight cysteinyl ligands for up to two [4Fe- 4S] centers, which show an unusual spacing of the cysteines, that is $Cx_5Cx_2Cx_3C$ and $Cx_2Cx_4Cx_3C$. Interestingly, similar inserts (providing one or both motifs) are found in all GRE AEs with the exception of Pfl- and Nrd-AEs (40) (compare figure 19) suggesting that these AEs also contain additional iron-sulfur clusters. Note, that all conserved amino acids in this stretch are cysteins.

Considering just the 60 amino acid insert, an ancient relationship to clostridial ferredoxins could be deduced from multiple sequence alignments. These ferredoxins are described to contain two redox active [4Fe-4S] clusters. Both clusters are coordinated by a $Cx_2Cx_2Cx_3CP$ motif. (Note that they are coordinated in a cross-over fashion: cluster I: C8,C11,C14,C47, cluster II C18,C37,C40,C43).

Even though a cross over binding could be anticipated for the binding of the insert clusters, the first mutational approach was to eliminate four cysteines in a row and exchange all eight cysteines individually to serines. All mutants described so far clearly affect catalysis. Therefore it seems likely, that both insert clusters are needed for a concerted action. Since no such cluster has been found in the well studied AE of Pfl and Nrd, a direct involvement in SAM cleavage seems unlikely; however, as deduced form 5' deoxyadenosine liberation, an involvement of the insert clusters in electron flow to the SAM cubane or a function as electron wire connecting an outside redox mediator and the active site SAM cubane is possible.

Nevertheless neither the cluster knockouts nor the single mutants generated so far affected the overall shape of the EPR signal. An involvement of Cys69 and Cys105 in cluster binding is very apparent, since mutations in this position almost abolished the EPR signals. While Cys60, Cys66 and Cys73 resemble the wild type signal and may therefore not be crucial for metal coordination or stability, a participation of Cys93, Cys96 and Cys101 is likely, since mutations of these residues yielded reduced signal intensities in EPR.

For all mutants the EPR line shape resembles the wild type signal and varies only in the signal intensities. It could be confirmed that only [4Fe-4S] clusters are present; no damaged [3Fe-4S] clusters or [2Fe-2S] clusters were visible.

A cross over binding of the cluster may be further postulated by these data, but needs to be further analyzed. Double knock-outs of Cys69 and Cys105 or triple knock outs of the seemingly similar single exchanges may be generated to elucidate the binding mode in more detail. Since cysteine to serine exchanges are rather soft concerning their effects in cluster binding, a replacement by alanine may further contribute to understand the cluster binding.

However, the possible combination of knockouts needed to fully understand the cluster binding properties by far exceeds the possibilities of this study and waits for future analysis.

To understand the role of the individual clusters in more detail, it would be extremely helpful to perform further measurements in the presence of SAM and investigate the nature of the clusters by Mössbauer spectroscopy. Since it could be shown, that the iron-sulfur clusters of the wild type could be reconstituted *in vitro*, further studies should be carried out with reconstituted mutants.

Activation - 5' deoxyadenosine as indictor for the activation process.

Concerning the activation process, one of the first findings distinguishing the arylacetate decarboxylases from the known glycyl radical enzymes, was the fast activation observed. To gain further insight into the activation process, a direct measurement to quantify the 5' deoxyadenosine was employed.

Measuring the arylacetate-decarboxylase system, it could be demonstrated indirectly that under assay conditions SAM is needed to generate the glycyl radical in the decarboxylase. It was calculated that, when the decarboxylase was present, both reactions (activation, futile cycle) take place in parallel. However, when substrate was missing an additional futile cycle could be observed, which further liberated 5' deoxyadenosine. Only this cycle was visible when monitoring the AE alone (in absence of decarboxylase and HPA) under reducing conditions with SAM.

In line with this is the finding, that all mutants of the insert cluster are catalytically impaired in both processes. This suggests that the insert clusters are involved in channeling the electron from an outside mediator to the SAM cubane in the active site (electron wire). A close proximity to the bound SAM molecule would also explain the futile cycle, since the liberated 5' deoxyadenosine radical may be quenched to a 5' deoxyadenosinylate by a second incoming electron from these clusters and an environmental proton.

Having a method at hand to quantify the reactions of the AE, it would be of further interest to investigate the kinetic properties (Michaelis-Menten) of the activation as well as of the futile SAM cycle in more detail. Additionally the very short lived nature of all reactions mediated by the AE could be established by applying photoreducing conditions and stop-flow and may contribute to a detailed analysis of the system in the future.

Redox states of the clusters - a way of regulation?

Having up to five [4Fe-4S] clusters in the decarboxylase system which exhibit different redox properties, a mode of regulation via these clusters may be postulated:

Concerning the AE, a fast mode of reduction could be established. The photoreducing experiments gave further evidence that the reduced clusters are extremely short lived during an activation process and only reduced under highly reductive conditions. Likewise a fast mode of reduction / activation was observed. All reactions of the activating enzyme could be controlled by changing the reductive environment (presence of light).

Considering an analogy of the insert clusters to the clostridial ferredoxins and taking the known redox potentials for SAM radical enzymes into account, a mid point potential of below -500mV could be anticipated for the clusters of the AE. The two redox centers in clostridial ferredoxins are at biologically relevant electron-transfer distances (center-to-center 12 Å, edge-to-edge 6.2 Å). They are described to exhibit equal potentials of -400 mV. Other bacterial ferredoxins are slightly longer (around 80 amino acids) and show a slightly modified binding of the second cluster. The midpoint potentials of these clusters is reported to be even more negative: -420 to -485 mV for cluster I and -585 to -675 mV for cluster II (111). From these considerations it may be estimated that the redox potential of the insert clusters may be equally low, though the contribution of the surrounding protein is unknown.

In this respect it should be noted that the reported redox potential for SAM cubanes is around -430 to -497 mV for lysine-2,3-aminomutase (LAM) (112) and -440 to -505 mV for Biotin-synthase (BioB) (113). Pfl-AE is believed to have a midpoint potential of around -500 mV (1) and Nrd-AE has been described to be -550 to -620 mV (84). Taking into consideration that the EPR spectra of clostridial arylacetate decarboxylase AE are not affected by SAM binding, it may be estimated that the major clusters visible under these conditions are the so called insert clusters.

Note that the redox potential of the used chemicals is -660mV (dithionite) and -480mV (Ti^{3+}). Interestingly the activation with Ti^{3+} only proceeds in the presence of Na_2SO_3; previous work suggests that in this case the sulfuranyl-radical anion is directly formed from Ti^{3+} and SO_2 [97]. Nevertheless the futile SAM cycle described in this work can be driven by Ti^{3+} alone; suggesting that at least one of the clusters can be reduced under these conditions.

In contrary the radical dissipation is a rather slow process involving the reduced cluster of the small subunit. It could be shown that radical quenching of the glycyl-radical site involves an almost equimolar oxidation of the reduced cluster of the small subunit, which exhibits a midpoint potential of around -278mV.

Since most experiments have been carried out under highly reductive conditions, the activation process as well as radical dissipation takes place in parallel. However, it seems likely that under in vivo conditions both processes need to be separated. Therefore it is likely that both actions relay on different cellular redox mediators.

Additionally, there is striking evidence that the presence of HPA dramatically change the reaction conditions; it not only terminates the futile SAM cycle of the AE but simultaneously prevents radical dissipation of the decarboxylase.

4.3 Conclusion

From the findings presented in this work a new way of regulation arylacetate decarboxylases may be deduced:

Besides the allosteric regulations mediated by complex formation and phosphorylation a redox dependent mechanism is postulated, involving the clusters of both protein partners. On the one hand it may be stated that for AE more than the essential SAM cluster is needed for catalysis, that this cluster(s) are coordinated by a 60 amino acid stretch not found in previously characterized GRE-AEs and that the activation process takes readily place without further cluster-reconstitution. It could also be established that the EPR signal does not change upon SAM binding, which makes a primary reduction of the additional clusters likely; they are believed to have a mid point potential below the usual SAM cluster (which is reported to be around -500 mV). It was also found that the reduced clusters in the AE are very short lived, which may further support highly reactive, low potential clusters. Under *in vitro* conditions this low redox state may drive the excess futile SAM cycle described in this work and lead to additional SAM cleavage. In contrary, this low redox potential may be *in vivo* needed to metabolically differentiate more precisely the redox state desired for activation and radical dissipation.

In line with that is the finding that the radical dissipation – found in the absence of HPA – is mediated by the decarboxylase itself and proceeds slowly over prolonged incubation times. The radical dissipation is favored under highly reductive conditions normally employed for the reconstituted system. Under photoreducing conditions however a reactivation seems possible, making a redox dependent regulation of the system extremely likely. Whereas the activation is terminated in the dark, radical dissipation proceeds and is accompanied by equimolar oxidation of previously reduced [4Fe-4S] cluster(s) of the decarboxylase.

The regulatory function of the small subunit could be further established and involves besides the role in radical quenching an impact in the formation of the catalytically active hetero-octameric complex as well as in the allosteric regulation of the system. First ideas of a differentiated function of the two clusters could be addressed and a gain of function mutant of the *T. forsythensis* system could validate the grouping into the glycyl-radical arylacetate decarboxylase family.

Altogether a complex mode of regulating the decarboxylase function could be elucidated, which involves redox state of the reduced [4Fe-4S] clusters of both protein partners.

4.4 Outlook

The data presented here clearly show, that GRE decarboxylases display a number of novel properties, which are not found in other systems and future work will focus on the elucidation of these features. The proper understanding of the individual processes involved in the SAM-dependent radical formation and in the SAM-independent quenching of the radical mediated by the decarboxylase will contribute to a more detailed understanding of the molecular mechanisms involved in the enzymatic handling of these highly reactive intermediates.

The first evidence of a redox dependent regulation needs to be further established. For this, additional mutants of the cluster binding sites in both protein partners are needed. Concerning the activating enzyme further studies concerning the [4Fe-4S] clusters by EPR and Mössbauer spectroscopy are desirable to elucidate changes upon SAM binding. Likewise, these experiments will define the redox properties of the individual clusters and give hints about their functional role during catalysis. The characterization of the futile SAM cycle and the biochemical properties of SAM cleavage may now be addressed by directly quantifying the amount of 5' deoxyadenosine liberated. However to establish the exact binding mode of the additional insert clusters a high number of double and triple knock-outs would be needed.

The analysis of the structural and functional properties of the decarboxylases will be facilitated in the future by the crystal structure of 4-hydroxyphenylacetate decarboxylase from *C. scatologenes*. Co-crystallization of the two protein partners may help to elucidate the structure of the activation enzymes. Likely, the crystal structures of the Hpd as well as the Tfd system will prove hallmarks in revealing the three dimensional structure of these proteins and in helping understand their complex regulation. Besides the binding mode of the small subunits, their contribution to complex formation, the substrate binding and binding of effector-molecules (possibly NAD) is of interest.

To further understand the mechanisms involved in radical dissipation, mutational studies of the small cluster need to be continued in the future. The structural and functional role of the two clusters found in this subunit needs to be further established, and the residues involved in the long distance electron flow to the active site of the decarboxylase wait to be established. Additionally the regulation via phosphorylation of the N-terminus of HpdB as well as the impact of cresol on the activation process may be further exemplified.

References

1. Walsby, C. J., Ortillo, D., Yang, J., Nnyepi, M. R., Broderick, W. E., Hoffman, B. M., and Broderick, J. B. (2005) Spectroscopic approaches to elucidating novel iron-sulfur chemistry in the "radical-Sam" protein superfamily. *Inorg Chem* 44, 727-741
2. Walsby, C. J., Ortillo, D., Broderick, W. E., Broderick, J. B., and Hoffman, B. M. (2002) An anchoring role for FeS clusters: chelation of the amino acid moiety of S-adenosylmethionine to the unique iron site of the [4Fe-4S] cluster of pyruvate formate-lyase activating enzyme. *J Am Chem Soc* 124, 11270-11271
3. Savage, D. C. (1977) Microbial ecology of the gastrointestinal tract. *Annu Rev Microbiol* 31, 107-133
4. Whitman, W. B., Coleman, D. C., and Wiebe, W. J. (1998) Prokaryotes: the unseen majority. *Proc Natl Acad Sci U S A* 95, 6578-6583
5. Backhed, F., Ley, R. E., Sonnenburg, J. L., Peterson, D. A., and Gordon, J. I. (2005) Host-bacterial mutualism in the human intestine. *Science* 307, 1915-1920
6. Benno, Y., Sawada, K., and Mitsuoka, T. (1984) The intestinal microflora of infants: composition of fecal flora in breast-fed and bottle-fed infants. *Microbiol Immunol* 28, 975-986
7. Stark, P. L., and Lee, A. (1982) The microbial ecology of the large bowel of breast-fed and formula-fed infants during the first year of life. *J Med Microbiol* 15, 189-203
8. Chaves-Olarte, E., Freer, E., Parra, A., Guzman-Verri, C., Moreno, E., and Thelestam, M. (2003) R-Ras glucosylation and transient RhoA activation determine the cytopathic effect produced by toxin B variants from toxin A-negative strains of Clostridium difficile. *J Biol Chem* 278, 7956-7963
9. Brito, G. A., Sullivan, G. W., Ciesla, W. P., Jr., Carper, H. T., Mandell, G. L., and Guerrant, R. L. (2002) Clostridium difficile toxin A alters in vitro-adherent neutrophil morphology and function. *J Infect Dis* 185, 1297-1306
10. Genth, H., Huelsenbeck, J., Hartmann, B., Hofmann, F., Just, I., and Gerhard, R. (2006) Cellular stability of Rho-GTPases glucosylated by Clostridium difficile toxin B. *FEBS Lett* 580, 3565-3569
11. Sebaihia, M., Wren, B. W., Mullany, P., Fairweather, N. F., Minton, N., Stabler, R., Thomson, N. R., Roberts, A. P., Cerdeno-Tarraga, A. M., Wang, H., Holden, M. T., Wright, A., Churcher, C., Quail, M. A., Baker, S., Bason, N., Brooks, K., Chillingworth, T., Cronin, A., Davis, P., Dowd, L., Fraser, A., Feltwell, T., Hance, Z., Holroyd, S., Jagels, K., Moule, S., Mungall, K., Price, C., Rabbinowitsch, E., Sharp,

S., Simmonds, M., Stevens, K., Unwin, L., Whithead, S., Dupuy, B., Dougan, G., Barrell, B., and Parkhill, J. (2006) The multidrug-resistant human pathogen Clostridium difficile has a highly mobile, mosaic genome. *Nat Genet* 38, 779-786

12. Elsden, S. R. H. M. G. a. W., J.M. (1976) The end products of the methabolism of aromatic amino acids by Clostridia. *Arch Microbiol* 107, 283-288
13. Barker, H. A. (1981) Amino acid degradation by anaerobic bacteria. *Annu Rev Biochem* 50, 23-40
14. Stickland, L. H. (1934) Studies in the metabolism of the strict anaerobes (genus Clostridium): The chemical reactions by which Cl. sporogenes obtains its energy. *Biochem J* 28, 1746-1759
15. Smith, E. A., and Macfarlane, G. T. (1997) Formation of Phenolic and Indolic Compounds by Anaerobic Bacteria in the Human Large Intestine. *Microb Ecol* 33, 180-188
16. Probst, E. L., Flickinger, E. A., Bauer, L. L., Merchen, N. R., and Fahey, G. C. (2003) A dose-response experiment evaluating the effects of oligofructose and inulin on nutrient digestibility, stool quality, and facal protein catabolites in healthy adult dogs. *J Anim Sci* 81, 3057-3066
17. Smith, E. A., and Macfarlane, G. T. (1996) Enumeration of human colonic bacteria producing phenolic and indolic compounds: effects of pH, carbohydrate availability and retention time on dissimilatory aromatic amino acid metabolism. *J Appl Bacteriol* 81, 288-302
18. Birkett, A. M., Jones, G. P., de Silva, A. M., Young, G. P., and Muir, J. G. (1997) Dietary intake and faecal excretion of carbohydrate by Australians: importance of achieving stool weights greater than 150 g to improve faecal markers relevant to colon cancer risk. *Eur J Clin Nutr* 51, 625-632
19. Birkett, A. M., Jones, G. P., and Muir, J. G. (1995) Simple high-performance liquid chromatographic analysis of phenol and p-cresol in urine and feces. *J Chromatogr B Biomed Appl* 674, 187-191
20. Birkett, A., Muir, J., Phillips, J., Jones, G., and O'Dea, K. (1996) Resistant starch lowers fecal concentrations of ammonia and phenols in humans. *Am J Clin Nutr* 63, 766-772
21. Brooks, J. B., Nunez-Montiel, O. L., Wycoff, B. J., and Moss, C. W. (1984) Frequency-pulsed electron capture gas-liquid chromatographic analysis of metabolites

produced by Clostridium difficile in broth enriched with amino acids. *J Clin Microbiol* 20, 539-548

22. Muramatsuo, T. (1990) Gut microflora and tissue protein turnover in vivo in animals. *Int J Biochem* 22, 793-800
23. Bone, E., Tamm, A., and Hill, M. (1976) The production of urinary phenols by gut bacteria and their possible role in the causation of large bowel cancer. *Am J Clin Nutr* 29, 1448-1454
24. Alles, M. S., Hartemink, R., Meyboom, S., Harryvan, J. L., Van Laere, K. M., Nagengast, F. M., and Hautvast, J. G. (1999) Effect of transgalactooligosaccharides on the composition of the human intestinal microflora and on putative risk markers for colon cancer. *Am J Clin Nutr* 69, 980-991
25. Brunet, P., Dou, L., Cerini, C., and Berland, Y. (2003) Protein-bound uremic retention solutes. *Adv Ren Replace Ther* 10, 310-320
26. Cerini, C., Dou, L., Anfosso, F., Sabatier, F., Moal, V., Glorieux, G., De Smet, R., Vanholder, R., Dignat-George, F., Sampol, J., Berland, Y., and Brunet, P. (2004) P-cresol, a uremic retention solute, alters the endothelial barrier function in vitro. *Thromb Haemost* 92, 140-150
27. Dou, L., Cerini, C., Brunet, P., Guilianelli, C., Moal, V., Grau, G., De Smet, R., Vanholder, R., Sampol, J., and Berland, Y. (2002) P-cresol, a uremic toxin, decreases endothelial cell response to inflammatory cytokines. *Kidney Int* 62, 1999-2009
28. Dou, L., Bertrand, E., Cerini, C., Faure, V., Sampol, J., Vanholder, R., Berland, Y., and Brunet, P. (2004) The uremic solutes p-cresol and indoxyl sulfate inhibit endothelial proliferation and wound repair. *Kidney Int* 65, 442-451
29. Atkinson, G., Bogan, J. A., Breeze, R. G., and Selman, I. E. (1977) Effects of 3-methylindole in cattle. *Br J Pharmacol* 61, 285-290
30. Carlson, J. R., Dickinson, E. O., Yokoyama, M. T., and Bradley, B. (1975) Pulmonary edema and emphysema in cattle after intraruminal and intravenous administration of 3-methylindole. *Am J Vet Res* 36, 1341-1347
31. Carlson, J. R., and Bray, T. M. (1983) Nutrition and 3-methylindole-induced lung injury. *Adv Nutr Res* 5, 31-55
32. Bray, T. M., and Kirkland, J. B. (1990) The metabolic basis of 3-methylindole-induced pneumotoxicity. *Pharmacology & Therapeutics* 46, 105-118

33. Dickinson, E. O., Yokoyama, M. T., Carlson, J. R., and Bradley, B. J. (1976) Induction of pulmonary edema and emphysema in goats by intraruminal administration of 3-methylindole. *Am J Vet Res* 37, 667-672

34. Ulvund, M. J. (1984) 3-Methylindole-induced pulmonary injury in lambs. A comparison with acute respiratory distress syndrome (ARDS). *Nordisk Veterinaermedicin* 36, 253-258

35. Updyke, L. W., Yoon, H. L., Kiorpes, A. L., Robinson, J. P., Pfeifer, R. W., and Marcus, C. B. (1991) 3-Methylindole-induced splenotoxicity: biochemical mechanisms of cytotoxicity. *Toxicol & Appl Pharmacol*109, 375-390

36. Updyke, L. W., Yoon, H. L., Robinson, J. P., Kiorpes, A. L., Marcus, C. B., and Pfeifer, R. W. (1991) 3-Methylindole-induced splenotoxicity: functional analysis of immune parameters and lymphocyte phenotyping by flow cytometry. *Toxicology & Appl Pharmacol* 109, 391-398

37. Yokoyama, M. T., Carlson, J. R., and Holdeman, L. V. (1977) Isolation and characteristics of a skatole-producing Lactobacillus sp. from the bovine rumen. *Appl Environ Microbiol* 34, 837-842

38. Ward, L. A., Johnson, K. A., Robinson, I. M., and Yokoyama, M. T. (1987) Isolation from swine feces of a bacterium which decarboxylates p-hydroxyphenylacetic acid to 4-methylphenol (p-cresol). *Appl Environ Microbiol* 53, 189-192

39. D'Ari, L., and Barker, H. A. (1985) p-Cresol formation by cell-free extracts of Clostridium difficile. *Arch Microbiol* 143, 311-312

40. Selmer, T., Pierik, A. J., and Heider, J. (2005) New glycyl radical enzymes catalysing key metabolic steps in anaerobic bacteria. *Biol Chem* 386, 981-988

41. Sjoberg, B. M., and Graslund, A. (1977) The free radical in ribonucleotide reductase from E. coli. *Ciba Found Symp*, 187-196

42. Lehtio, L., and Goldman, A. (2004) The pyruvate formate lyase family: sequences, structures and activation. *Protein Eng Des Sel* 17, 545-552

43. Eklund, H., and Fontecave, M. (1999) Glycyl radical enzymes: a conservative structural basis for radicals. *Structure Fold Des* 7, R257-262

44. Sawers, G., and Watson, G. (1998) A glycyl radical solution: oxygen-dependent interconversion of pyruvate formate-lyase. *Mol Microbiol* 29, 945-954

45. Buckel, W., and Golding, B. T. (2006) Radical enzymes in anaerobes. *Annu Rev Microbiol* 60, 27-49

46. Wagner, A. F., Frey, M., Neugebauer, F. A., Schafer, W., and Knappe, J. (1992) The free radical in pyruvate formate-lyase is located on glycine-734. *Proc Natl Acad Sci U S A* 89, 996-1000

47. Unkrig, V., Neugebauer, F. A., and Knappe, J. (1989) The free radical of pyruvate formate-lyase. Characterization by EPR spectroscopy and involvement in catalysis as studied with the substrate-analogue hypophosphite. *Eur J Biochem* 184, 723-728

48. Mulliez, E., Fontecave, M., Gaillard, J., and Reichard, P. (1993) An iron-sulfur center and a free radical in the active anaerobic ribonucleotide reductase of *Escherichia coli*. *J Biol Chem* 268, 2296-2299

49. Young, P., Andersson, J., Sahlin, M., and Sjoberg, B. M. (1996) Bacteriophage T4 anaerobic ribonucleotide reductase contains a stable glycyl radical at position 580. *J Biol Chem* 271, 20770-20775

50. Yu, L., Blaser, M., Andrei, P. I., Pierik, A. J., and Selmer, T. (2006) 4-hydroxyphenylacetate decarboxylases: properties of a novel subclass of glycyl radical enzyme systems. *Biochem* 45, 9584-9592

51. Krieger, C. J., Roseboom, W., Albracht, S. P., and Spormann, A. M. (2001) A stable organic free radical in anaerobic benzylsuccinate synthase of Azoarcus sp. strain T. *J Biol Chem* 276, 12924-12927

52. Verfurth, K., Pierik, A. J., Leutwein, C., Zorn, S., and Heider, J. (2004) Substrate specificities and electron paramagnetic resonance properties of benzylsuccinate synthases in anaerobic toluene and m-xylene metabolism. *Arch Microbiol* 181, 155-162

53. Rabus, R., Wilkes, H., Behrends, A., Armstroff, A., Fischer, T., Pierik, A. J., and Widdel, F. (2001) Anaerobic initial reaction of n-alkanes in a denitrifying bacterium: evidence for (1-methylpentyl)succinate as initial product and for involvement of an organic radical in n-hexane metabolism. *J Bacteriol* 183, 1707-1715

54. Fontecave, M., Mulliez, E., and Ollagnier-de-Choudens, S. (2001) Adenosylmethionine as a source of 5'-deoxyadenosyl radicals. *Curr Opin Chem Biol* 5, 506-511

55. Leuthner, B., Leutwein, C., Schulz, H., Horth, P., Haehnel, W., Schiltz, E., Schagger, H., and Heider, J. (1998) Biochemical and genetic characterization of benzylsuccinate synthase from Thauera aromatica: a new glycyl radical enzyme catalysing the first step in anaerobic toluene metabolism. *Mol Microbiol* 28, 615-628

56. Selmer, T., and Andrei, P. I. (2001) p-Hydroxyphenylacetate decarboxylase from Clostridium difficile. A novel glycyl radical enzyme catalysing the formation of p-cresol. *Eur J Biochem* 268, 1363-1372

57. Raynaud, C., Sarcabal, P., Meynial-Salles, I., Croux, C., and Soucaille, P. (2003) Molecular characterization of the 1,3-propanediol (1,3-PD) operon of Clostridium butyricum. *Proc Natl Acad Sci U S A* 100, 5010-5015

58. Becker, A., Fritz-Wolf, K., Kabsch, W., Knappe, J., Schultz, S., and Wagner, A. F. V. (1999) Structure and mechanism of the glycyl radical enzyme pyruvate formate-lyase. *Nature Struct Biol* 6, 969-975

59. O'Brien, J. R., Raynaud, C., Croux, C., Girbal, L., Soucaille, P., and Lanzilotta, W. N. (2004) Insight into the mechanism of the B12-independent glycerol dehydratase from Clostridium butyricum: preliminary biochemical and structural characterization. *Biochem* 43, 4635-4645

60. Logan, D. T., Andersson, J., Sjoberg, B. M., and Nordlund, P. (1999) A glycyl radical site in the crystal structure of a class III ribonucleotide reductase. *Science* 283, 1499-1504

61. Becker, A., and Kabsch, W. (2002) X-ray Structure of Pyruvate Formate-Lyase in Complex with Pyruvate and CoA. How the enzyme uses the cyx-418 thiyl radical for pyruvate cleavage. *J Biol Chem* 277, 40036-40042

62. Leppanen, V. M., Merckel, M. C., Ollis, D. L., Wong, K. K., Kozarich, J. W., and Goldman, A. (1999) Pyruvate formate lyase is structurally homologous to type I ribonucleotide reductase. *Structure* 7, 733-744

63. Lehtio, L., Grossmann, J. G., Kokona, B., Fairman, R., and Goldman, A. (2006) Crystal structure of a glycyl radical enzyme from Archaeoglobus fulgidus. *J Mol Biol* 357, 221-235

64. Reddy, S. G., Wong, K. K., Parast, C. V., Peisach, J., Magliozzo, R. S., and Kozarich, J. W. (1998) Dioxygen inactivation of pyruvate formate-lyase: EPR evidence for the formation of protein-based sulfinyl and peroxyl radicals. *Biochem* 37, 558-563

65. Kessler, D., Herth, W., and Knappe, J. (1992) Ultrastructure and pyruvate formate-lyase radical quenching property of the multienzymic AdhE protein of Escherichia coli. *J Biol Chem* 267, 18073-18079

66. Fontecave, M. (1998) Ribonucleotide reductases and radical reactions. *Cell Mol Life Sci* 54, 684-695

67. Coschigano, P. W., Wehrman, T. S., and Young, L. Y. (1998) Identification and analysis of genes involved in anaerobic toluene metabolism by strain T1: putative role of a glycine free radical. *Appl Environ Microbiol* 64, 1650-1656

68. Leutwein, C., and Heider, J. (1999) Anaerobic toluene-catabolic pathway in denitrifying Thauera aromatica: activation and beta-oxidation of the first intermediate, (R)-(+)-benzylsuccinate. *Microbiology* 145 (Pt 11), 3265-3271

69. Buckel, W., and Golding, B. T. (1999) Radical species in the catalytic pathways of enzymes from anaerobes. *FEMS Microbiol. Rev.* 22, 523-541

70. Sofia, H. J., Chen, G., Hetzler, B. G., Reyes-Spindola, J. F., and Miller, N. E. (2001) Radical SAM, a novel protein superfamily linking unresolved steps in familiar biosynthetic pathways with radical mechanisms: functional characterization using new analysis and information visualization methods. *Nucleic Acids Res* 29, 1097-1106

71. Pierrel, F., Hernandez, H. L., Johnson, M. K., Fontecave, M., and Atta, M. (2003) MiaB protein from Thermotoga maritima. Characterization of an extremely thermophilic tRNA-methylthiotransferase. *J Biol Chem* 278, 29515-29524

72. Pierrel, F., Douki, T., Fontecave, M., and Atta, M. (2004) MiaB protein is a bifunctional radical-S-adenosylmethionine enzyme involved in thiolation and methylation of tRNA. *J Biol Chem* 279, 47555-47563

73. Hanzelmann, P., and Schindelin, H. (2004) Crystal structure of the S-adenosylmethionine-dependent enzyme MoaA and its implications for molybdenum cofactor deficiency in humans. *Proc Natl Acad Sci U S A* 101, 12870-12875

74. Layer, G., Pierik, A. J., Trost, M., Rigby, S. E., Leech, H. K., Grage, K., Breckau, D., Astner, I., Jansch, L., Heathcote, P., Warren, M. J., Heinz, D. W., and Jahn, D. (2006) The substrate radical of Escherichia coli oxygen-independent coproporphyrinogen III oxidase HemN. *J Biol Chem* 281, 15727-15734

75. Leonardi, R., and Roach, P. L. (2004) Thiamine biosynthesis in Escherichia coli: in vitro reconstitution of the thiazole synthase activity. *J Biol Chem* 279, 17054-17062

76. Leonardi, R., Fairhurst, S. A., Kriek, M., Lowe, D. J., and Roach, P. L. (2003) Thiamine biosynthesis in Escherichia coli: isolation and initial characterisation of the ThiGH complex. *FEBS Lett* 539, 95-99

77. Graham, D. E., Xu, H., and White, R. H. (2003) Identification of the 7,8-didemethyl-8-hydroxy-5-deazariboflavin synthase required for coenzyme F(420) biosynthesis. *Arch Microbiol* 180, 455-464

78. Fang, Q., Peng, J., and Dierks, T. (2004) Post-translational formylglycine modification of bacterial sulfatases by the radical S-adenosylmethionine protein AtsB. *J Biol Chem* 279, 14570-14578

79. Curatti, L., Ludden, P. W., and Rubio, L. M. (2006) NifB-dependent in vitro synthesis of the iron-molybdenum cofactor of nitrogenase. *Proc Natl Acad Sci U S A* 103, 5297-5301

80. Peters, J. W., Szilagyi, R. K., Naumov, A., and Douglas, T. (2006) A radical solution for the biosynthesis of the H-cluster of hydrogenase. *FEBS Lett* 580, 363-367

81. Paraskevopoulou, C., Fairhurst, S. A., Lowe, D. J., Brick, P., and Onesti, S. (2006) The Elongator subunit Elp3 contains a Fe4S4 cluster and binds S-adenosylmethionine. *Mol Microbiol* 59, 795-806

82. Blaschkowski, H. P., Neuer, G., Ludwig-Festl, M., and Knappe, J. (1982) Routes of flavodoxin and ferredoxin reduction in Escherichia coli. CoA-acylating pyruvate: flavodoxin and NADPH: flavodoxin oxidoreductases participating in the activation of pyruvate formate-lyase. *Eur J Biochem* 123, 563-569

83. Ollagnier, S., Mulliez, E., Schmidt, P. P., Eliasson, R., Gaillard, J., Deronzier, C., Bergman, T., Graslund, A., Reichard, P., and Fontecave, M. (1997) Activation of the anaerobic ribonucleotide reductase from Escherichia coli. The essential role of the iron-sulfur center for S-adenosylmethionine reduction. *J Biol Chem* 272, 24216-24223

84. Mulliez, E., Padovani, D., Atta, M., Alcouffe, C., and Fontecave, M. (2001) Activation of class III ribonucleotide reductase by flavodoxin: a protein radical-driven electron transfer to the iron-sulfur center. *Biochem* 40, 3730-3736

85. Krebs, C., Broderick, W.E., Henshaw, T.F., Broderick, J.B., and Huynh, B.H. (2002) Coordination of adenosylmethionine to a unique iron site of the [4Fe-4S] of pyruvate formate-lyase activating enzyme: A Mössbauer spectroscopic study. *J Am Chem Soc* 124, 912-913

86. Berkovitch, F., Nicolet, Y., Wan, J. T., Jarrett, J. T., and Drennan, C. L. (2004) Crystal structure of biotin synthase, an S-adenosylmethionine-dependent radical enzyme. *Science* 303, 76-79

87. Layer, G., Moser, J., Heinz, D. W., Jahn, D. and Schubert, W.-D. (2003) Crystal structure of coproporphyrinogen III oxidase reveals cofactor geometry of Radical SAM enzymes. *EMBO J* 22, 6214-6224

88. Jarrett, J. T. (2003) The generation of 5'-deoxyadenosyl radicals by adenosylmethionine-dependent radical enzymes. *Curr Opin Chem Biol* 7, 174-182

89. Layer, G., Heinz, D. W., Jahn, D., and Schubert, W. D. (2004) Structure and function of radical SAM enzymes. *Curr Opin Chem Biol* 8, 468-476

90. Lepore, B. W., Ruzicka, F. J., Frey, P. A., and Ringe, D. (2005) The x-ray crystal structure of lysine-2,3-aminomutase from Clostridium subterminale. *Proc Natl Acad Sci U S A* 102, 13819-13824

91. Douglas, P., Kriek, M., Bryant, P., and Roach, P. L. (2006) Lipoyl Synthase Inserts Sulfur Atoms into an Octanoyl Substrate in a Stepwise Manner. *Angew Chem Int Ed Engl*

92. Tse Sum Bui, B., Mattioli, T. A., Florentin, D., Bolbach, G., and Marquet, A. (2006) Escherichia coli biotin synthase produces selenobiotin. Further evidence of the involvement of the [2Fe-2S]2+ cluster in the sulfur insertion step. *Biochem* 45, 3824-3834

93. Hanzelmann, P., and Schindelin, H. (2006) Binding of 5'-GTP to the C-terminal FeS cluster of the radical S-adenosylmethionine enzyme MoaA provides insights into its mechanism. *Proc Natl Acad Sci U S A* 103, 6829-6834

94. Skerra, A. (1994) Use of the tetracycline promoter for the tightly regulated production of a murine antibody fragment in Escherichia coli. *Gene* 151, 131-135

95. Pierik, A. J., Wolbert, R. B. G., Mutsaers, P. H., Hagen, W. R., and Veeger, C. (1992) Purification and biochemical characterisation of a putative [6Fe-6S] prismane-cluster-containing protein from *Desulfovibrio vulgaris* (Hildenborough). *Eur J Biochem* 206, 679-704

96. Selmer, T., Pierik, A. J. & Heider, J. (2005) New glycyl radical enzymes catalysing key metabolic steps in anaerobic bacteria. *Biol Chem* 386, 981-988

97. Stubbe, J., Booker, S., Broderick, J., Mao, S. S., Ator, M., Harris, G., Ashley, G., Linn, A. E., and Yu, G. X. (1993) Ribonucleotide reductases: radical enzymes with suicidal tendencies. *Nucleic Acids Symp Ser*, 107

98. Bennati, M., Robblee, J. H., Mugnaini, V., Stubbe, J., Freed, J. H., and Borbat, P. (2005) EPR distance measurements support a model for long-range radical initiation in E. coli ribonucleotide reductase. *J Am Chem Soc* 127, 15014-15015

99. Andrei, P. I., Pierik, A. J., Zauner, S., Andrei-Selmer, L. C., and Selmer, T. (2004) Subunit composition of the glycyl radical enzyme p-hydroxyphenylacetate decarboxylase. A small subunit, HpdC, is essential for catalytic activity. *Eur J Biochem* 271, 2225-2230

100. Ling, Y. (2006) Untersuchung zur Kresolbildung durch *Clostridium difficile*. In Diploma-thesis Fachbereich Biologie, Phillips-Universität Marburg

101. Yu, L. (2006) Two novel glycyl radical decarboxylase systems from *Clostridium scatologenes* and *Tannerella forsythensis*. In Thesis Fachbereich Biologie, Philipps-Universität-Marburg

102. Torrents, E., Buist, G., Liu, A., Eliasson, R., Kok, J., Gibert, I., Graslund, A., and Reichard, P. (2000) The Anaerobic (Class III) Ribonucleotide Reductase from Lactococcus lactis. Catalytic properties and allosteric regulation of the pure enzyme system. *J Biol Chem* 275, 2463-2471

103. Paulsen, I. T., Brown, M. H. & Skurray, R. A. (1996) Proton-dependent multidrug efflux systems. *Microbiol Rev.* 60, 575-608

104. Pao, S. S., Paulsen, I. T. & Saier, M. H., Jr. (1998) Major facilitator superfamily. *Microbiol Mol Biol Rev.* 62, 1-34

105. Stubbe, J., Nocera, D. G., Yee, C. S., and Chang, M. C. Y. (2003) Radical Initiation in the Class I Ribonucleotide Reductase: Long-Range Proton-Coupled Electron Transfer? *Chem. Rev.* 103, 2167-2202

106. Walsby, C. J., Hong, W., Broderick, W. E., Cheek, J., Ortillo, D., Broderick, J. B., and Hoffman, B. M. (2002) Electron-nuclear double resonance spectroscopic evidence that S-adenosylmethionine binds in contact with the catalytically active [4Fe-4S](+) cluster of pyruvate formate-lyase activating enzyme. *J Am Chem Soc* 124, 3143-3151

107. Tamarit, J., Gerez, C., Meier, C., Mulliez, E., Trautwein, A., and Fontecave, M. (2000) The activating component of the anaerobic ribonucleotide reductase from Escherichia coli. An iron-sulfur center with only three cysteines. *J Biol Chem* 275, 15669-15675.

108. Kuelzer, R., Pils, T., Kappl, R., Huttermann, J., and Knappe, J. (1998) Reconstitution and characterization of the polynuclear iron-sulfur cluster in pyruvate formate-lyase-activating enzyme. Molecular properties of the holoenzyme form. *J Biol Chem* 273, 4897-4903

109. Grillo, M. A., and Colombatto, S. (2006) S-adenosylmethionine and radical-based catalysis. *Amino Acids*

110. Hewitson, K. S., Ollagnier-de Choudens, S., Sanakis, Y., Shaw, N. M., Baldwin, J. E., Munck, E., Roach, P. L., and Fontecave, M. (2002) The iron-sulfur center of biotin synthase: site-directed mutants. *J Biol Inorg Chem* 7, 83-93

111. Giastas, P., Pinotsis, N., Efthymiou, G., Wilmanns, M., Kyritsis, P., Moulis, J. M., and Mavridis, I. M. (2006) The structure of the 2[4Fe-4S] ferredoxin from Pseudomonas aeruginosa at 1.32-A resolution: comparison with other high-resolution structures of ferredoxins and contributing structural features to reduction potential values. *J Biol Inorg Chem* 11, 445-458

112. Hinckley, G. T., and Frey, P. A. (2006) Cofactor dependence of reduction potentials for [4Fe-4S]2+/1+ in lysine 2,3-aminomutase. *Biochem* 45, 3219-3225

113. Ugulava, N. B., Gibney, B. R., and Jarrett, J. T. (2001) Biotin synthase contains two distinct iron-sulfur cluster binding sites: chemical and spectroelectrochemical analysis of iron-sulfur cluster interconversions. *Biochem* 40, 8343-8351

Acknowledgements

I would like to thank god and (in alphabetical order) Dr. Andrei, Paula; Becker, Gero; Blaser, Antonia; Blaser, Bruno; Blaser, Christiane; Blaser, Felix; Blaser Georg; Prof. Dr. Buckel, Wolfgang; Friedrich, Marc; Ling, Yan; Löbrich, Sven; Mittelsteadt, Luca; Mittelsteadt, Mael; Mittelsteadt, Noah, Mittelsteadt, Silvia Balateera; PD Dr. Selmer, Thorsten; Streubel, Gundula; Szyska, Brigitta; Werner, Silke; Wiedemann, Johanna; Dr. Yu, Lihua;

I would like to gratefully acknowledge all the people who gave me support and help during my Ph.D program. I also acknowledge the funding by the Graduate College 'Protein function on an atomic level' by the Deutsche Forschungsgemeinschaft (DFG). Likewise I give my special thanks to Prof. Dr. Erhard Bremer for further financial support by the SFB 593, which allowed my to safely finish my Ph.D.

I give my deep thanks to my supervisor Dr. Thorsten Selmer who led me to the research field of (micro-)biology and biochemistry. With his constant guidance and tremendous knowledge, I was able to get through my work and finish this dissertation. He gave me all the opportunities to practice and gain more experience in my research field.

I am especially grateful to Prof. Dr. Wolfgang Buckel, who gave me the chance to study in this friendly and knowledgeable interdisciplinary team and coordinated the graduate college. And I am also greatly thankful to all the members of his team for their friendship and help. And great thanks to Prof. Dr. R. K. Thauer for allowing us to take the EPR measurements in the MPI.

I am greatly thankful to Dr. Antonio Pierik for his powerful help about EPR analysis and for his kind support and good ideas during my Ph.D. work.

I would like to give my thanks to Dr. Paula Andrei for her former work in this project and Dr. Lihua Yu for our really nice cooperation's.

Publication

Yu, L., **Blaser, M**., Andrei, P. I., Pierik, A. J., and Selmer, T. (2006) 4-hydroxyphenylacetate decarboxylases: properties of a novel subclass of glycyl radical enzyme systems. *Biochemistry* 45, 9584-9592

.

Curriculum Vitae

name:	Martin Blaser
date of birth:	10.Mai 1977
School	
1983 - 1987	Elementary School (Grundschule), Bad Homburg,
1987 - 1996	High-School (Gymnasium), Bad Homburg, Abitur (2,2),
Military Service	
1996 - 1997	Schule für Nachrichtenwesen (SNBw), Bad Ems,
University	
1997 - 2003	Justus-Liebig-Universität, Giessen, "Food&Nutrition" (Ökotrophologie), Diplom (1,3),
Promotion	
2003 - 2006	Scholarship of the graduate school "Protein function at the atomic Level". Phillips Universität, Marburg, Institut für Mikrobiologie; "Activation and Regulation of the 4-Hydroxy-phenylacetate Decarboxylase System from *C. difficile*."

Erklärung

Ich versichere, dass ich meine Dissertation

Activation and Regulation of the 4-Hydroxyphenylacetate Decarboxylase System from *C. difficile*
selbständig, ohne unerlaubte Hilfe angefertigt und mich dabei keiner anderen als der von mir ausdrücklich bezeichneten Quellen und Hilfen bedient habe.

Die Dissertation wurde in der jetzigen oder einer ähnlichen Form noch bei keiner anderen Hochschule eingereicht und hat noch keinen sonstigen Prüfungszwecken gedient.

_____ _____

(Ort/Datum) (Unterschrift mit Vor- und Zuname)